Calhoun: The NPS Institutional Archive

DSpace Repository

Theses and Dissertations 1. Thesis and Dissertation Collection, all items

1956

# A study of the metal flow during integral end closure extrusion cladding.

Wegner, William

Cambridge, Massachusetts : Massachusetts Institute of Technology

http://hdl.handle.net/10945/26796

*Downloaded from NPS Archive: Calhoun*

Calhoun is the Naval Postgraduate School's public access digital repository for research materials and institutional publications created by the NPS community. Calhoun is named for Professor of Mathematics Guy K. Calhoun, NPS's first appointed -- and published -- scholarly author.

Dudley Knox Library / Naval Postgraduate School
411 Dyer Road / 1 University Circle
Monterey, California USA 93943

http://www.nps.edu/library

# A STUDY OF METAL FLOW DURING INTEGRAL END CLOSURE EXTRUSION CLADDING

William Wegner

# A STUDY OF METAL FLOW DURING INTEGRAL END CLOSURE EXTRUSION CLADDING

by

William Wegner

B.S., United States Naval Academy

(1948)

M.S. in Naval Architecture, Webb Institute of Naval Architecture

(1953)

Submitted in Partial Fulfillment of the
Requirements for the Degree of
MASTER OF SCIENCE
at the
Massachusetts Institute of Technology

July 18, 1956

# A STUDY OF METAL FLOW DURING INTEGRAL END CLOSURE EXTRUSION CLADDING

by

William Wegner

Submitted to the Department of Chemical Engineering, Massachusetts Institute of Technology, in partial fulfillment of the requirements for the degree of Master of Science.

## ABSTRACT

Lead and lead-antimony alloys of three various stiffnesses were co-extruded through a circular die at area reduction ratios of 4, 9, 16, and 25. The interface between the two cylindrical billets was made in the shape of a cone with various preset apex angles of 180°, 170°, 160° and 150°. This comprised a set of 144 different test samples that were extruded by the direct process in order to study the effects of the above mentioned variables. These experiments were carried out at constant conditions of die geometry, lubrication, room temperature, and ram speed.

The results showed that for a particular ratio of stiffnesses between the billets ($K_1/K_2$) and a given cone angle, as the extrusion ratio was increased the interface distortion increased. Also, other conditions being fixed, as $K_1/K_2$ increases, the interface distortion, if plotted in the form of a defect area, will result in an S-shaped curve which has a maximum and minimum which are reached somewhere in the neighborhood where the stiffness of the first metal out is slightly greater than that which follows.

It was also found that when $K_1/K_2$ was small (about 0.5) voids would form between the extruded billets.

The variation of the apex cone angle showed that, in general, if the cone angle was decreased the size of the interface distortion decreased. This decrease continued to a certain point and then the interface would reverse itself and increase in the opposite direction. This situation was not studied since the lowest cone angle used was 150°.

# TABLE OF CONTENTS

I Introduction 1

II The Experiment 8

III The Apparatus 16

IV Preparation of the Billet 19

V Analysis 20

A Preparation of the Sample 20

B Determination of the Extrusion Constant 22

C Determination of the Extrusion Defect Area 26

VI Results and Discussion of Results 39

A Normalized Extrusion Defects 39

B Effect of Varying $K_1/K_2$ Ratio 55

C Effect of Varying Cone Angle 67

D Formation of Voids 72

VII Conclusions 73

VIII Recommendations 75

IX Appendix

A Equipment and Condensed Photographic Results 76

B Plasticine Experiments 97

C Double Extrusion Experiment with Aluminum 100

## LIST OF ILLUSTRATIONS

| Figure No. | Title | Page |
|---|---|---|
| 1. | Direct Extrusion Process Showing Orthogonal Grid Lines Prior to Extrusion | 3 |
| 2. | Direct Extrusion Process Showing Grid Lines After Extrusion | 3 |
| 3. | Extrusion Billet Consisting of Two Dissimilar Metals (A and B) Prior to Extrusion | 4 |
| 4. | Extrusion Billet After Extrusion Showing Interface Between Two Dissimilar Metals | 4 |
| 5. | Billet Arrangement for First Extrusion in a Double Extrusion Process | 10 |
| 6. | Billet Arrangement for Second Extrusion in a Double Extrusion Process | 10 |
| 7 - 10. | Figures Showing Results Obtained with Double Extrusion when Extrusion Ratios of First and Second Extrusions are Equal | 11 |
| 11. | Extrusion Billet | 13 |
| 12. | Tinius-Olsen Tensile Testing Machine Used For Extrusion Testing | 18 |
| 13. | Split-Ring for Preventing Flashing | 13 |
| 14. | Typical Recording of Load vs Ram Travel from Tinius-Olsen Tensile Machine | 25 |
| 15. | Parameters Used for Analyzing Extrusion Defects | 27 |
| 16. | Extrusion Defects Normalized to Common Base | 42 |
| 17. | Extrusion Defects Normalized to Common Base | 43 |
| 18. | Extrusion Defects Normalized to Common Base | 44 |
| 19. | Extrusion Defects Normalized to Common Base | 45 |
| 20. | Extrusion Defects Normalized to Common Base | 46 |
| 21. | Extrusion Defects Normalized to Common Base | 47 |
| 22. | Extrusion Defects Normalized to Common Base | 48 |

## LIST OF ILLUSTRATIONS, contd.

| Figure No. | Title | Page |
|---|---|---|
| 23. | Extrusion Defects Normalized to Common Base | 49 |
| 24. | Extrusion Defects Normalized to Common Base | 50 |
| 25. | Extrusion Defects Normalized to Common Base | 51 |
| 26. | Extrusion Defects Normalized to Common Base | 52 |
| 27. | Extrusion Defects Normalized to Common Base | 53 |
| 28. | Extrusion Defects Normalized to Common Base | 54 |
| 29. | Plot of $K_1/K_2$ Vs Extrusion Defect Area for Varying Angles and E. R. = 4 | 59 |
| 30. | Plot of $K_1/K_2$ Vs Extrusion Defect Area for Varying Angles and E. R. = 9 | 60 |
| 31. | Plot of $K_1/K_2$ Vs Extrusion Defect Area for Varying Angles and E. R. = 16 | 61 |
| 32. | Plot of $K_1/K_2$ Vs Extrusion Defect Area for Varying Angles and E. R. = 25 | 62 |
| 33. | Plot of $K_1/K_2$ Vs Extrusion Defect Area for Varying Extrusion Ratios and Cone Angle of 0° | 63 |
| 34. | Plot of $K_1/K_2$ Vs Extrusion Defect Area for Varying Extrusion Ratios and Cone Angle of 5° | 64 |
| 35. | Plot of $K_1/K_2$ Vs Extrusion Defect Area for Varying Extrusion Ratios and Cone Angle of 10° | 65 |
| 36. | Plot of $K_1/K_2$ Vs Extrusion Defect Area for Varying Extrusion Ratios and Cone Angle of 15° | 66 |
| 37. | Three-Dimensional Plot of $K_1/K_2$ Vs Cone Angle Vs Extrusion Defect Area. Extrusion Ratio = 4 | 68 |
| 38. | Three-Dimensional Plot of $K_1/K_2$ Vs Cone Angle Vs Extrusion Defect Area. Extrusion Ratio = 9 | 69 |
| 39. | Three-Dimensional Plot of $K_1/K_2$ Vs Cone Angle Vs Extrusion Defect Area. Extrusion Ratio = 16 | 70 |
| 40. | Three-Dimensional Plot of $K_1/K_2$ Vs Cone Angle Vs Extrusion Defect Area. Extrusion Ratio = 25 | 71 |

## LIST OF ILLUSTRATIONS, contd.

| Figure No. | Title | Page |
|---|---|---|
| A-1 | Extrusion Cylinder | 77 |
| A-2 | Extrusion Dies | 78 |
| A-3 | Extrusion Stand | 79 |
| A-4 | Extrusion Ram | 79 |
| A-5 | Assembly of Extrusion Apparatus | 80 |
| A-6 | Photographs of Composite Lead Billets After Extrusion Showing Interface. Extrusion Ratio = 4 | 81 |
| A-7 | Photographs of Composite Lead Billets After Extrusion Showing Interface. Extrusion Ratio = 9 | 82 |
| A-8 | Photographs of Composite Lead Billets After Extrusion Showing Interface. Extrusion Ratio = 16 | 83 |
| A-9 | Photographs of Composite Lead Billets After Extrusion Showing Interface. Extrusion Ratio = 25 | 84 |
| A-10 | Photographs of Composite Lead Billets After Extrusion Showing Interface. Extrusion Ratio = 4 | 85 |
| A-11 | Photographs of Composite Lead Billets After Extrusion Showing Interface. Extrusion Ratio = 4 | 86 |
| A-12 | Photographs of Composite Lead Billets After Extrusion Showing Interface. Extrusion Ratio = 4 | 87 |
| A-13 | Photographs of Composite Lead Billets After Extrusion Showing Interface. Extrusion Ratio = 9 | 88 |
| A-14 | Photographs of Composite Lead Billets After Extrusion Showing Interface. Extrusion Ratio = 16 | 89 |
| A-15 | Photographs of Composite Lead Billets After Extrusion Showing Interface. Extrusion Ratio = 25 | 90 |
| A-16 | Photographs of Composite Lead Billets After Extrusion Showing Interface. Extrusion Ratio = 9 | 91 |
| A-17 | Photographs of Composite Lead Billets After Extrusion Showing Interface. Extrusion Ratio = 16 | 92 |
| A-18 | Photographs of Composite Lead Billets After Extrusion Showing Interface. Extrusion Ratio = 25 | 93 |

## LIST OF ILLUSTRATIONS, contd.

| Figure No. | Title | Page |
|---|---|---|
| A-19 | Photographs of Composite Lead Billets After Extrusion Showing Interface. Extrusion Ratio = 9 | 94 |
| A-20 | Photographs of Composite Lead Billets After Extrusion Showing Interface. Extrusion Ratio = 16 | 95 |
| A-21 | Photographs of Composite Lead Billets After Extrusion Showing Interface. Extrusion Ratio = 25 | 96 |
| C-1 | Billet for Aluminum Double Extrusion | 101 |
| C-2 | Radiograph of Aluminum Billet After First Extrusion Showing Distortion of Copper-Filled Hole. Direction of First Extrusion was from Right to Left. | 102 |
| C-3 | Radiograph of Aluminum Billet After Second Extrusion Showing Distortion of Copper-Filled Hole. Direction of Second Extrusion was from Left to Right. | 102 |

## LIST OF TABLES

| Table No. | Subject | Page |
|---|---|---|
| I | Summary Sheet for Identifying Extrusions | 14 |
| II | Experiment Extrusion Data | 29 |
| III | Ratio of Extrusion Constants | 55 |
| IV | Extrusion Constants (K) | 57 |
| V | Void Formation | 72 |

# ACKNOWLEDGMENTS

The author is indebted to Professor A. R. Kaufmann for his able and willing assistance throughout this investigation.

Gratitude is also extended to Dr. W. B. Nowak for his constant help and many suggestions. Mention must also be made of the willing assistance of many people at Nuclear Metals, Inc. of Cambridge, Massachusetts, where this investigation was conducted.

# I. INTRODUCTION

In the process of manufacturing fuel elements for reactors it is necessary to clad the nuclear fuel with a more corrosion resistant metal so that the fuel elements can be subjected to the flow of the heat-dissipating medium and also be capable of withstanding shock. One method of doing this in the case of cylindrical fuel elements has been to co-extrude the fuel material along with the cladding metal. This is normally done by "canning" the fuel material prior to extrusion. Dimensions are chosen so that after extrusion the proper thickness of clad is obtained. This, in itself, presents no great difficulty, and is accomplished with extreme accuracy. However, since these elements are of finite length and must be extruded as such, difficulty arises at the ends where the clad material faces on to the fuel material. Instead of getting a flat interface between the two metals, as one would like to have, the normal result is an irregularly shaped interface.

Typical of all extrusions is a phenomenon which is called an "extrusion defect", or just the "defect". As in the flow of fluids, once a steady state condition is reached and no discontinuities are introduced the flow pattern remains constant. Such would be the case with extrusions if only one stiffness of metal were used; but in the case of co-extrusion, at least two different stiffnesses of metal are used.

In order to illustrate the significance of the "defect", consider a single metal being extruded through a die in which a grid has been superimposed on a center plane as in Figure 1.

As force is applied to the piston, a point will be reached when the shear stress is greater than the shear modulus of the metal and flow will

commence. The first squares of the orthogonal grid will be distorted to a new shape and successive squares will result in varying shapes until a steady state condition is reached. This steady state condition is shown in Figure 2.

Finally, as the last of the metal approaches the die, the pattern changes again and neither resembles the initial pattern nor the steady state pattern. These variations of grid pattern at the beginning and end of the extrusion as compared to the steady flow pattern are examples of "defects". Some authors refer to the distortion of the orthogonal grid pattern as a "defect", but this experimenter will use the term "grid distortion" for this in order to differentiate between the two. In other words, every element of an extrusion undergoes grid distortion, whereas the defect occurs only at discontinuities.

Imagine now, two materials of different stiffnesses arranged as in Figure 3 being extruded through the same arrangement as before.

Depending upon the relative stiffnesses and many other variables, the result will, in general, be as is shown in Figure 4.

The fact that the interface between the two dissimilar materials is no longer a straight line and can extend for great lengths is the problem to be attacked by this paper.

Were it possible to weld or somehow cap the ends of extrusions, the defect would present no problem because one long extrusion could be made, cut into desired lengths, and capped. Due to the nature of the metals concerned and to the desirability of a metallic bond at the end between the meat and the clad this is not possible at the present time and consequently some means had to be developed to eliminate or reduce the defect.

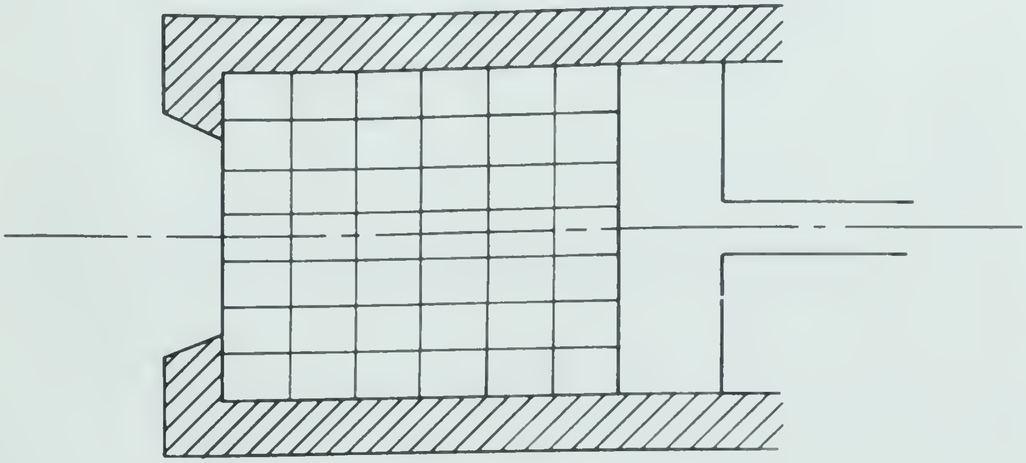

FIGURE 1

Direct Extrusion Process Showing Orthogonal Grid Lines Prior to Extrusion

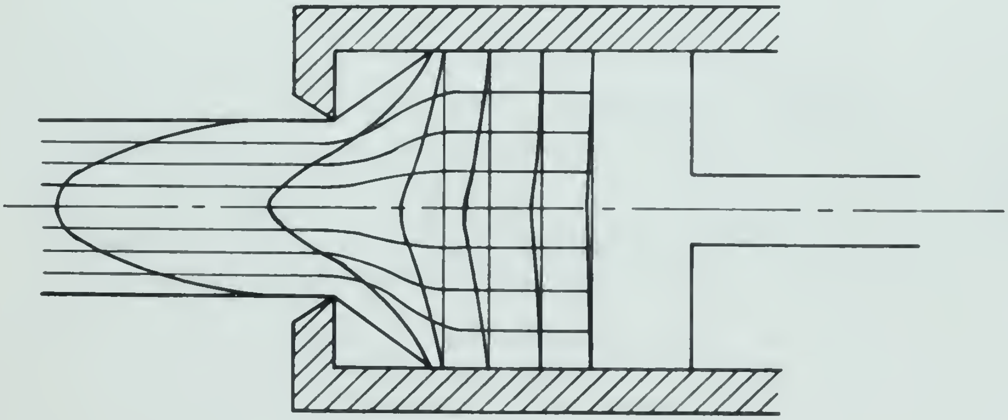

FIGURE 2

Direct Extrusion Process Showing Grid Lines After Extrusion

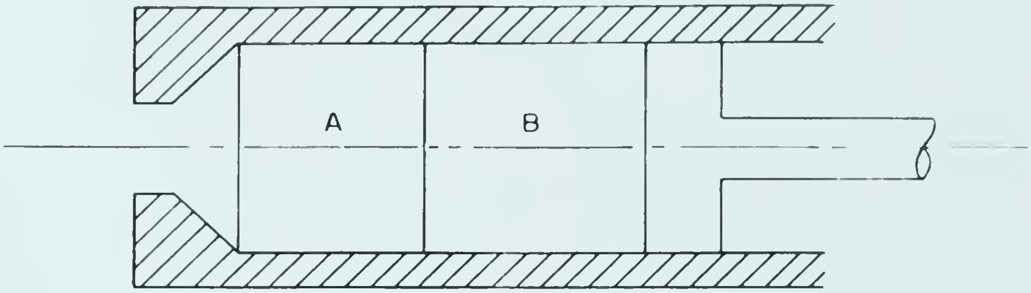

FIGURE 3

Extrusion Billet Consisting of Two Dissimilar Metals (A and B) Prior to Extrusion

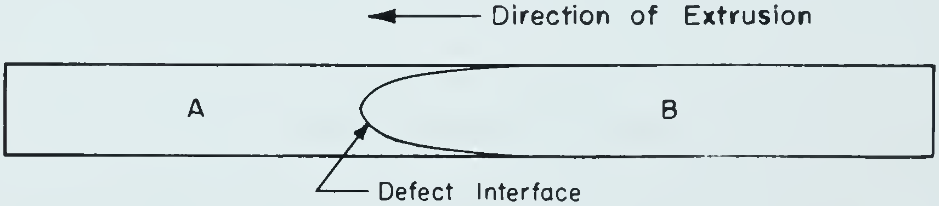

FIGURE 4

Extrusion Billet After Extrusion Showing Interface Between Two Dissimilar Metals

Presently this is done by preshaping the interface so that a straight interface is approached in the final result. The exact geometry of the preshape is arrived at by experimental methods for each particular case and can be called nothing more than a trial-and-error method. It will be the object of this paper to investigate systematically the formation of the defect.

Since the main problem in this investigation centered around the behaviors of two metals having different stiffnesses, the first problem was to arrive at an experiment which would show the effects of this property. In the beginning, the idea of using a commercial plastic clay called "Plasticine" was tried and many experiments were carried out with this material. Plasticine had possible advantages in that different stiffnesses might be easily attained by merely adding given amounts of talc and kneading the clay until it was homogeneous. Also there was quite a large background of material available where Plasticine had been used to study the flow of metal during extrusions, rolling and etc. Also in its favor was its relative ease of fabrication, its ability to be made in various colors, and its extremely low extrusion pressure.

Its disadvantages lie in the fact that its properties are so dependent upon temperature that a few degrees' change will alter its characteristics noticeably. Another difficulty encountered was dimensional stability of the billets prior to extrusion. Since the whole investigation centered around the interface, it was mandatory that the original billet interface be quite exact and very reproducible for hundreds of extrusions. The very softness of the Plasticine prevented this stability to any great degree but it is felt that this problem could

have been solved by lowering the temperature of the Plasticine during the making of the billet in order to make it easier to maintain tolerances.

Appendix B details some of the experiments carried out with Plasticine prior to the time that a new material was selected.

In the selection of the new material certain qualities were predominant: (1) it should be a metal, (2) it should be relatively soft so that the testing equipment available could be used, (3) it must be possible to vary its stiffness but not change its over-all characteristics, and (4) it should be a material which is readily available and safe to use. After looking over the field it was decided that lead fulfilled the specifications since antimony could be added in small percentages to increase its hardness.

The only objection to this selection was the fact that at room temperature lead and antimony would not form a solid solution and the possibility existed of having variations in the metal due to non-homogeneity. In order to find out if this problem was of sufficient magnitude to exclude the use of these two metals, a test was made by extruding a long billet containing 10 percent antimony and testing each piece of this billet by extruding through another die to determine if its properties changed with respect to position in the originally cast billet. No differences were noted so it was tacitly assumed that all cast billets were homogeneous.

By calling local lead distributors it was learned that lead containing any desired amounts of antimony was obtainable by order, but that 3 percent and 10 percent were readily available and required no special procurement. Pure lead (99.99 percent) was also available as a

standard stock item. Thus, the selection was made to use three different types of lead: pure, 3 percent antimony, and 10 percent antimony.

Having selected the material to be used, the next step was to determine the experiment which would enable an investigation concerning the extrusion interface to be studied.

## II. THE EXPERIMENT

Since most of the extrusions made in general practice are of the direct extrusion type, it was decided that this experiment would also use the direct process. Figure 1 is an example of the direct extrusion process. The simplest geometry for extrusion is the cylindrical type where the cross-sections of the billet and of the extrusion are circles. This type of geometry was selected.

The next selection was the size of the billets and the extrusion. The determining factor here was the apparatus available which is described in Chapter III. A few simple calculations showed that a 3/4-inch diameter billet could be extruded through a 25 to 1 reduction ratio and from this limiting arrangement the billet size was fixed at .748-inch diameter (.002-inch under the .750-inch value so that the billet would fit into a .750-inch diameter cylinder). Four different values of reduction ratio were selected:

(1) 4 to 1
(2) 9 to 1
(3) 16 to 1
(4) 25 to 1

It was felt that this range would cover the possible range now being used for extrusions and would yield sufficient data to investigate the problem. Thus, at this point there are three different materials and four different extrusion ratios, resulting in a possibility of twelve different conditions. If it is now allowed to use two different billets in the cylinder instead of one, and also specify the material which is first extruded, the possibilities are tripled and thirty-six combinations are available.

The introduction of one more variable now completes the necessary variations which are required: that of preshaping the interface of the billet. In order to understand why the particular shapes were chosen, it is necessary to explain some profound results obtained in the Plasticine experiments.

After working with Plasticine for several weeks trying to obtain a flat interface by preshaping the billets, the idea came to this investigator of double extrusion. In this process a billet consisting of two materials having a flat interface was extruded at an extrusion ratio roughly the square root of the final extrusion ratio required. See Figure 5. This resulted in a billet having an extrusion defect as shown in Figure 6. It was now proposed to re-extrude this billet, but in the opposite direction, so that the final extrusion would again contain a flat interface as in Figure 5. The idea was to let the physical properties of the metal and the extrusion determine the complicated preshaping of the billet so as to result in a flat interface.

This experiment was performed many times and always resulted in the confusing and then-unexplainable situation of an extrusion defect much larger and in the opposite direction of the final extrusion. In other words, the billet in Figure 7 was extruded in the direction shown, resulting in Figure 8. Then the billet in Figure 8 was extruded in the direction shown in Figure 9, and resulted in Figure 10. Theory available could not explain this result. At first it was felt that the Plasticine was the reason for this difficulty, so an experiment was carried out using aluminum and the same result was obtained. See Appendix C.

Careful analysis and precise evaluation shows that the result obtained could be predicted if one realizes that there is some angle in

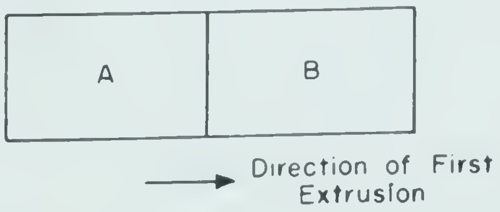

FIGURE 5

Billet Arrangement for First Extrusion in a Double Extrusion Process

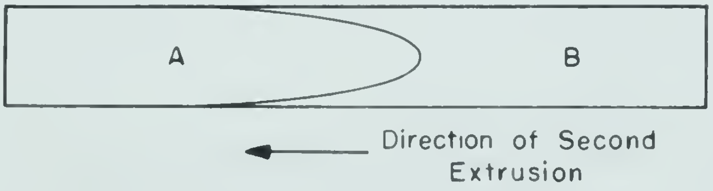

FIGURE 6

Billet Arrangement for Second Extrusion in a Double Extrusion Process

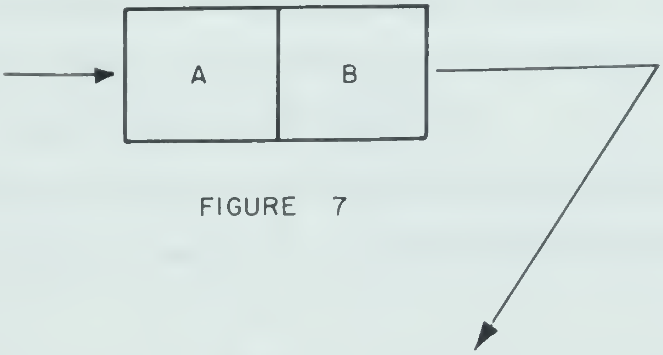

FIGURE 7

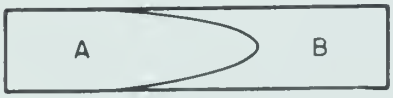

FIGURE 8

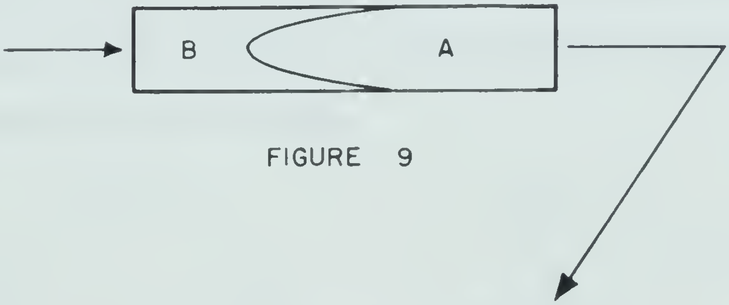

FIGURE 9

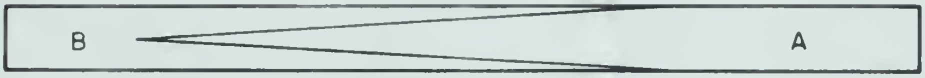

FIGURE 10

Figures Showing Results Obtained with Double Extrusion when Extrusion Ratios of First and Second Extrusions are Equal.

the preshaped interface, after which the first extrusion defect will not reverse itself, but will indeed increase in defect length. An analysis based on preservation of volume shows this angle to be around 15° for all materials and will be discussed in detail later on.

Having arrived at this angle of 15° for preshaping, it was decided to investigate four different angles in the lead experiment, namely:

(1) 0°

(2) 5°

(3) 10°

(4) 15°

Figure 11 shows the general shape of the billet with the cone-shaped interface. With these four new combinations available the final combinations rose to 144, which was the final number of experiments as actually performed. Table I gives a schedule of these different experiments. No two of these extrusions were the same.

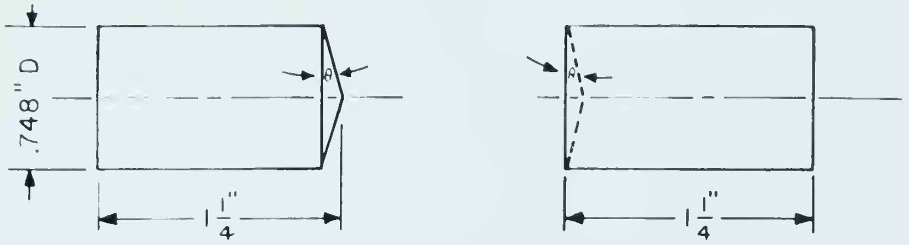

$\theta = 0°, 5°, 10°, 15°$

Material Lead (Pure, 3% & 10% Antimony)

FIGURE 11

Extrusion Billet

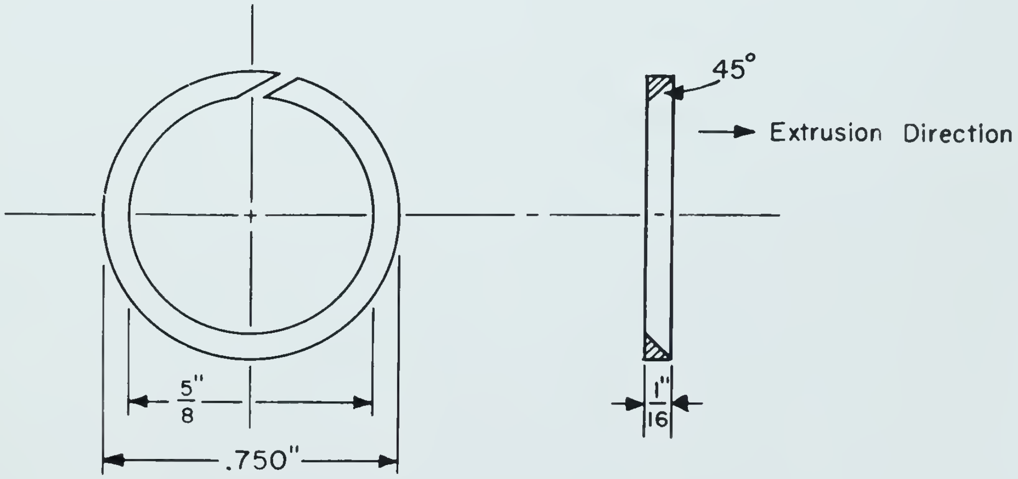

FIGURE 13

Split-Ring for Preventing Flashing

TABLE I

| θ | EXTRUSION RATIO $A_1/A_2$ | | | | | | | |
|---|---|---|---|---|---|---|---|---|
| | 4 | | 9 | | 16 | | 25 | |
| 0° | P→P | #1 | P→P | #10 | P→P | #19 | P→P | #28 |
| | 3→3 | #5 | 3→3 | #11 | 3→3 | #20 | 3→3 | #29 |
| | 10→10 | #2 | 10→10 | #12 | 10→10 | #21 | 10→10 | #30 |
| | P→3 | #6 | P→3 | #13 | P→3 | #22 | P→3 | #31 |
| | P→10 | #4 | P→10 | #14 | P→10 | #23 | P→10 | #32 |
| | 3→P | #7 | 3→P | #15 | 3→P | #24 | 3→P | #33 |
| | 3→10 | #8 | 3→10 | #16 | 3→10 | #25 | 3→10 | #34 |
| | 10→P | #3 | 10→P | #17 | 10→P | #26 | 10→P | #35 |
| | 10→3 | #9 | 10→3 | #18 | 10→3 | #27 | 10→3 | #36 |
| 5° | P→P | #37 | P→P | #91 | P→P | #100 | P→P | #109 |
| | 3→3 | #38 | 3→3 | #92 | 3→3 | #101 | 3→3 | #110 |
| | 10→10 | #39 | 10→10 | #93 | 10→10 | #102 | 10→10 | #111 |
| | P→3 | #40 | P→3 | #94 | P→3 | #103 | P→3 | #112 |
| | P→10 | #41 | P→10 | #95 | P→10 | #104 | P→10 | #113 |
| | 3→P | #42 | 3→P | #96 | 3→P | #105 | 3→P | #114 |
| | 3→10 | #43 | 3→10 | #97 | 3→10 | #106 | 3→10 | #115 |
| | 10→P | #44 | 10→P | #98 | 10→P | #107 | 10→P | #116 |
| | 10→3 | #45 | 10→3 | #99 | 10→3 | #108 | 10→3 | #117 |

TABLE I (Continued)

| | 4 | | 9 | | 16 | | 25 | |
|---|---|---|---|---|---|---|---|---|
| 10° | P→P | #46 | P→P | #118 | P→P | #127 | P→P | #136 |
| | 3→3 | #47 | 3→3 | #119 | 3→3 | #128 | 3→3 | #137 |
| | 10→10 | #48 | 10→10 | #120 | 10→10 | #129 | 10→10 | #138 |
| | P→3 | #49 | P→3 | #121 | P→3 | #130 | P→3 | #139 |
| | P→10 | #50 | P→10 | #122 | P→10 | #131 | P→10 | #140 |
| | 3→P | #51 | 3→P | #123 | 3→P | #132 | 3→P | #141 |
| | 3→10 | #52 | 3→10 | #124 | 3→10 | #133 | 3→10 | #142 |
| | 10→P | #53 | 10→P | #125 | 10→P | #134 | 10→P | #143 |
| | 10→3 | #54 | 10→3 | #126 | 10→3 | #135 | 10→3 | #144 |
| 15° | P→P | #55 | P→P | #64 | P→P | #73 | P→P | #82 |
| | 3→3 | #56 | 3→3 | #65 | 3→3 | #74 | 3→3 | #83 |
| | 10→10 | #57 | 10→10 | #66 | 10→10 | #75 | 10→10 | #84 |
| | P→3 | #58 | P→3 | #67 | P→3 | #76 | P→3 | #85 |
| | P→10 | #59 | P→10 | #68 | P→10 | #77 | P→10 | #86 |
| | 3→P | #60 | 3→P | #69 | 3→P | #78 | 3→P | #87 |
| | 3→10 | #61 | 3→10 | #70 | 3→10 | #79 | 3→10 | #88 |
| | 10→P | #62 | 10→P | #71 | 10→P | #80 | 10→P | #89 |
| | 10→3 | #63 | 10→3 | #72 | 10→3 | #81 | 10→3 | #90 |

## III. THE APPARATUS

A 20,000-pound Tinius-Olsen Testing Machine was used to provide the power for the extrusions. Means were available on this machine to accurately set the speed of the cross-head which, in effect, was the ram-speed of the extrusion. Since the extrusion pressure is greatly dependent upon the ram-speed, it was decided that the ram-speed would be held constant for all the extrusions and was ultimately set at one inch per minute.

This machine also provided means for recording the load versus ram travel graphically and these graphs were used to obtain a permanent record throughout the entire run of the extrusion. An example of one of these records is presented in Figure 14.

The actual extrusion apparatus was made as simple as possible and consisted of a cylinder, ram, dies, and stand. Plans of these are shown in Appendix A. These were all made from cold-rolled steel and were not heat-treated since it was felt that by using the relatively soft lead no particular abuse would be experienced by the apparatus. This confidence was borne out by the experiment.

Since four dies were required, it was necessary to either make the dies removable from the cylinder or make four dies integral with the cylinder. Realizing that it would be impossible to extrude 100 percent of the billet and that the remainder would have to be removed from the cylinder, it was decided that the better arrangement would be to have the die detachable from the cylinder, thus facilitating the removal of the spent billet.

Use was made of an anti-flashing ring between the ram and the billet. Great care was used in machining the cylinder hole and the ram so as to obtain a tight but movable fit. However, enough clearance was left to permit flashing of the lead between the cylinder and the ram. If allowed, this flashing eventually results in binding the ram. In order to alleviate this situation a small steel split ring was used as a seal between the lead and the ram face. See Figure 13. As the ram forced the ring into the lead, the tapered inner face of the ring caused the ring to expand outward, sealing off any lead which might try to slip between the ram and cylinder. This method worked very successfully.

The next consideration was that of lubrication. From experience it was known that some form of lubrication was required in the extrusion of lead and most references indicated some form of graphite. However, in this experiment the problem of lubrication was made complicated by the fact that there should be no lubrication on the interface. This, at the onset, ruled out the use of a liquid lubricant unless the interface could somehow be closed off. At first the notion of pressing the two billets together under extreme pressure in a closed container was tried, but with the pressures available this was unsuccessful. Since the lubricant recommended was some form of graphite and dry film graphite was available, the problem was solved. The billets, prior to extrusion, were sprayed with "DGF-123", a quick-drying product produced by the A. P. Products Corporation of Toledo, Ohio. This method proved to be successful in that it provided lubrication to the cylinder wall and still did not lubricate the interface. A small amount of liquid graphite was placed on the die face to facilitate the initial phase of the extrusion.

Figure 12 shows the apparatus as set up for extruding the lead billets.

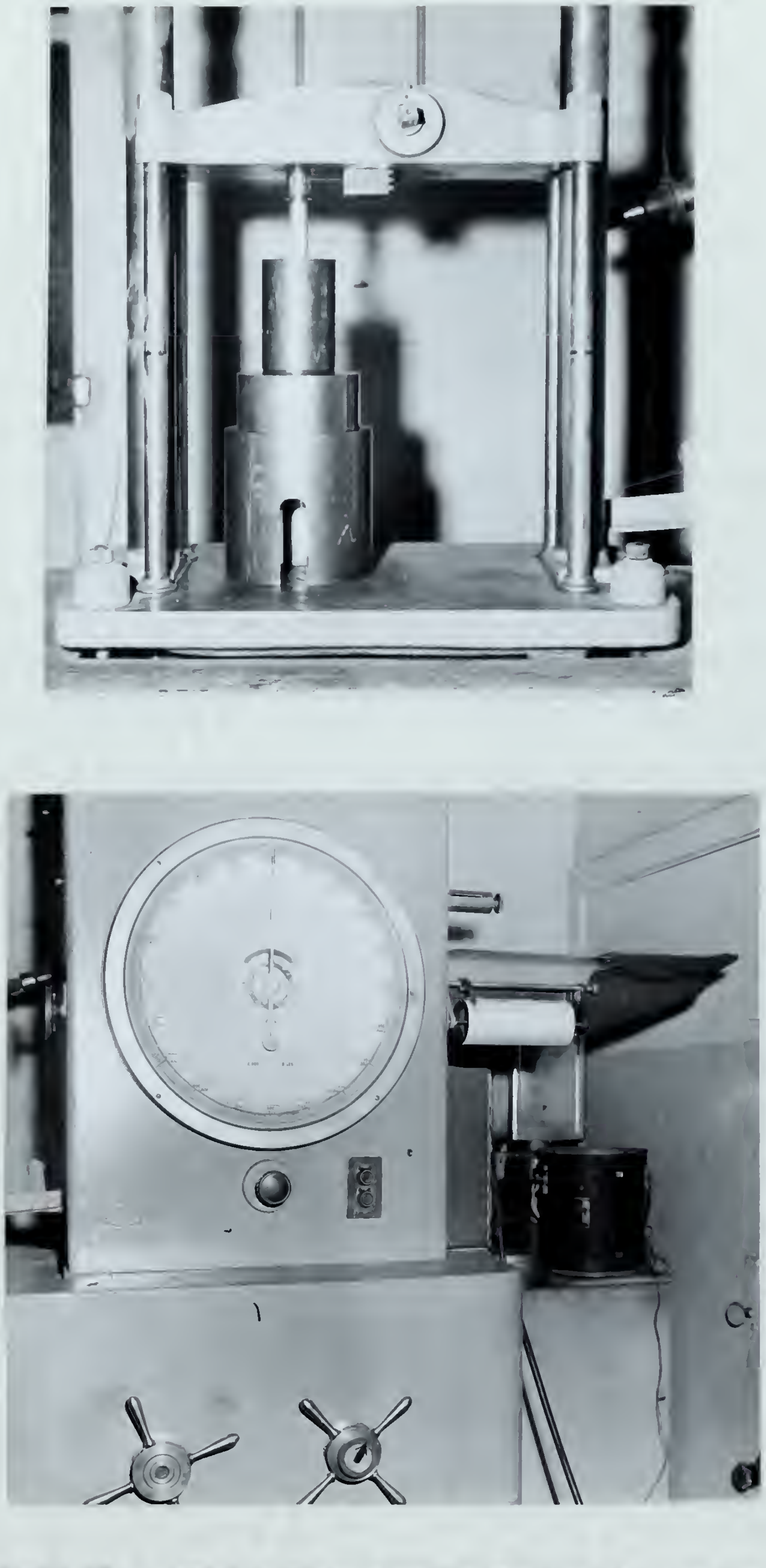

Figure 12 - Tinius-Olsen Tensile Testing Machine Used For Extrusion Testing

## IV. PREPARATION OF THE BILLET

The three types of lead were obtained in pig form and were melted down in the laboratory under conditions which were intended to prevent any contamination which might have caused a variation in its properties. The molten lead was poured into a hollow graphite cylinder which had an inside diameter of 2 inches. This billet was cooled slowly in air and caused to solidify from the bottom up by using a torch to apply heat at the top. This was done in order to assure that no pipe would form.

After cooling, the billet was removed from the graphite cylinder and the top inch was sawed off and discarded. This billet was then extruded in a 100-ton extrusion press using a .756-inch die. The extrusion was performed at room temperature. These rods were then drawn down to .748-inch diameter on a regular drawing machine.

After cutting into 1½-inch length cylinders, the cylinders were faced off on one end and the required cone machined on the other. Each billet was labeled as to its cone angle and percent antimony. Although the accuracy of the angle as machined could not be attested to, it was the procedure that once the lathe was set up for cutting a particular angle, all the samples were done at once, both the male and female, to insure that all the angles were the same within that group of cone angle designation.

# V. ANALYSIS

## A. Preparation of the Sample

The extrusions were performed in the order shown in Table I. Each extrusion was given a number and all pictures, diagrams, and calculations can be identified by this number and reference to Table I.

As each extrusion was completed, the extruded metal was scrutinized in order to locate some tell-tale sign by which the position of the interface could be determined. Usually this presented no particular problem because a definite discontinuity would develop. Sometimes where the two metals were of the same composition, finding the exact location of the interface was quite a problem and long test samples had to be taken. The direction of extrusion was scribed on the metal.

Since the information could only be obtained along the cross-section of the test sample, it was necessary first to embed the lead into a metallographic mounting substance called Casto-Mold, manufactured by the Cosmos Products, Inc., of New York City. This facilitated mounting the samples in a strong resiliant plastic without the application of heat.

Each sample was then ground down to the diameter by use of a wet-belt sander and the application of a great deal of water as a coolant for the lead. Extreme care was exercised in this process for the lead had a tendency to smear if too much pressure was applied, or if the lead was allowed to heat up. At first an attempt was made to mill each sample down, but this proved to be a great time-consuming process. By using the wet-belt sander, a sample was prepared in just a couple of minutes.

After this initial rough-grind, the sample was then further polished using emery paper down to 2/0 with liberal amounts of kerosene as a

lubricant and coolant to prevent smearing. No finer paper than 2/0 was used because the interest was in the interface rather than in the grain structure of the lead.

At this point, many of the samples displayed the interface very clearly and needed no further preparation prior to photographing; however, some form of etching was called for to facilitate the photographic process. Three basic types of etches were used, depending upon the composition of the sample, namely:

(1) Glacial Acetic Acid

(2) Nitric Acid (concentrated)

(3) Hydrogen Peroxide (30 percent)

It will be recalled that each sample could be composed of any two of the three types of lead. If the two metals in the sample consisted of dissimilar metals, such as pure lead and 10 percent antimony lead, then a light cotton swabbing with full strength Glacial acetic acid was sufficient to clearly bring out the interface because the greater the percentage of antimony in the lead, the lighter in color would be the etch. Pure lead turned almost black.

When the two leads in the sample were of the same metal, such as pure lead and pure lead, then the problem was to try to burn out the interface with the hope that the grain structure at the interface would be weaker and thus more susceptible to a strong oxidizing agent. The first etching solution tried was:

16 parts $H_2O$
4 parts Acetic Acid (Glacial)
6 parts $HNO_3$

In many cases this solution was sufficient to bring out the interface. In some isolated cases the aforementioned solution was not successful and the following was used:

1 part $H_2O_2$ (30 percent)

1 part Acetic Acid (Glacial)

Each sample was then photographed and printed. A complete set of the photographs are presented in Appendix A.

## B. Determination of Extrusion Constant

One of the few basic relationships which apply to the process of extrusion is the concept of the Extrusion Constant (K). This states that the extrusion pressure is proportional to the natural logarithm of the ratio of the initial to the final cross-sectional areas.

$$P = K \ln (A_1/A_2) \quad (1)$$

where $P$ = extrusion pressure (psi)

$A_1$ = cross-sectional area of pre-extruded billet (area)

$A_2$ = cross-sectional area of extruded billet (area)

$K$ = Extrusion constant (psi)

This relationship requires that many conditions remain fixed during any series of extrusions. Thus, there is no particular value of K for a particular metal since so many other variables can effect K. Some examples of parameters which have a profound effect on K are: the ram speed, the temperature, the type and amount of lubrication, the type of extrusion, and the geometry of the dies.

Realizing that these factors all contributed to the determination of K, it was mandatory that the experiment be so conducted as to have these factors remain constant for all the tests. This was not too

difficult to achieve because of the nature of the factors involved. The only items which could not be absolutely fixed were the temperature and the lubrication. All the tests were conducted at room temperature which varied, over the period of tests, about 10°F. It was assumed that this variation did not effect the results within the accuracy desired. In the matter of the lubrication, it was realized that the exact amount of dry film graphite could not be repeated for each test, but that so little variation existed that this too was felt to be within the experimental error anticipated.

Thus, with all other conditions remaining fixed, K depended only on P, $A_1$, and $A_2$. $A_1$ and $A_2$ were accurately measurable since the cylinder and dies were machined to within .001-inch. From the inception of the design the area ratios were selected as definite parameters such that $A_1/A_2$ varied in steps 4, 9, 16, and 25. These are called the area reduction ratios or extrusion ratios (E.R.)

$$E.R. = A_1/A_2 \qquad (2)$$

It then follows:

| E.R. | ln E.R. |
|---|---|
| 4 | 1.39 |
| 9 | 2.20 |
| 16 | 2.77 |
| 25 | 3.22 |

Then for a given E.R., K is directly proportional to the extrusion pressure, if (1) is valid. During the actual process of the extrusion, the load being applied to the ram was being recorded by means of a revolving drum and stylus connected by linkages to the recording dials of the Tinius-Olsen machine. This resulted in a graph of load versus travel

of the ram. Knowing the cross-sectional area of the ram, it was possible to convert directly from the load reading to a pressure reading.

Determining that particular value of the load to use presented a problem since at no time was a constant value attained. In Figure 14, which is a typical example of the type of curve obtained from the machine, several interesting things can be noticed. Since the ram speed was constant, the initial load was applied at a constant rate and is evidenced by the characteristic straight line at the beginning of the plot. This is analogous to the proportional region of a stress-strain curve for metal. As the load finally reached the point where the metal was stressed beyond the elastic limit, the extrusion began. At this point, a definite maximum occurred which was the stress required to start the extrusion. Once the extrusion began, the stress dropped to a lower value and reflected that stress which was required to maintain the extrusion. For the direct type of extrusion, this value did not remain constant because the friction experienced by the billet was decreasing as the billet length was becoming shorter. This downward trend is very evident in all the curves and appeared to be of constant slope for all tests.

As the interface between the two metals approached the die, there appeared to be a definite discontinuity in the recorded curve. Depending on the metals involved and the angle of the cone, this discontinuity varied slightly. After this discontinuity passed through the die, then, once again, the stress (or load) settled down to the relatively constant extrusion pressure characteristic of the second billet material.

One thing very noticeable on all the curves was the harmonic-like vibration which occurred whenever a discontinuity passed through the die.

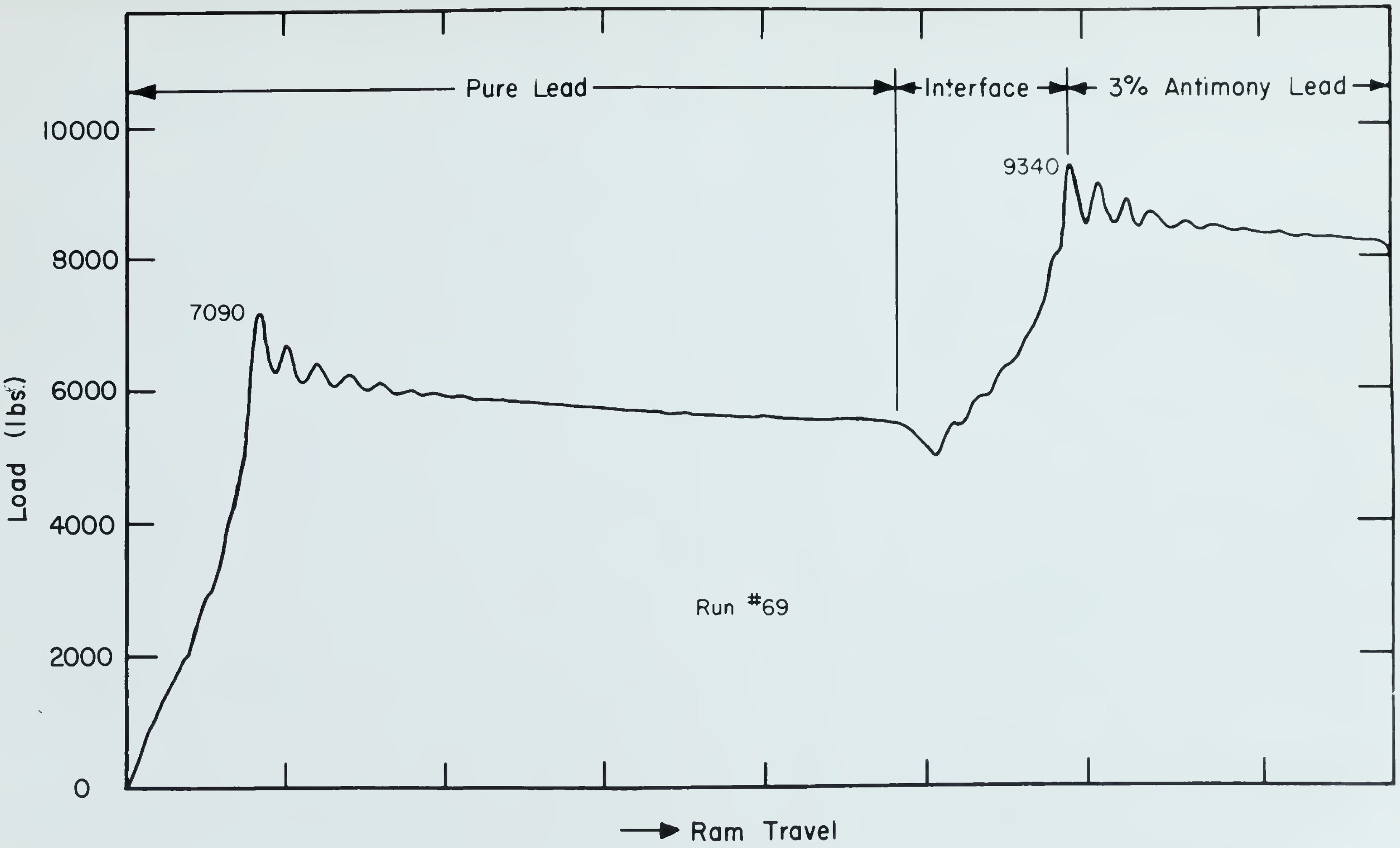

Figure 14 Typical Recording of Load vs Ram Travel from Tinius-Olsen Tensile Machine

This was always evident at the beginning of the extrusion and when the interface passed through the die. This phenomenon, not being of particular interest at this point, will be discussed in more detail later on.

In order to arrive at a mean value of the extrusion pressure for each region of the curve, a smooth curve was drawn through the slowly varying region, disregarding the initial peak value. Then by taking the value at the mid-point of this curve, the so-called mean extrusion pressure was determined. It is obvious that some engineering judgment had to be used in arriving at these values, but, as Table III indicates, very good values were obtained.

From this point it was a simple matter to arrive at K for each region and ultimately obtain $K_1/K_2$.

## C. Determination of Extrusion Defect Area

The photographs shown in Appendix A clearly show the interface between the two extruded billets and the object now was to determine just what parameter would be used to classify the defect. Not knowing how the information would finally be used, it was decided to get as much information as possible from the photographs. Figure 15 is a typical example of an interface and shows the points and areas under consideration.

By using a calibrated planimeter, the area acbf was determined from the photograph. Since all the photographs were made to varying scales, these areas had to be multiplied by the area magnification of each photograph. This factor was arrived at by measuring the line de in both the photograph and the sample. By taking the squared ratio of these numbers, the area multiplication factor was determined. Then, by

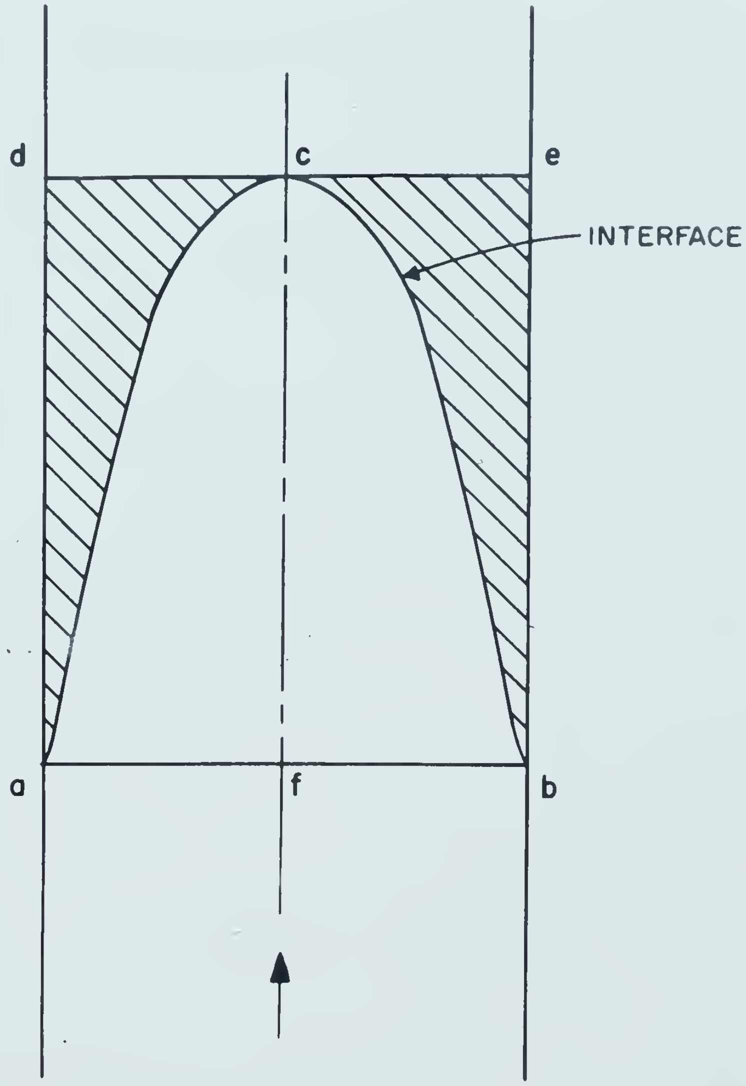

FIGURE 15

Parameters Used for Analyzing Extrusion Defects

dividing the area of *acbf* of the photograph by this factor, the actual area of the sample for *acbf* was determined. See Table II.

It was also felt that the area *acd* plus *ceb* was of importance and so the line *cf* was measured, multiplied by line *de*, and divided by the area multiplication factor. This determined area *adeb* and from this area was subtracted the already known area *acbf*, giving area *acd* plus *ceb*.

Unfortunately, not all the interfaces were symmetrical about the centerline, and in these cases the line *ab* was drawn, connecting the points where the interface terminated at the outer edge. Point *f* was the mid-point of line *ab*. Line *de* was drawn through point *c* and perpendicular to the centerline of the extrusion. Results of these calculations are also shown in Table II.

## TABLE II

## EXTRUSION EXPERIMENTAL DATA

| Extrusion Number | Extrusion Pressure First Metal (PSI) | Extrusion Pressure Second Metal (PSI) | $K_1$ (PSI) | $K_2$ (PSI) | $K_1/K_2$ | Cross-Sectional Area of Defect (Sq. In.) | Length of Defect x Diameter (Sq. In.) | Difference (sq. In.) | Key |
|---|---|---|---|---|---|---|---|---|---|
| 1 | 8040 | 8500 | 5800 | 6130 | .947 | .0393 | .0925 | .0572 | E |
| 2 | 16530 | 15400 | 11920 | 11100 | 1.072 | .0968 | .1545 | .0577 | D |
| 3 | 9180 | 15400 | 6630 | 11100 | .598 | .0222 | .0316 | .0094 | A |
| 4 | 14480 | 8380 | 10440 | 6050 | 1.728 | .0534 | .1197 | .0663 | I |
| 5 | 13590 | 12100 | 9810 | 8730 | 1.122 | .0750 | .1340 | .0590 | F |
| 6 | 12690 | 8500 | 9160 | 6130 | 1.494 | .0397 | .0743 | .0346 | H |
| 7 | 8490 | 12920 | 6450 | 9330 | .692 | .0227 | .0338 | .0111 | B |
| 8 | 16650 | 12920 | 12020 | 9330 | 1.288 | .1088 | .1590 | .0502 | G |
| 9 | 12800 | 14270 | 9240 | 10290 | .898 | .0557 | .0923 | .0423 | C |
| 10 | 12680 | 11540 | 5780 | 5260 | 1.100 | .1535 | .2490 | .0955 | E |
| 11 | 21750 | 20150 | 9910 | 9170 | 1.080 | .0957 | .1625 | .0668 | F |
| 12 | 24900 | 22100 | 11330 | 10050 | 1.127 | .1437 | .2650 | .1213 | D |
| 13 | 21900 | 13000 | 9970 | 5290 | 1.685 | .1805 | .3430 | .1625 | H |

## TABLE II (Continued)

| Extrusion Number | Extrusion Pressure First Metal (PSI) | Extrusion Pressure Second Metal (PSI) | $K_1$ (PSI) | $K_2$ (PSI) | $K_1/K_2$ | Cross-Sectional Area of Defect (Sq. In.) | Length of Defect x Diameter (Sq. In.) | Difference (Sq. In.) | Key |
|---|---|---|---|---|---|---|---|---|---|
| 14 | 24700 | 12450 | 11240 | 5670 | 1.985 | .1430 | .2320 | .0890 | I |
| 15 | 13600 | 18450 | 6190 | 8380 | .738 | .0745 | .1075 | .0330 | B |
| 16 | 23750 | 19000 | 10820 | 8650 | 1.253 | .1605 | .2520 | .0915 | G |
| 17 | 13600 | 21900 | 6190 | 9970 | .622 | .0718 | .0907 | .0189 | A |
| 18 | 20650 | 22200 | 9400 | 10100 | .930 | .0853 | .1468 | .0615 | C |
| 19 | 15640 | 14950 | 5650 | 5400 | 1.046 | .0201 | .0668 | .0457 | E |
| 20 | 28300 | 25500 | 10220 | 9210 | 1.110 | .1365 | .1800 | .0435 | F |
| 21 | 31150 | 30300 | 11250 | 10950 | 1.032 | .1450 | .2550 | .1100 | D |
| 22 | 28300 | 17900 | 10220 | 6460 | 1.585 | .0975 | .2195 | .1220 | H |
| 23 | 33900 | 17650 | 12230 | 6370 | 1.922 | .0540 | .1158 | .0618 | I |
| 24 | 17900 | 24550 | 6470 | 8860 | .730 | .1285 | .1760 | .0475 | B |
| 25 | 31700 | 26500 | 11440 | 9580 | 1.195 | .1980 | .3800 | .1820 | G |
| 26 | 18350 | 28650 | 6620 | 10350 | .638 | .1345 | .1700 | .0355 | A |
| 27 | 28500 | 29100 | 10280 | 10500 | .978 | .1255 | .2050 | .0795 | C |

TABLE II (Continued)

| Extrusion Number | Extrusion Pressure First Metal (PSI) | Extrusion Pressure Second Metal (PSI) | $K_1$ (PSI) | $K_2$ (PSI) | $K_1/K_2$ | Cross-Sectional Area of Defect (Sq. In.) | Length of Defect x Diameter (Sq. In.) | Difference (Sq. In.) | Key |
|---|---|---|---|---|---|---|---|---|---|
| 28 | 19900 | 18350 | 6180 | 5700 | 1.085 | .1005 | .1650 | .0645 | E |
| 29 | 33100 | 31000 | 10270 | 9630 | 1.068 | .3950 | .4640 | .1610 | F |
| 30 | 36700 | 34900 | 11400 | 10850 | 1.052 | .1235 | .2250 | .1015 | D |
| 31 | 31900 | 18350 | 9930 | 5700 | 1.742 | —— | —— | .0760 | H |
| 32 | 40700 | 19000 | 12630 | 5910 | 2.135 | .2600 | .4350 | .1750 | I |
| 33 | 21500 | 29000 | 6680 | 9020 | .742 | .3530 | .4630 | .1100 | B |
| 34 | 37100 | 30700 | 11520 | 9530 | 1.210 | .3150 | .4950 | .1800 | G |
| 35 | 24550 | 37400 | 7630 | 11620 | .657 | .1325 | .2100 | .0775 | A |
| 36 | 36500 | 37100 | 11350 | 11520 | .985 | —— | —— |  | C |
| 37 | 11440 | 9510 | 8270 | 6870 | 1.205 | .0757 | .1165 | .0408 | E |
| 38 | 14720 | 13700 | 10620 | 9890 | 1.075 | .0560 | .0918 | .0350 | F |
| 39 | 15150 | 16540 | 10940 | 11950 | .916 | .0479 | .0700 | .0221 | D |
| 40 | 15850 | 10180 | 11450 | 7350 | 1.558 | .0378 | .0682 | .0304 | H |
| 41 | 18100 | 9510 | 13060 | 6870 | 1.904 | .0564 | .1132 | .0568 | I |

TABLE II (Continued)

| Extrusion Number | Extrusion Pressure First Metal (PSI) | Extrusion Pressure Second Metal (PSI) | $K_1$ (PSI) | $K_2$ (PSI) | $K_1/K_2$ | Cross-Sectional Area of Defect (Sq. In.) | Length of Defect x Diameter (Sq. In.) | Difference (Sq. In.) | Key |
|---|---|---|---|---|---|---|---|---|---|
| 42 | 8380 | 13700 | 6050 | 9890 | .612 | .0189 | .0294 | .0105 | B |
| 43 | 16540 | 14050 | 11950 | 10140 | 1.178 | .0748 | .1146 | .0398 | G |
| 44 | 9970 | 15400 | 7200 | 11120 | .648 | .0248 | .0341 | .0093 | A |
| 45 | 14050 | 16050 | 10140 | 11600 | .874 | .0521 | .0735 | .0214 | C |
| 46 | 8610 | 9510 | 6220 | 6870 | .905 | .0655 | .1056 | .0550 | E |
| 47 | 14720 | 13820 | 10620 | 9980 | 1.063 | .0522 | .0833 | .0311 | F |
| 48 | 17650 | 15400 | 12750 | 11120 | 1.146 | .0799 | .1162 | .0363 | D |
| 49 | 15400 | 9730 | 11120 | 7020 | 1.585 | .0478 | .0838 | .0360 | H |
| 50 | 17900 | 9280 | 12920 | 6700 | 1.930 | .0770 | .1498 | .0728 | I |
| 51 | 10180 | 13820 | 7350 | 9980 | .737 | .0265 | .0395 | .0130 | B |
| 52 | 16540 | 13820 | 11950 | 9980 | 1.197 | .0730 | .1272 | .0542 | G |
| 53 | 9850 | 15150 | 7100 | 10920 | .650 | .0289 | .0417 | .0128 | A |
| 54 | 13350 | 14150 | 9640 | 10220 | .944 | .0647 | .0937 | .0290 | C |
| 55 | 9730 | 8830 | 7020 | 6370 | 1.100 | .0714 | .1357 | .0643 | E |

## TABLE II (Continued)

| Extrusion Number | Extrusion Pressure First Metal (PSI) | Extrusion Pressure Second Metal (PSI) | $K_1$ (PSI) | $K_2$ (PSI) | $K_1/K_2$ | Cross-Sectional Area of Defect (Sq. In.) | Length of Defect x Diameter (Sq. In.) | Difference (Sq. In.) | Key |
|---|---|---|---|---|---|---|---|---|---|
| 56 | 13350 | 13590 | 9640 | 9820 | .983 | .0519 | .0823 | .0304 | F |
| 57 | 16420 | 16300 | 11850 | 11750 | 1.008 | .0603 | .0915 | .0312 | D |
| 58 | 15050 | 9280 | 10860 | 6700 | 1.620 | .0366 | .0715 | .0349 | H |
| 59 | 17900 | 9280 | 12920 | 6700 | 1.930 | .0715 | .1220 | .0505 | I |
| 60 | 8040 | 14350 | 5820 | 10350 | .562 | .0115 | .0170 | .0055 | B |
| 61 | 17750 | 13900 | 12820 | 10040 | 1.275 | .1175 | .1785 | .0610 | G |
| 62 | 10950 | 17200 | 7900 | 12420 | .637 | .0220 | .0309 | .0089 | A |
| 63 | 15500 | 15850 | 11180 | 11430 | .979 | .0379 | .0565 | .0186 | C |
| 64 | 15850 | 14500 | 7220 | 6600 | 1.092 | .1285 | .2130 | .0845 | E |
| 65 | 21900 | 20600 | 9950 | 9370 | 1.063 | .0624 | .1329 | .0705 | F |
| 66 | 25850 | 25100 | 11750 | 11400 | 1.032 | .1015 | .1748 | .0733 | D |
| 67 | 23300 | 14050 | 10600 | 6390 | 1.658 | .0858 | .1236 | .0378 | H |
| 68 | 26400 | 13480 | 12000 | 6130 | 1.958 | .1305 | .1426 | .0121 | I |
| 69 | 13040 | 19000 | 5930 | 8640 | .687 | .0081 | .0114 | .0033 | B |

TABLE II (Continued)

| Extrusion Number | Extrusion Pressure First Metal (PSI) | Extrusion Pressure Second Metal (PSI) | $K_1$ (PSI) | $K_2$ (PSI) | $K_1/K_2$ | Cross-Sectional Area of Defect (Sq. In.) | Length of Defect x Diameter (Sq. In.) | Difference (Sq. In.) | Key |
|---|---|---|---|---|---|---|---|---|---|
| 70 | 23900 | 19800 | 10850 | 9000 | 1.207 | .1338 | .1905 | .0567 | G |
| 71 | 14040 | 23100 | 6380 | 10500 | .608 | .0103 | .0138 | .0035 | A |
| 72 | 20600 | 21850 | 9380 | 9930 | .943 | .0765 | .1090 | .0325 | C |
| 73 | 17100 | 15250 | 6180 | 5520 | 1.123 | .0418 | .0827 | .0409 | E |
| 74 | 27400 | 25400 | 9900 | 9180 | 1.078 | .0600 | .0950 | .0350 | F |
| 75 | 38500 | 36500 | 13900 | 13180 | 1.055 | .0279 | .0610 | .0331 | D |
| 76 | 34200 | 17450 | 12350 | 6300 | 1.962 | .1515 | .2770 | .1255 | H |
| 77 | 37200 | 17200 | 13420 | 6220 | 2.160 | .1475 | .2960 | .1485 | I |
| 78 | 21500 | 28100 | 7770 | 10150 | .766 | .1345 | .1520 | .0175 | B |
| 79 | 29800 | 25200 | 10750 | 9080 | 1.182 | .0702 | .0967 | .0265 | G |
| 80 | 21700 | 35100 | 7830 | 12650 | .619 | .0042 | .0062 | .0020 | A |
| 81 | 37400 | 36500 | 13500 | 13200 | 1.023 | .0763 | .0945 | .0185 | C |
| 82 | 19800 | 17950 | 6150 | 5580 | 1.100 | .0138 | .0208 | .0070 | E |
| 83 | 31300 | 29900 | 9730 | 9280 | 1.048 | .0798 | .1165 | .0367 | F |
| 84 | 37900 | 35500 | 11750 | 11050 | 1.050 | .1065 | .1685 | .0380 | D |

TABLE II (Continued)

| Extrusion Number | Extrusion Pressure First Metal (PSI) | Extrusion Pressure Second Metal (PSI) | $K_1$ (PSI) | $K_2$ (PSI) | $K_1/K_2$ | Cross-Sectional Area of Defect (Sq. In.) | Length of Defect x Diameter (Sq. In.) | Difference (Sq. In.) | Key |
|---|---|---|---|---|---|---|---|---|---|
| 85 | 29200 | 19350 | 9080 | 6020 | 1.510 | .1075 | .1845 | .0770 | H |
| 86 | 38900 | 18550 | 12050 | 5770 | 2.090 | .1368 | .2660 | .1292 | I |
| 87 | 21050 | 31500 | 6540 | 9780 | .668 | .0196 | .0217 | .0021 | B |
| 88 | 37000 | 29200 | 11480 | 9080 | 1.267 | .2590 | .3370 | .0780 | G |
| 89 | 20900 | 34400 | 6500 | 10680 | .609 | .0025 | .0055 | .0030 | A |
| 90 | 31000 | 34700 | 9630 | 10780 | .895 | 0 | 0 | 0 | C |
| 91 | 12900 | 11550 | 5870 | 5250 | 1.117 | .0469 | .0713 | .0244 | E |
| 92 | 20800 | 20800 | 9460 | 9460 | 1.000 | .0318 | .0540 | .0222 | F |
| 93 | 23450 | 23100 | 10670 | 10500 | 1.015 | .0492 | .0647 | .0155 | D |
| 94 | 18800 | 12450 | 8550 | 5660 | 1.513 | .0940 | .1785 | .0845 | H |
| 95 | 22400 | 12650 | 10180 | 5750 | 1.773 | .0993 | .1720 | .0727 | I |
| 96 | 12250 | 18800 | 5580 | 8550 | .654 | .0612 | .0727 | .0115 | B |
| 97 | 22650 | 20100 | 10300 | 9140 | 1.128 | .0483 | .0800 | .0317 | G |
| 98 | 12900 | 21050 | 5870 | 9580 | .613 | .0568 | .0788 | .0220 | A |
| 99 | 20000 | 21700 | 9100 | 9880 | .921 | .0583 | .0932 | .0349 | C |

TABLE II (Continued)

| Extrusion Number | Extrusion Pressure First Metal (PSI) | Extrusion Pressure Second Metal (PSI) | $K_1$ (PSI) | $K_2$ (PSI) | $K_1/K_2$ | Cross-Sectional Area of Defect (Sq. In.) | Length of Defect x Diameter (Sq. In.) | Difference (Sq. In.) | Key |
|---|---|---|---|---|---|---|---|---|---|
| 100 | 19900 | 16550 | 7190 | 5980 | 1.200 | .1160 | .1710 | .0550 | E |
| 101 | 32650 | 25700 | 11800 | 9280 | 1.270 | .0755 | .1480 | .0725 | F |
| 102 | 39000 | 33500 | 14080 | 12100 | 1.165 | .1320 | .2590 | .1270 | D |
| 103 | 24300 | 15600 | 8780 | 5630 | 1.560 | .1330 | .2650 | .1320 | H |
| 104 | 27900 | 17100 | 10060 | 6180 | 1.625 | .1362 | .2715 | .1353 | I |
| 105 | 17200 | 24200 | 6220 | 8740 | .712 | .0456 | .0662 | .0206 | B |
| 106 | 38700 | 26900 | 13950 | 9720 | 1.435 | .0715 | .1245 | .0530 | G |
| 107 | 16100 | 29200 | 5820 | 10550 | .552 | 0 | 0 | 0 | A |
| 108 | 30300 | 31200 | 10940 | 11270 | .972 | .0785 | .1450 | .0665 | C |
| 109 | 19850 | 19250 | 6170 | 5980 | 1.030 | .0162 | .0200 | .0038 | E |
| 110 | 38300 | 32800 | 11900 | 10180 | 1.168 | .1240 | .2440 | .1200 | F |
| 111 | 37100 | 35100 | 11530 | 10900 | 1.058 | .0818 | .0430 | .0388 | D |
| 112 | 38300 | 19950 | 11880 | 6200 | 1.915 | .0277 | .0414 | .0137 | H |
| 113 | 35300 | 19450 | 10960 | 6040 | 1.815 | 0 | 0 | 0 | I |
| 114 | 20600 | 28800 | 6400 | 8950 | .716 | .1180 | .1860 | .0680 | B |

TABLE II (Continued)

| Extrusion Number | Extrusion Pressure First Metal (PSI) | Extrusion Pressure Second Metal (PSI) | $K_1$ (PSI) | $K_2$ (PSI) | $K_1/K_2$ | Cross-Sectional Area of Defect (Sq. In.) | Length of Defect x Diameter (Sq. In.) | Difference (Sq. In.) | Key |
|---|---|---|---|---|---|---|---|---|---|
| 115 | 38500 | 30800 | 11950 | 9570 | 1.250 | .4550 | .6060 | .1510 | G |
| 116 | 19350 | 34900 | 6020 | 10830 | .555 | .0041 | .0064 | .0023 | A |
| 117 | 36100 | 34700 | 11220 | 10780 | 1.042 | .4240 | .5950 | .1710 | C |
| 118 | 12450 | 12450 | 5660 | 5660 | 1.000 | .0418 | .0619 | .0201 | E |
| 119 | 19100 | 21050 | 8680 | 9580 | .907 | .0139 | .0203 | .0064 | F |
| 120 | 23200 | 23000 | 10550 | 10450 | 1.010 | .0693 | .1095 | .0402 | D |
| 121 | 19500 | 12450 | 8880 | 5660 | 1.570 | .0454 | .0683 | .0429 | H |
| 122 | 23200 | 11550 | 10550 | 5250 | 2.010 | .0825 | .1625 | .0800 | I |
| 123 | 12450 | 19950 | 5660 | 9070 | .625 | .0076 | .0098 | .0022 | B |
| 124 | 24300 | 19050 | 11040 | 8660 | 1.275 | .1225 | .1872 | .0647 | G |
| 125 | 11550 | 22500 | 5250 | 10220 | .513 | .0278 | .0365 | .0087 | A |
| 126 | 19450 | 24000 | 8850 | 10900 | .812 | .0379 | .0537 | .0158 | C |
| 127 | 15600 | 16200 | 5630 | 5850 | .965 | .0044 | .0081 | .0037 | E |
| 128 | 29000 | 26500 | 10450 | 9580 | 1.090 | .0393 | .0643 | .0250 | F |
| 129 | 31300 | 30000 | 11300 | 10850 | 1.041 | .1061 | .1650 | .0390 | D |

TABLE II (Continued)

| Extrusion Number | Extrusion Pressure First Metal (PSI) | Extrusion Pressure Second Metal (PSI) | $K_1$ (PSI) | $K_2$ (PSI) | $K_1/K_2$ | Cross-Sectional Area of Defect (Sq. In.) | Length of Defect x Diameter (Sq. In.) | Difference (Sq. In.) | Key |
|---|---|---|---|---|---|---|---|---|---|
| 130 | 24200 | 15150 | 8730 | 5570 | 1.570 | .0199 | .0427 | .0228 | H |
| 131 | 31300 | 14800 | 11300 | 5350 | 2.110 | .1372 | .2570 | .1198 | I |
| 132 | 15400 | 24600 | 5560 | 8880 | .627 | .0932 | .1100 | .0177 | B |
| 133 | 31500 | 24900 | 11350 | 9000 | 1.262 | .1556 | .2475 | .0919 | G |
| 134 | 15600 | 32500 | 5640 | 11150 | .508 | .0059 | .0072 | .0013 | A |
| 135 | 26300 | 30700 | 9500 | 11100 | .858 | .0767 | .1063 | .0296 | C |
| 136 | 19250 | 18900 | 5980 | 5880 | 1.017 | .0122 | .0235 | .0113 | E |
| 137 | 34500 | 29500 | 10720 | 9160 | 1.170 | .0757 | .1475 | .0718 | F |
| 138 | 37500 | 35400 | 11650 | 11000 | 1.060 | .0691 | .0820 | .0129 | D |
| 139 | 31000 | 19050 | 9650 | 5920 | 1.630 | .1645 | .2970 | .1325 | H |
| 140 | 37500 | 17900 | 11650 | 5560 | 2.095 | .2430 | .4180 | .1750 | I |
| 141 | 19450 | 29850 | 6030 | 9250 | .652 | 0 | 0 | 0 | B |
| 142 | 37800 | 28500 | 11750 | 8850 | 1.325 | .2075 | .3770 | .1695 | G |
| 143 | 18350 | 36500 | 5700 | 11350 | .502 | .0032 | .0042 | .0010 | A |
| 144 | 30800 | 34700 | 9580 | 10850 | .883 | .1425 | .1850 | .0425 | C |

# VI. RESULTS AND DISCUSSION OF RESULTS

## A. Normalized Extrusion Defects (Figures 16 - 28)

From the negatives obtained in photographing the etched interfaces, a normalized interface was drawn, using a photographic enlarger. On a piece of white paper a one inch line was drawn and the enlarger magnification was so adjusted as to make the diameter of the extrusion at the interface coincide with this drawn line. A pencil sketch was then made of the interface. Thus, all 144 samples were normalized, as it were, to a common one inch base. In redrawing the grouped sketches shown in the figures, a free hand was taken in making the interfaces symmetrical about the centerline, since very few of the samples were truly symmetrical.

In the grouping of the normalized defects, it was planned to group first of all, all those extrusions in which the metal compositions were identical. Thus in Figure 16-a is seen only those cases where pure lead was pushing pure lead for a particular extrusion ratio of 4. The only variation in Figure 16-a, and all the subsequent figures, is the presst cone angle. The numbers inside the parenthesis indicate this angle and those numbers outside indicate the extrusion number tabulated in Table I.

Figures 16 - 18 are all at an extrusion ratio of 4, whereas Figures 19 - 22 are at an extrusion ratio of 9. This pattern continues throughout the remainder of the figures.

In analyzing these curves one must bear in mind that as the defect curve approaches the outer edge in many cases it becomes parallel to this edge and the determination of the cut off point is almost impossible. For this reason, it is wise to utilize two parameters, or in effect, to observe two characteristics of the curves. The most important thing to

observe is the overall shape of the curve, especially the region near the vertex, and secondly the relative heights, or as is commonly referred to as the defect length. Recall that these curves are normalized and that comparison of height will have no justification between varying extrusion ratios. In the early stages of the experiment it was thought that the included angle at the vertex would lend itself as a convenient parameter but these figures show that little or no information would be gained from this point of view.

It might be well to mention at this point that the area included under these curves is not the so-called defect area as determined in Table II and used subsequently for analysis. Recall that the defect area is the shaded portion as shown in Figure 15.

Certain basis results are evident from these curves. This information, in itself, is not profound but merely agrees with generally well-known characteristics of the extrusions.

1. As the extrusion ratio increases, other variables being fixed, the defect length increases.

2. As the extrusion ratio increases, other variables being fixed, the interface vertex angle becomes more acute.

3. Generally, but not in all cases, as the preshaped cone angle is increased from the flat interface, the defect becomes less and the vertex becomes flatter.

Other characteristics seem to show certain trends which are either in disagreement with present theory or are not found in present day

references. Briefly mentioned below are these trends which will be analyzed further using defect area parameter:

1. For a given extrusion ratio and cone angle, as the $K_1/K_2$ ratio is initially increased, there is a steady increase to the defect length, however as the $K_1/K_2$ ratio exceeds unity and extends out to about 1.5, there is a sharp drop in the defect length. After this drop, with the $K_1/K_2$ ratio increasing still further, the defect length increases still further.

2. For low extrusion ratios, variation in angle or metal composition shows little effect on the extrusion defect length or shape of the vertex. At high extrusion ratios, small variations in any variable produce tremendous changes in the shape of the defect.

3. Formation of voids, which will be covered separately.

4. The formation of reverses or "dimples" in the interface occurred with equal probability at cone angles of 10° and 15° and did not occur at 0° and 5°.

5. Increasing the cone angle did not necessarily reduce the defect.

6. No simple rule existed which would allow one to preduct interface shapes.

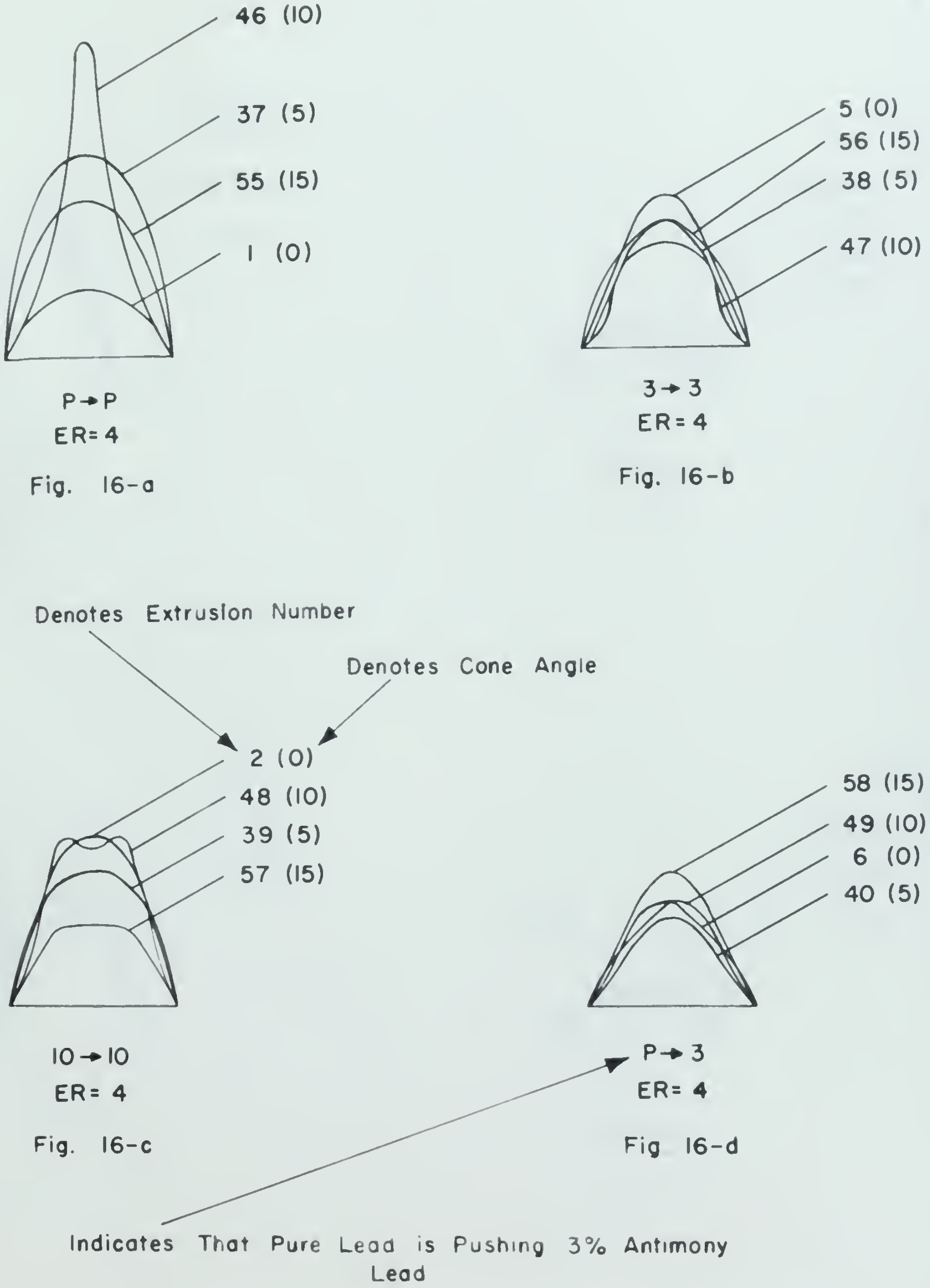

P → P
ER = 4

Fig. 16-a

3 → 3
ER = 4

Fig. 16-b

Denotes Extrusion Number

Denotes Cone Angle

10 → 10
ER = 4

Fig. 16-c

P → 3
ER = 4

Fig 16-d

Indicates That Pure Lead is Pushing 3% Antimony Lead

Extrusion Defects Normalized to Common Base

Figure 16

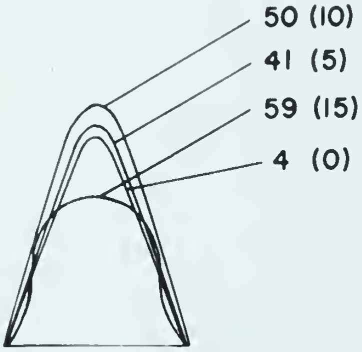

P → 10
ER = 4

Fig. 17-a

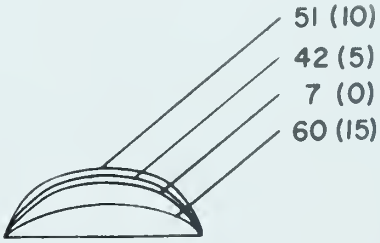

3 → P
ER = 4

Fig. 17-b

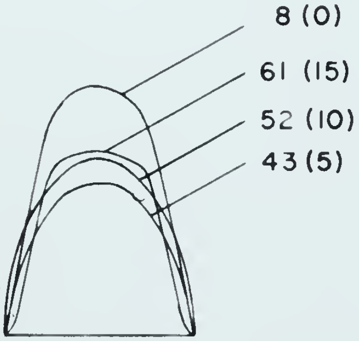

3 → 10
ER = 4

Fig. 17-c

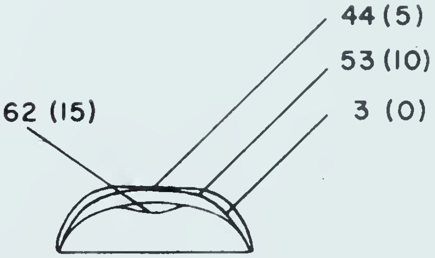

10 → P
ER = 4

Fig. 17-d

Extrusion Defects Normalized to Common Base

Figure 17

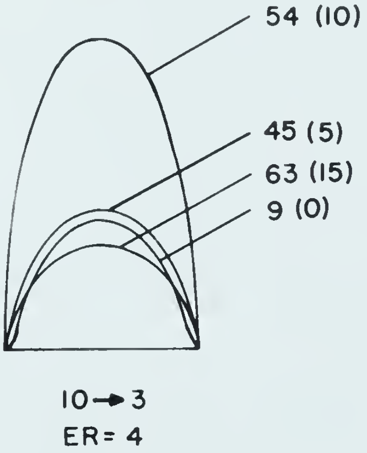

Extrusion Defects Normalized to Common Base

Figure 18

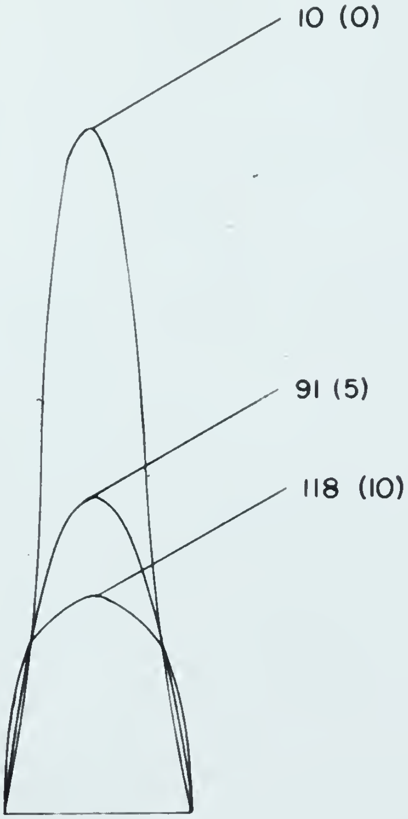

P→P
ER=9

Fig. 19-a

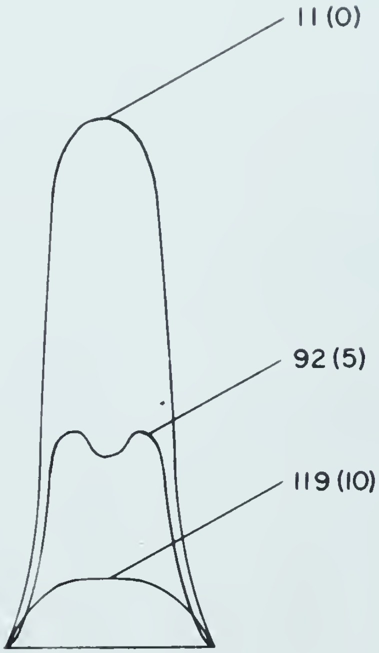

3→3
ER=9

Fig. 19-b

Extrusion Defects Normalized to Common Base

Figure 19

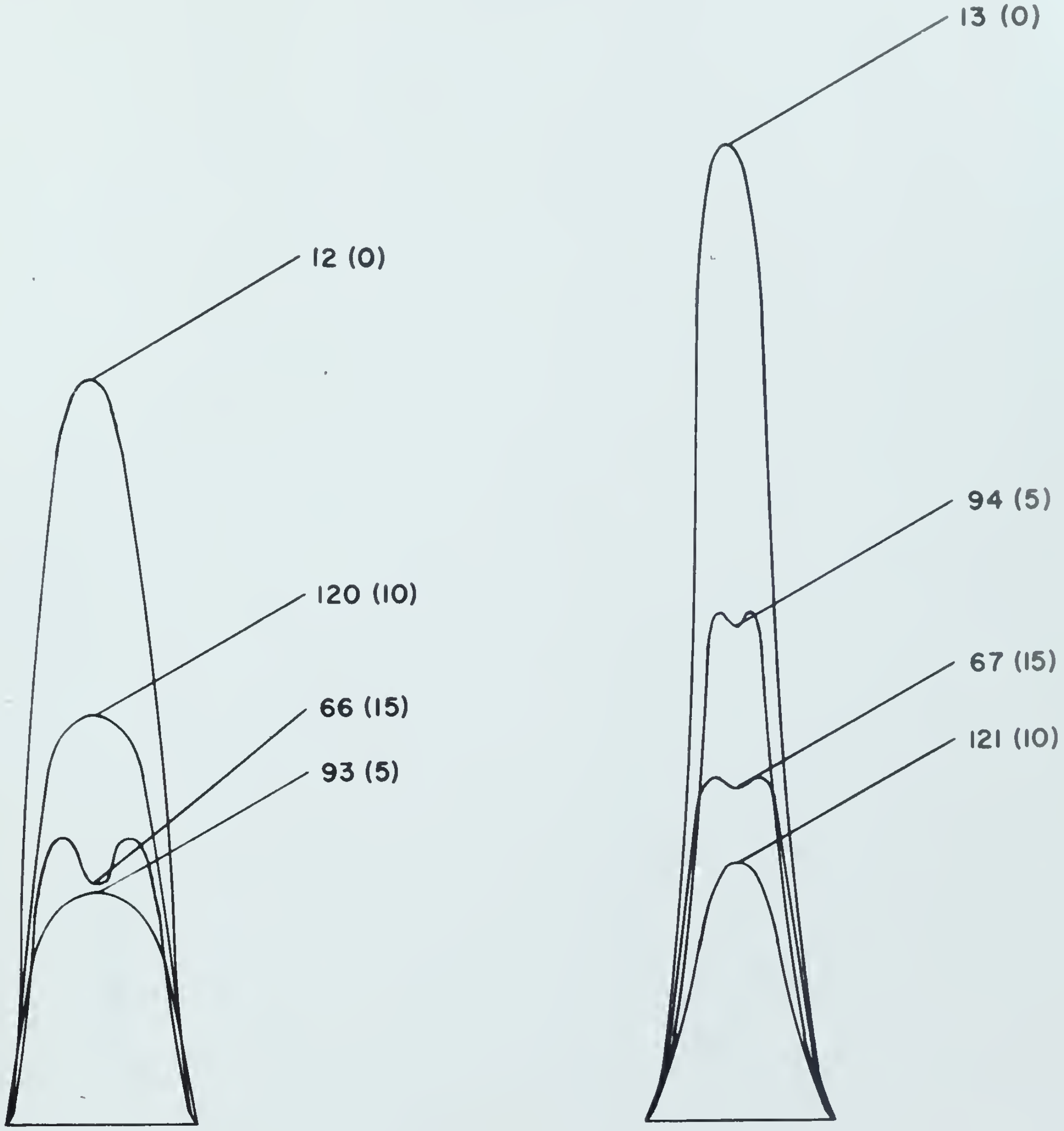

10→10
ER= 9

Fig. 20-a

P→3
ER=9

Fig. 20-b

Extrusion Defects Normalized to Common Base

Figure 20

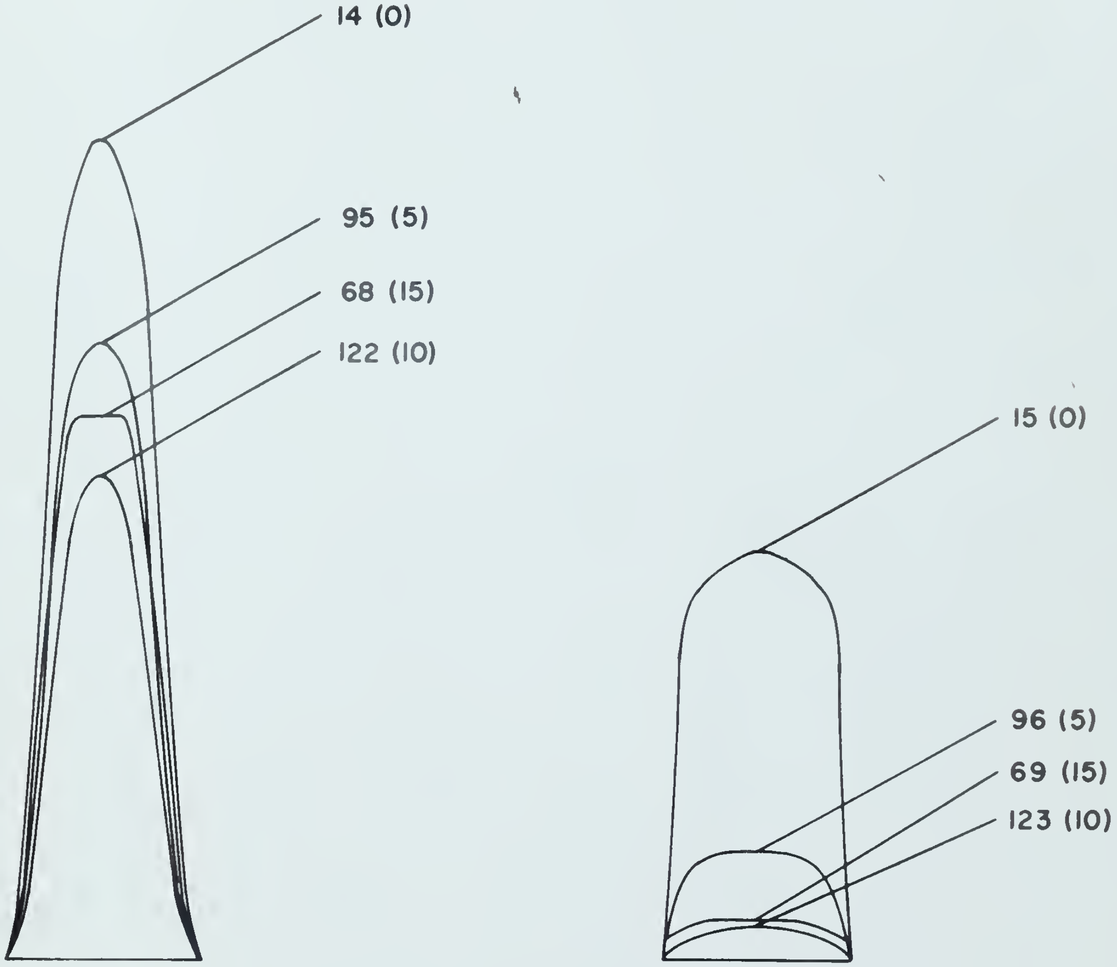

P→10
ER=9

Fig. 21–a

3→P
ER=9

Fig. 21-b

Extrusion Defects Normalized to Common Base

Figure 21

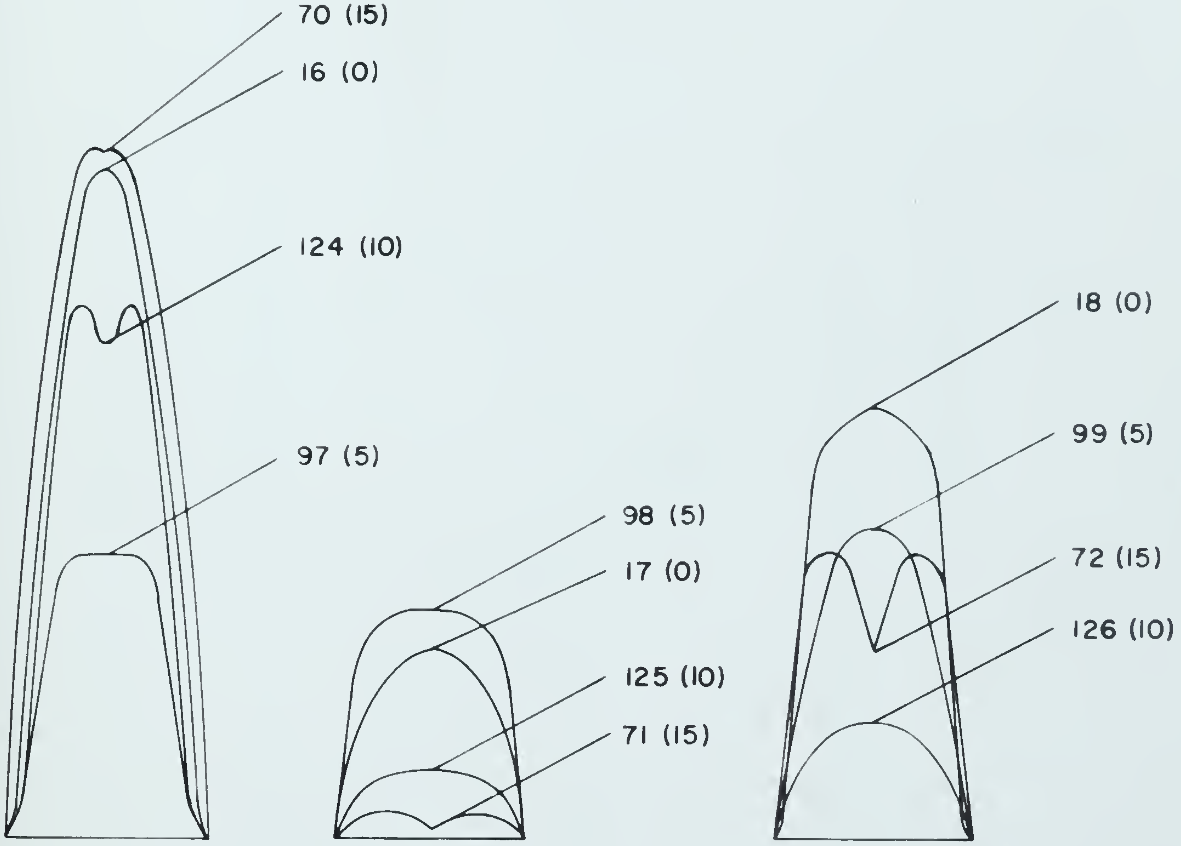

3 → 10
ER = 9

Fig. 22-a

10 → P
ER = 9

Fig. 22-b

10 → 3
ER = 9

Fig. 22-c

Extrusion Defects Normalized to Common Base

Figure 22

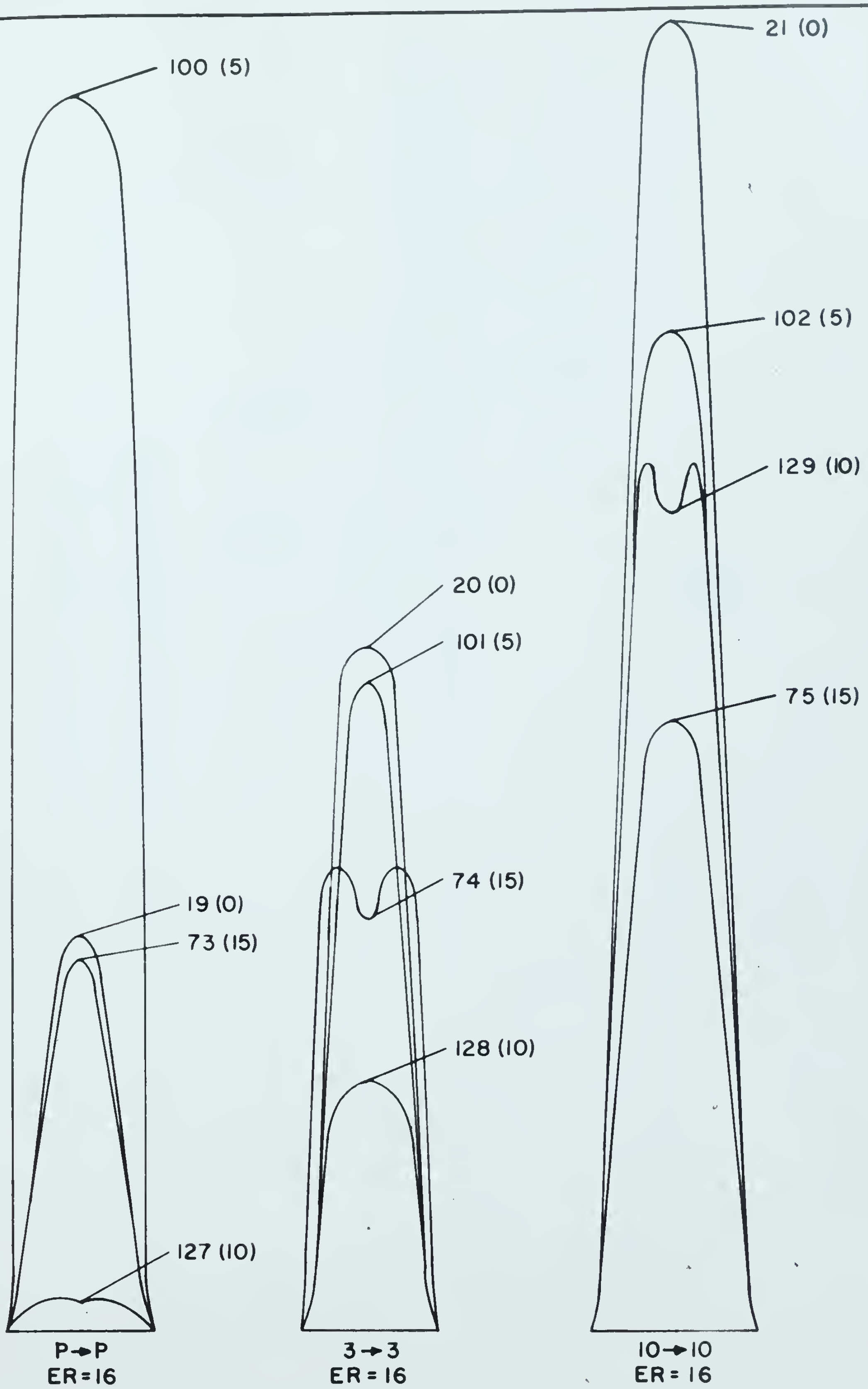

Fig. 23-a Fig. 23-b Fig. 23-c

Figure 23 Extrusion Defects Normalized to Common Base

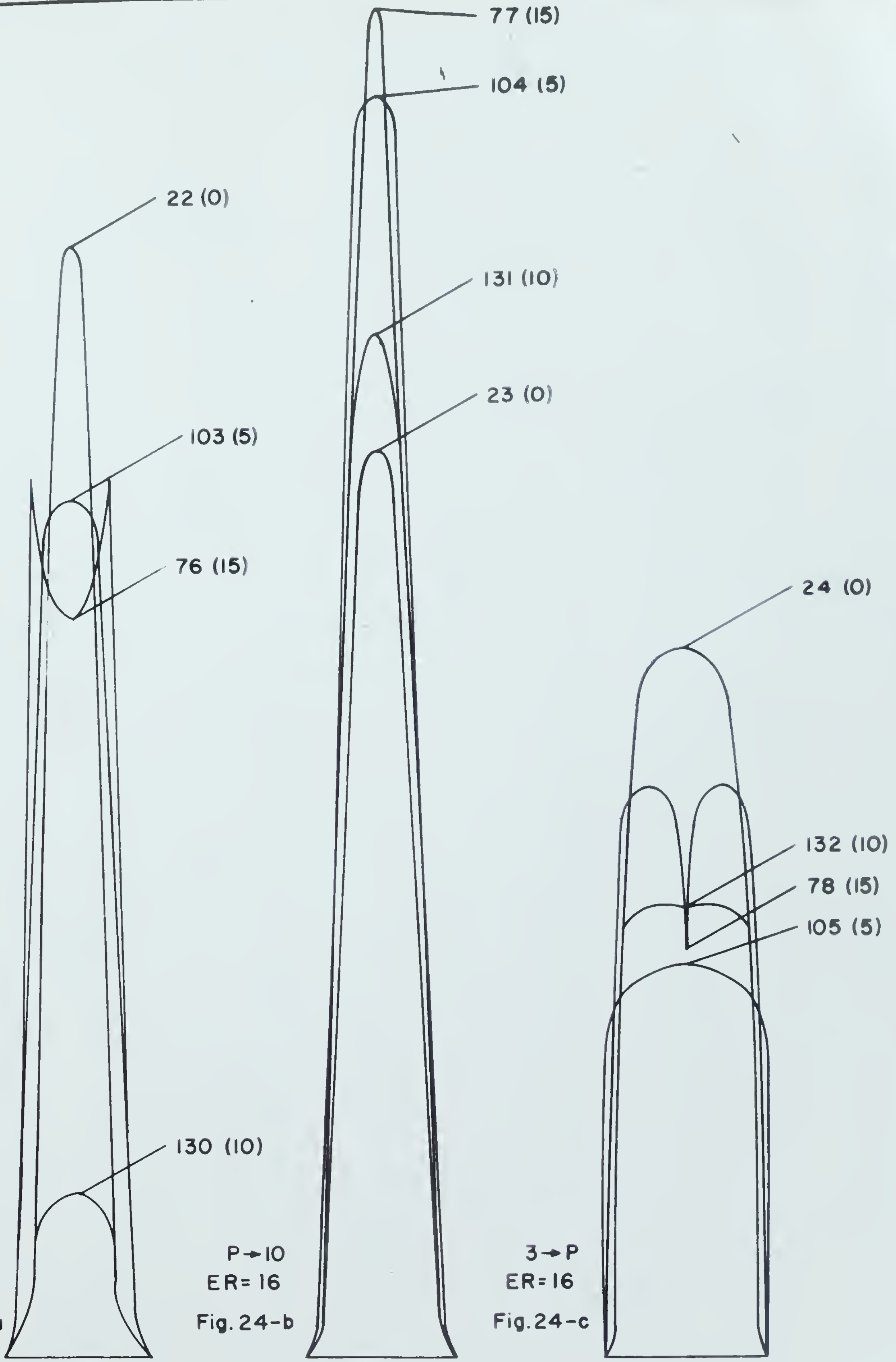

P → 3
ER = 16
Fig. 24-a

P → 10
ER = 16
Fig. 24-b

3 → P
ER = 16
Fig. 24-c

Figure 24 Extrusion Defects Normalized to Common Base

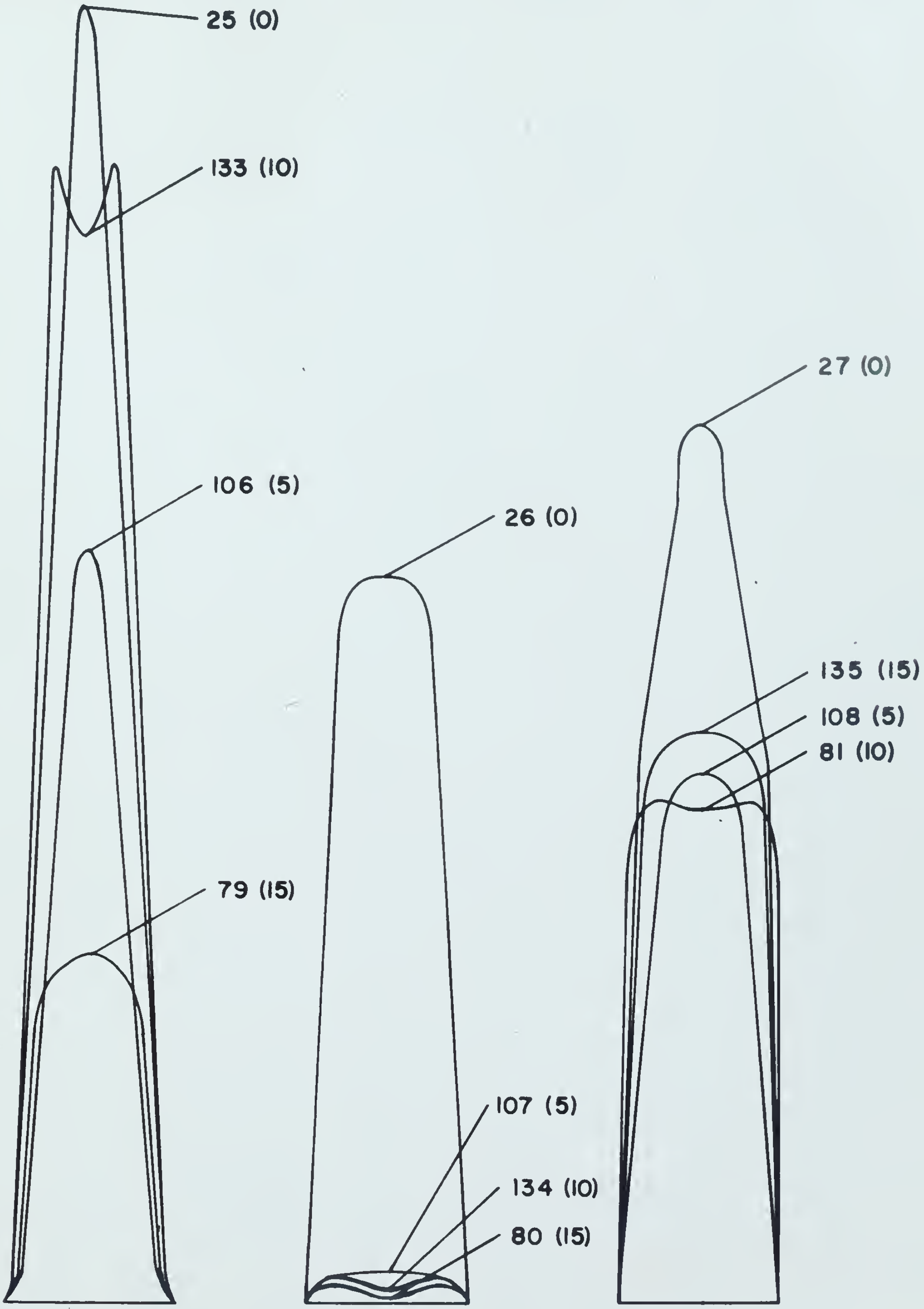

3 → 10
ER = 16
Fig. 25-a

10 → P
ER = 16
Fig. 25-b

10 → 3
ER = 16
Fig. 25-c

Figure 25 Extrusion Defects Normalized to Common Base

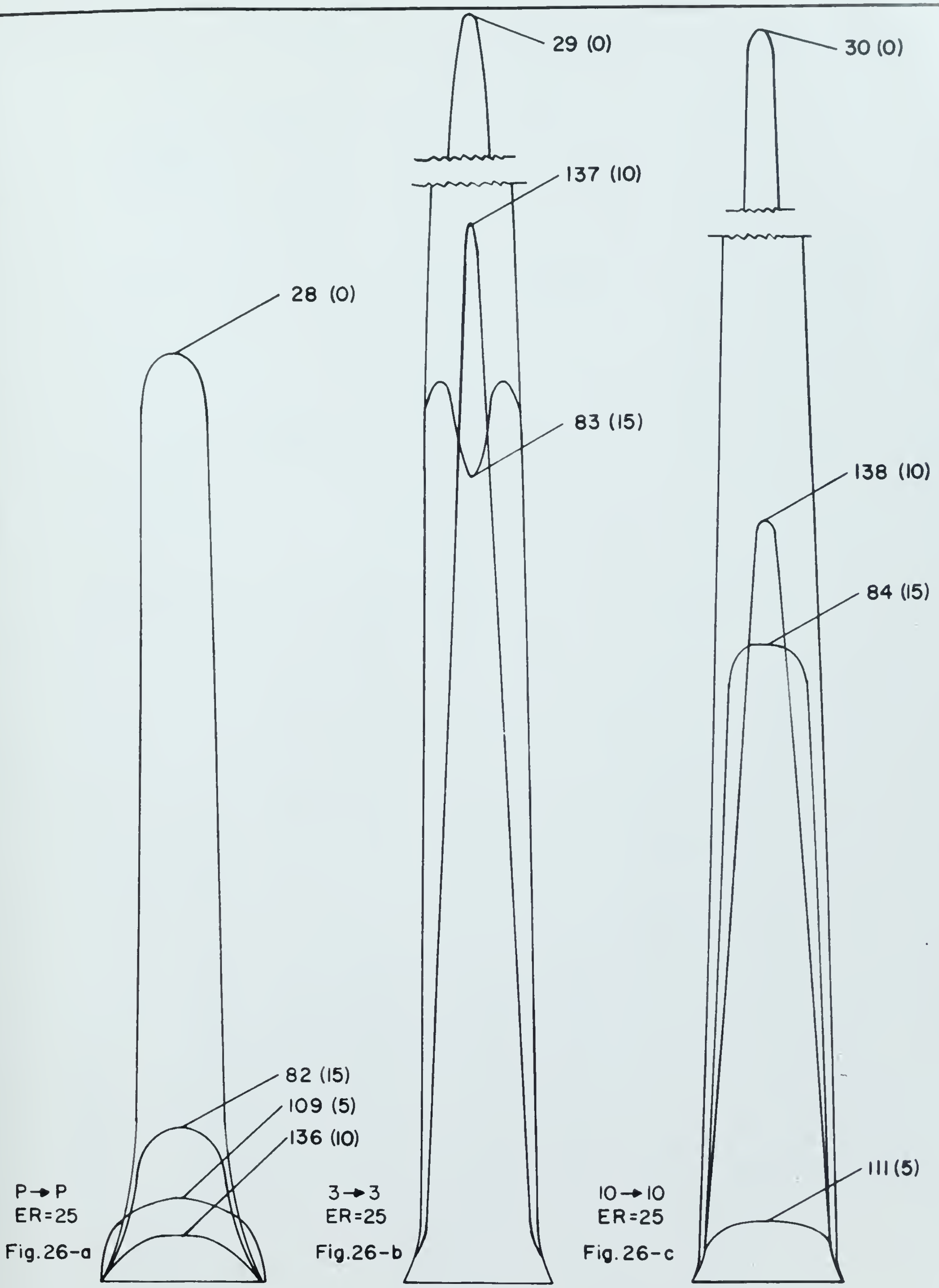

P → P
ER=25
Fig.26-a

3 → 3
ER=25
Fig.26-b

10 → 10
ER=25
Fig.26-c

Figure 26

Extrusion Defects Normalized to Common Base

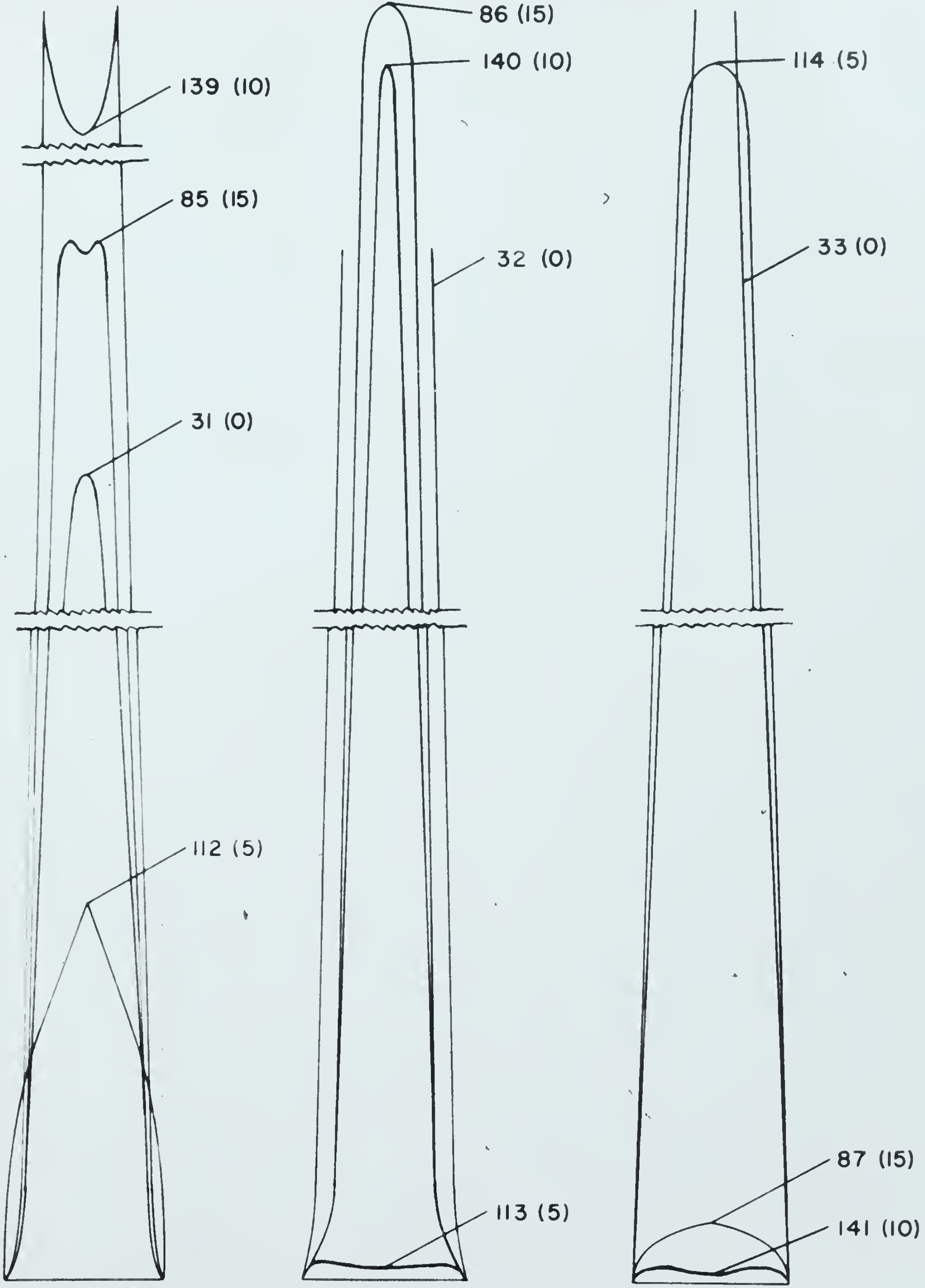

P→3
ER=25
Fig. 27-a

P→10
ER=25
Fig. 27-b

3→P
ER=25
Fig. 27-c

Figure 27 Extrusion Defects Normalized to Common Base

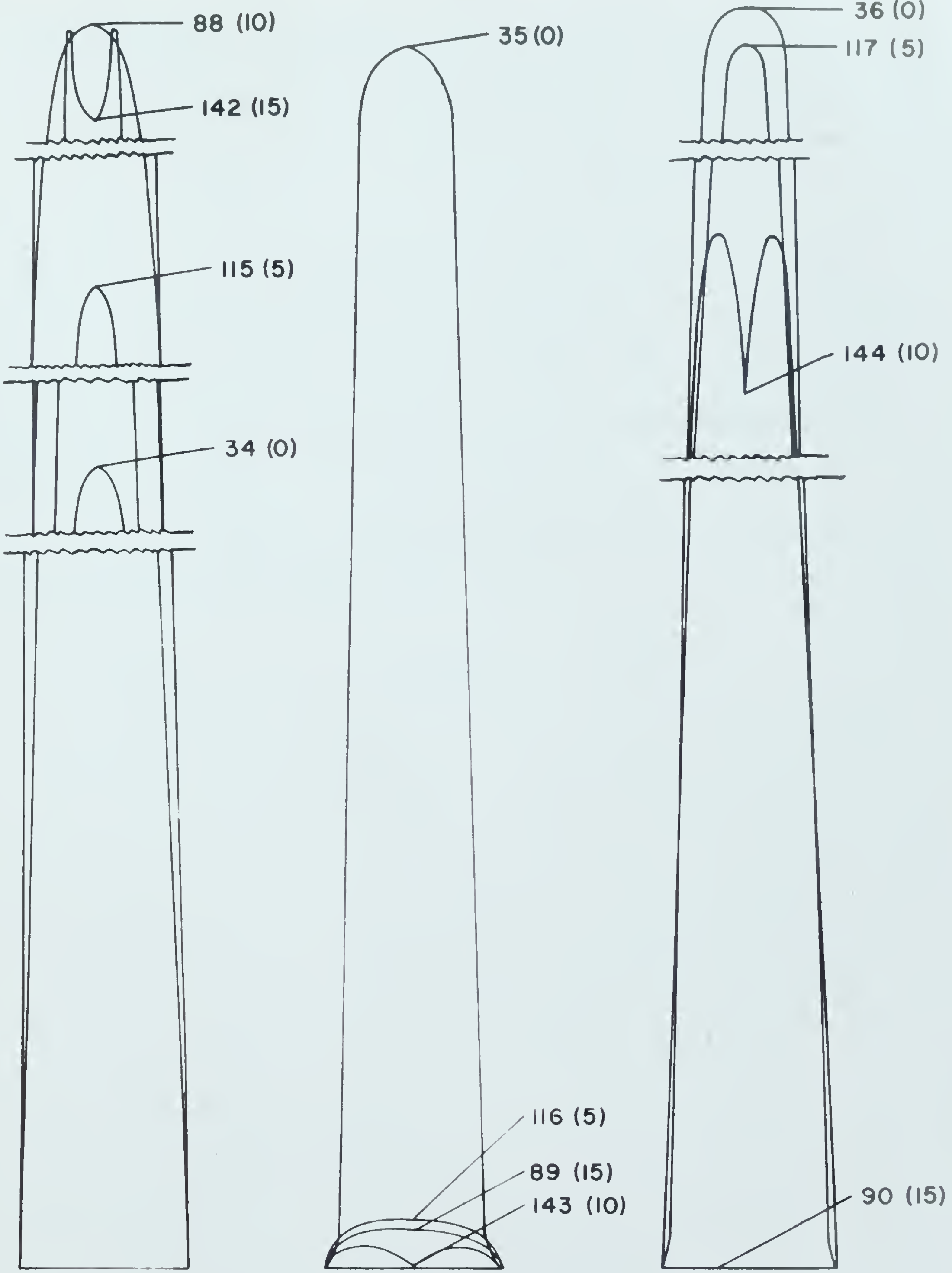

3 → 10
ER=25
Fig. 28–a

10 → P
ER=25
Fig. 28–b

10 → 3
ER=25
Fig. 28–c

Extrusion Defects Normalized to Common Base

Figure 28

## B. Effect of Varying $K_1/K_2$ Ratio (Figures 29 - 36)

Figures 29 - 32 show the effect on the defect area with variation of the $K_1/K_2$ ratio. Information to plot these curves was obtained from Table II.

Since the metal used for each classification came from the same batch and can be assumed to be homogeneous, it might be suspected that the $K_1/K_2$ ratio for all the P- P extrusions, for example, would be the same. This was basically true, but since a particular $K_1/K_2$ value was found for each run, that value was plotted. It was of interest to determine the average value for all the various combinations and the results are shown in Table III.

TABLE III

| TYPE | $K_1/K_2$ | METAL COMBINATION |
|---|---|---|
| A | .596 | 10- P * |
| B | .683 | 3- P |
| C | .934 | 10- 3 |
| D | 1.053 | 10- 10 |
| E | 1.065 | P- P |
| F | 1.081 | 3- 3 |
| G | 1.245 | 3- 10 |
| H | 1.635 | P- 3 |
| I | 1.948 | P- 10 |

*Indicates 10 percent antimony lead pushing pure lead.

The type designation was assigned so that Type A had the lowest $K_1/K_2$ ratio. Of interest is the fact that for Types D, E, and F, the $K_1/K_2$ ratio is slightly above 1.00. This is completely understandable if one recognizes that part of the load registered by the tensile machine is due to the friction between the lead and the cylinder wall. In the beginning the friction is greatest because there is more friction area. As the extrusion continues this area is reduced and consequently the friction is reduced, giving a lower reading for the second billet than the first.

Note also the very good agreement found in Types D, E, and F as to variation in $K_1/K_2$. This would give credence to the values obtained for the other types.

Table IV is a compilation of the extrusion constants (K) for the metals used, depending upon whether it was the first or second billet out of the die. These values agree fairly well with published data, but as was stated earlier, so many other variables enter into the determination of K that before comparisons can be made, the complete picture must be analyzed as to temperature, lubrication, die geometry, and ram speed. Sufficient, however, is the fact that K did remain a constant for this series of experiments.

Referring again to the series of curves plotted in Figures 29 - 32, it will be noted that they are all similar to a modified S-curve. At the low values of $K_1/K_2$, that is, where a hard metal is pushing a soft metal, the defect area is small. Carrying this example to the extreme, assume that the hard metal was steel and that the soft metal were a liquid, say water. It can be visualized that a very small defect would form because

the water, under hydrostatic pressure, with negligible shear, would flow completely out of the die before the steel was extruded. It is true that as the steel was extruded it would not come out flat, but would have a defect. It is this aspect which would restrict one from obtaining a completely flat interface by variation of the $K_1/K_2$ alone. It is still necessary to preshape the billet. This point of view is merely academic, because in dealing with extrusion problems, the selection of $K_1/K_2$ is seldom allowed but rather pre-determined.

TABLE IV

EXTRUSION CONSTANTS (K)

| METAL | EXTRUSION CONSTANTS (PSI) |
|---|---|
| Pure Lead (1st Billet) | 6374 |
| Pure Lead (2nd Billet) | 6032 |
| 3% Antimony (1st Billet) | 10163 |
| 3% Antimony (2nd Billet) | 9347 |
| 10% Antimony (1st Billet) | 11712 |
| 10% Antimony (2nd Billet) | 11011 |

As the ratio of $K_1/K_2$ increases from this low value (less than 1) to values around unity, the curves increase until a maximum is reached which generally lies somewhere between $K_1/K_2 = 1.0$ and 2.0. Herein is

the situation where both metals are of the same hardness. As could be expected in this range, an increase in the extrusion ratio causes an increase in the defect area.

Any further increase in $K_1/K_2$ causes a sharp drop in the defect area which, up to this point, is the most significant aspect noticed. Increasing $K_1/K_2$ still further produces a minimum to the curve after which it again starts to climb and as far as these experiments were concerned, did not reach a plateau or reverse itself again.

The fact that these curves were not smoothly varying curves without maximums or minimums points up the strong dependence of the defect area on the $K_1/K_2$ value. For example, if one has a pre-determined $K_1/K_2$ and extrusion ratio, then one does not know where he might be in relation to the maximum or minimum without having one of these experimental curves available. Basic theory cannot, and does not predict these S-curves.

The minimum values reached were unquestionably noted and repeated themselves to the point of almost certainty. Again going to extreme situation, assume that water is pushing steel and it can be visualized that a large defect would form because again the water acting under hydraulic pressure will exert itself equally on the surface of the steel. As the steel flows out, the central mass is flowing faster than the edge mass and a large defect would develop. Thus, the large defect values found for high $K_1/K_2$ are understandable.

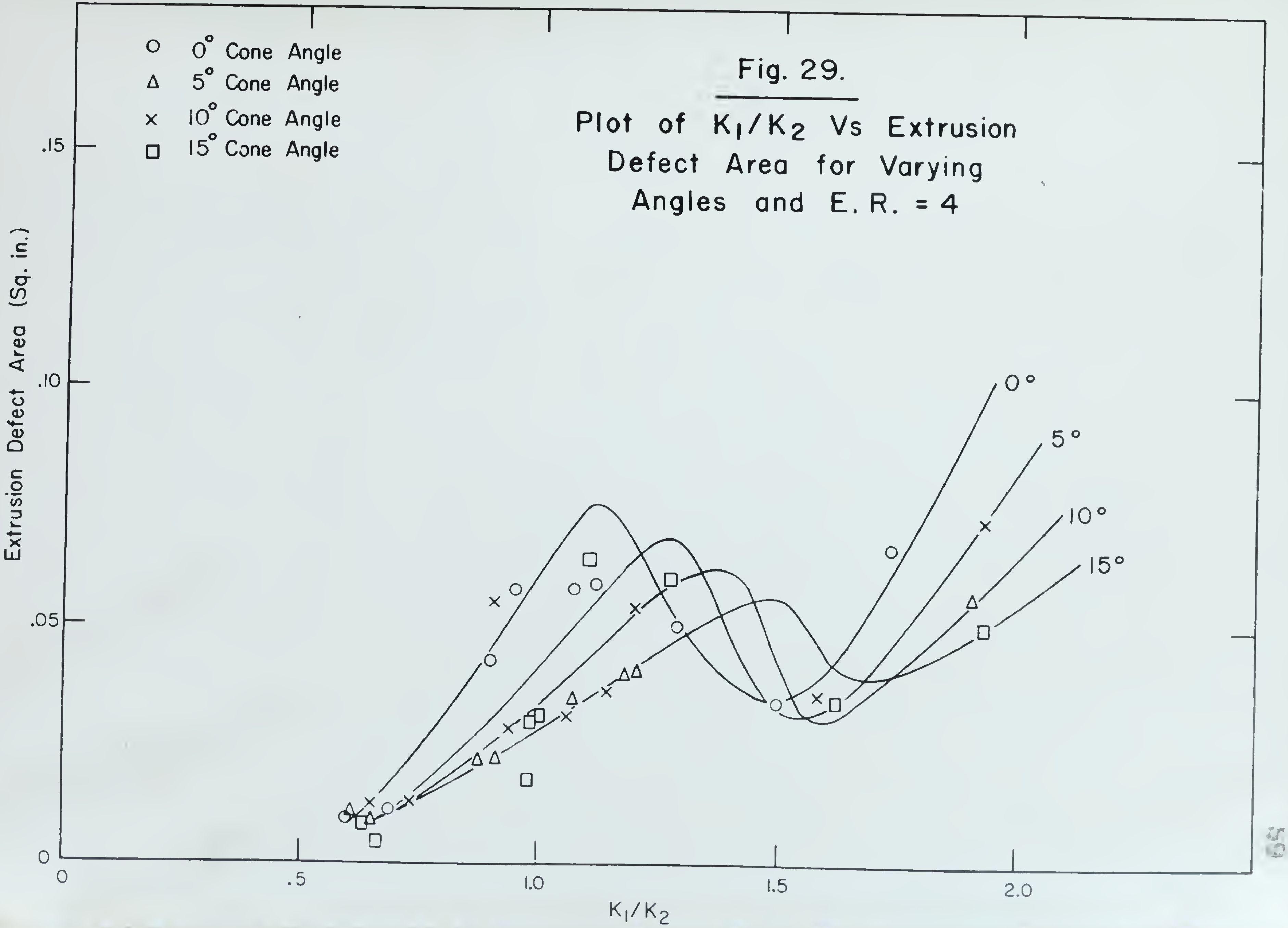

Fig. 29.

Plot of $K_1/K_2$ Vs Extrusion Defect Area for Varying Angles and E. R. = 4

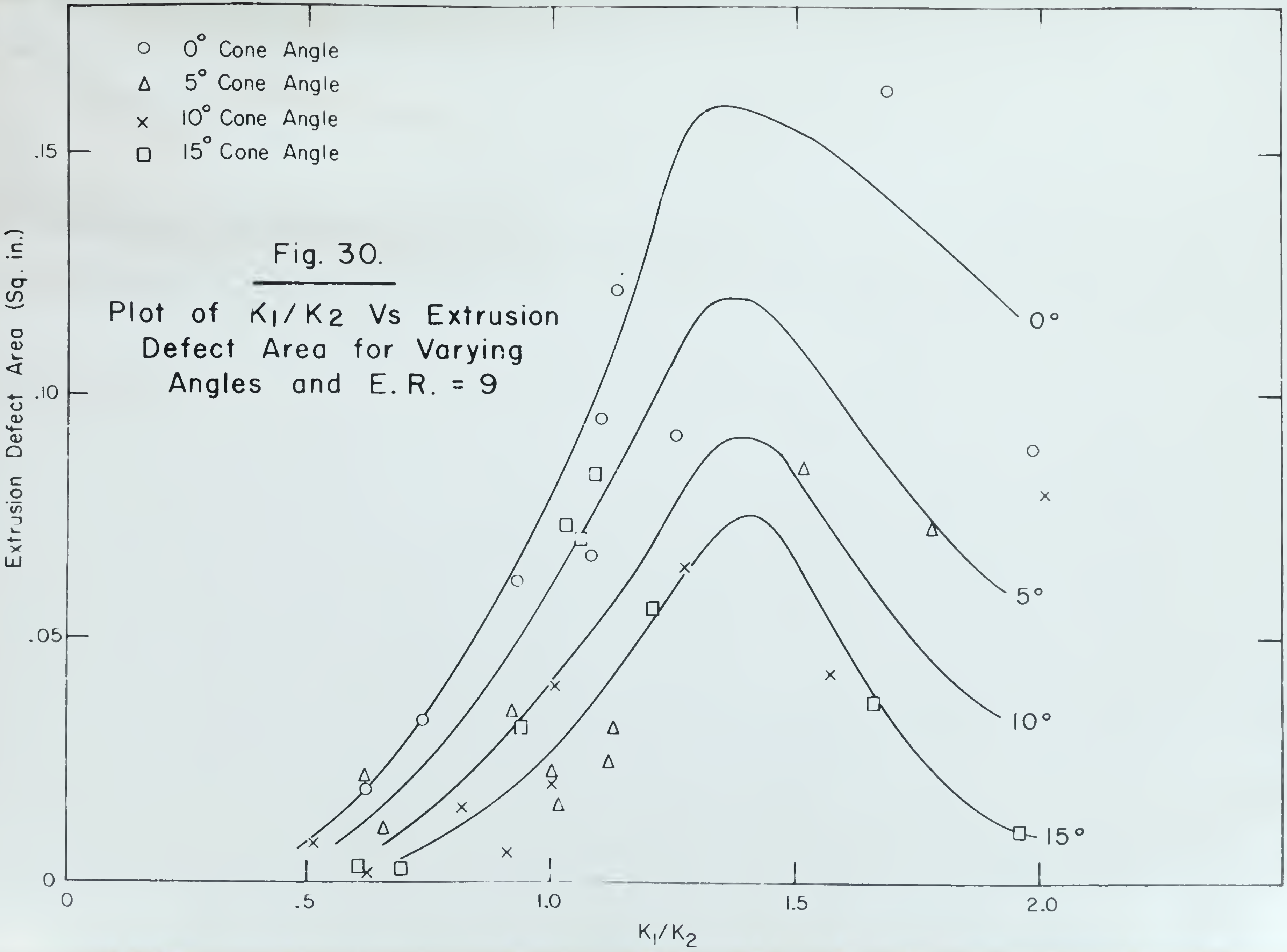

Fig. 30.

Plot of $K_1/K_2$ Vs Extrusion Defect Area for Varying Angles and E. R. = 9

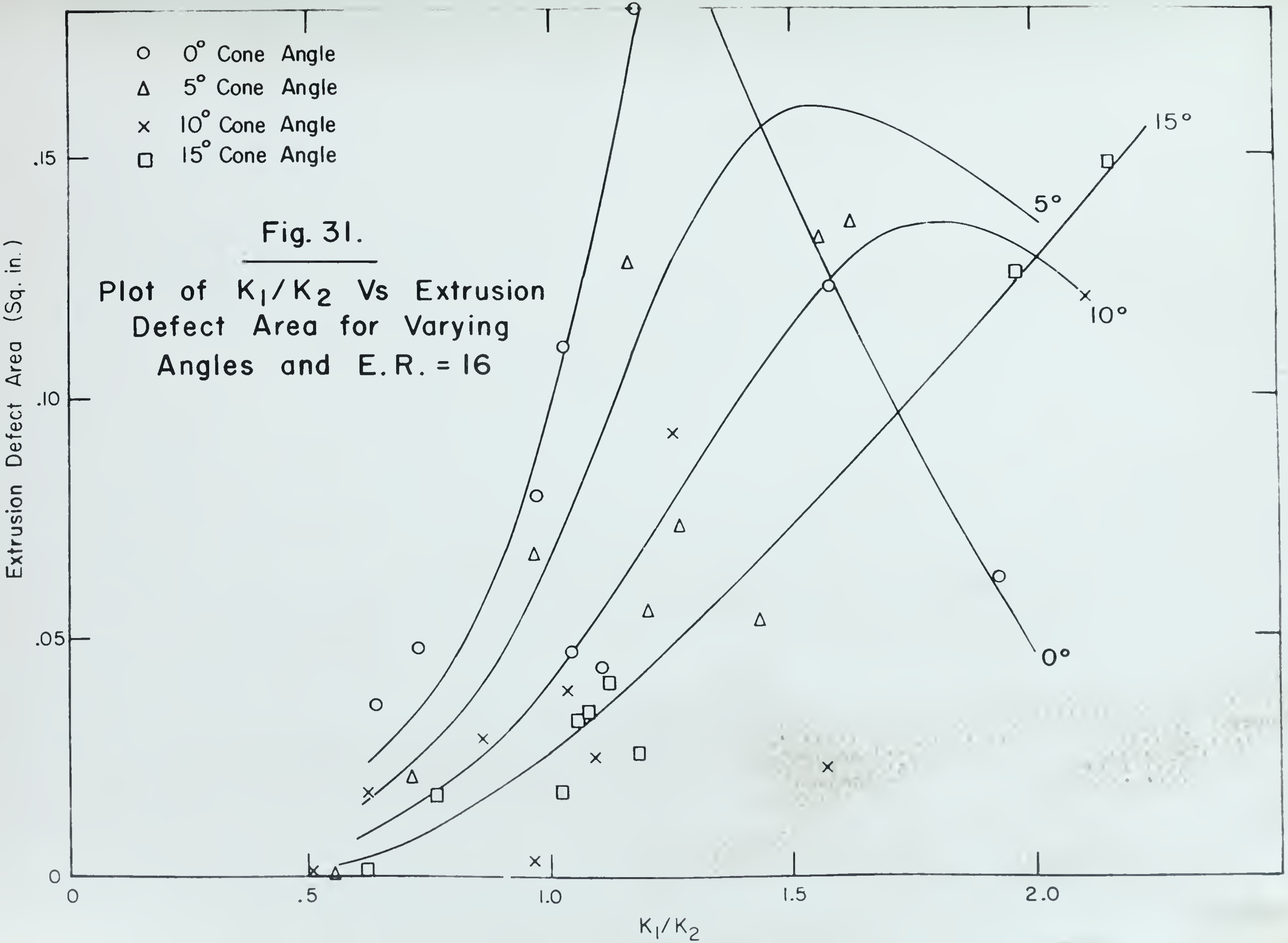

Fig. 31.

Plot of $K_1/K_2$ Vs Extrusion Defect Area for Varying Angles and E. R. = 16

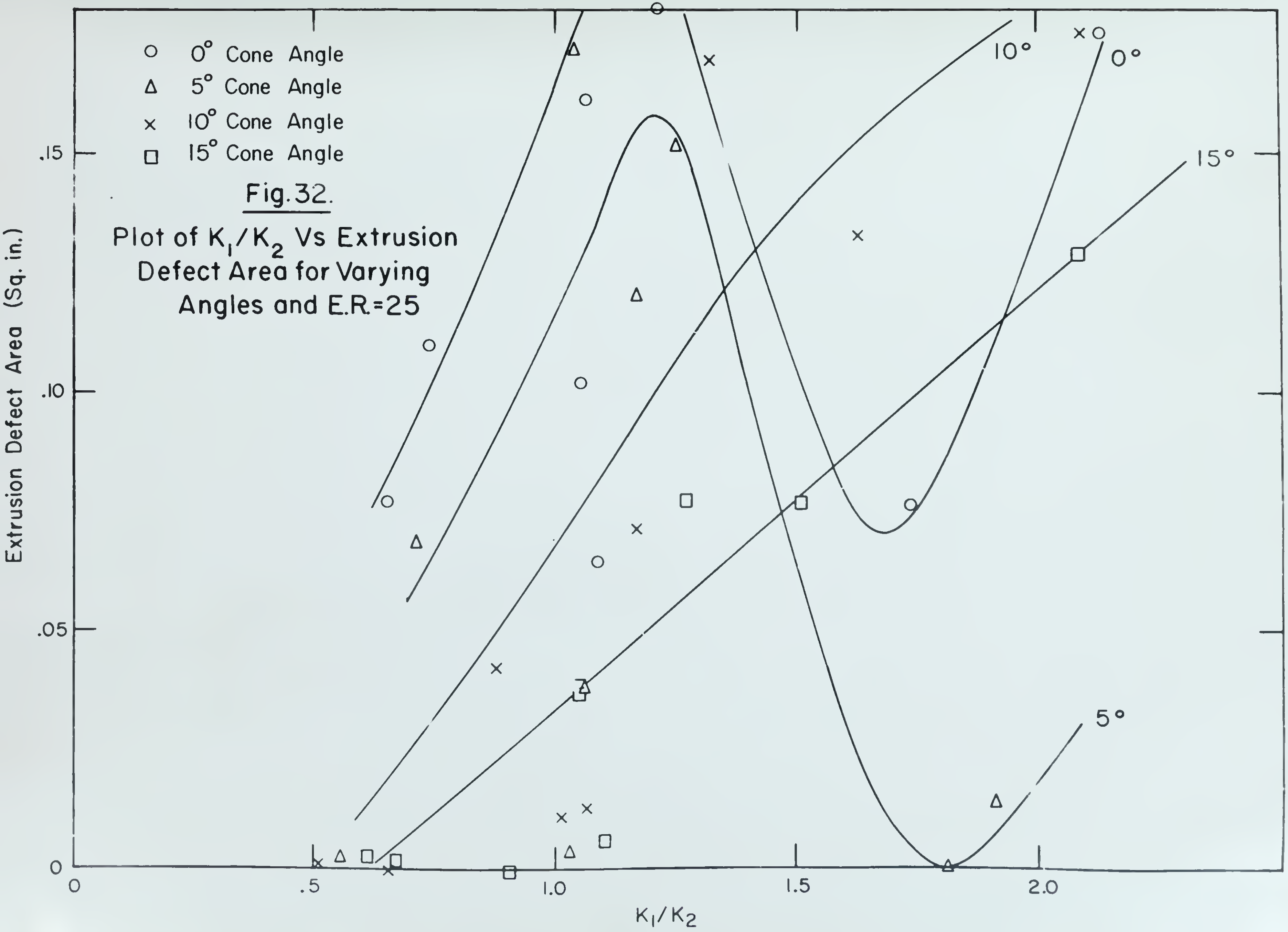

Fig. 32.

Plot of $K_1/K_2$ Vs Extrusion Defect Area for Varying Angles and E.R.=25

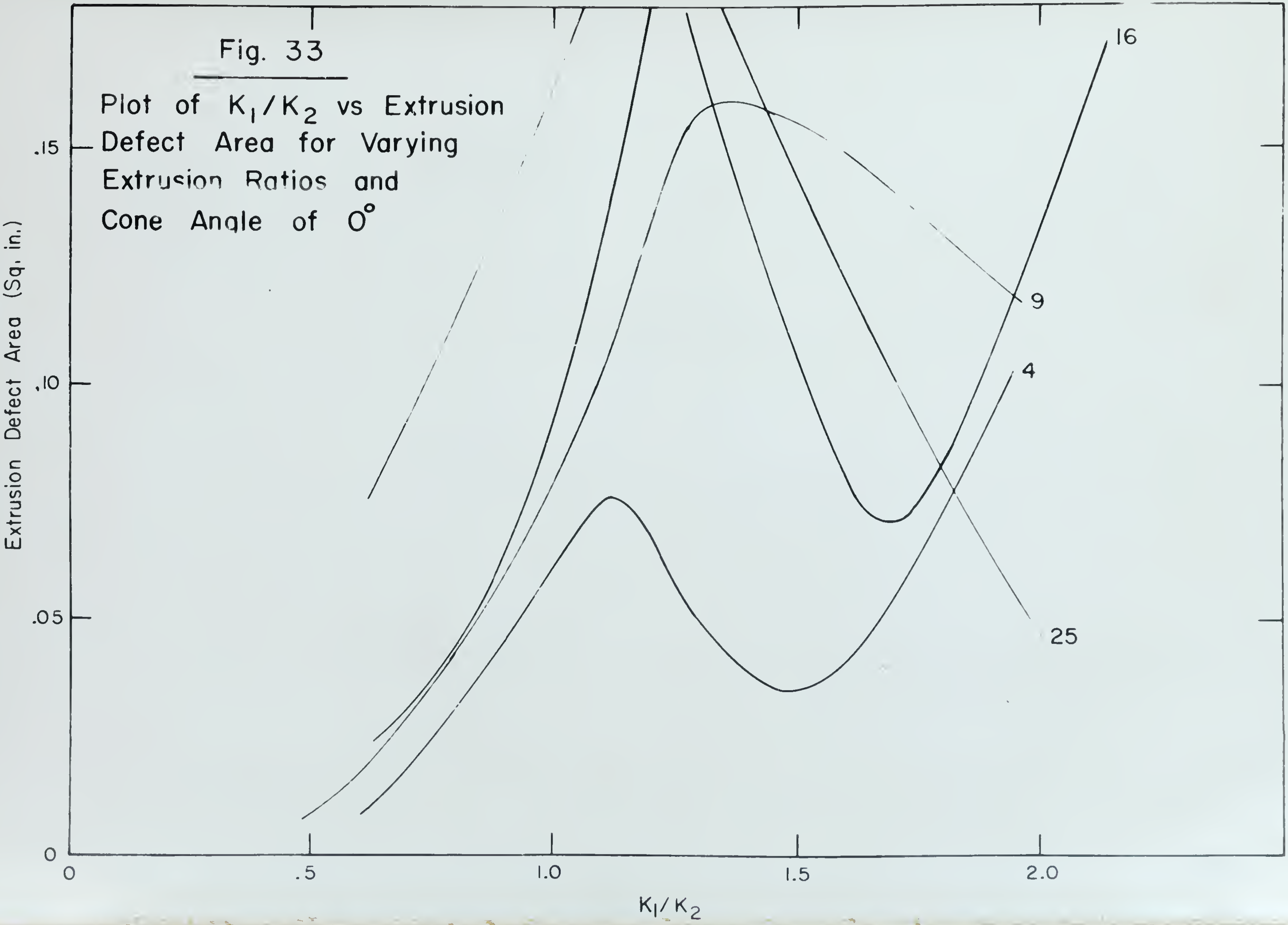

Fig. 33

Plot of $K_1/K_2$ vs Extrusion Defect Area for Varying Extrusion Ratios and Cone Angle of 0°

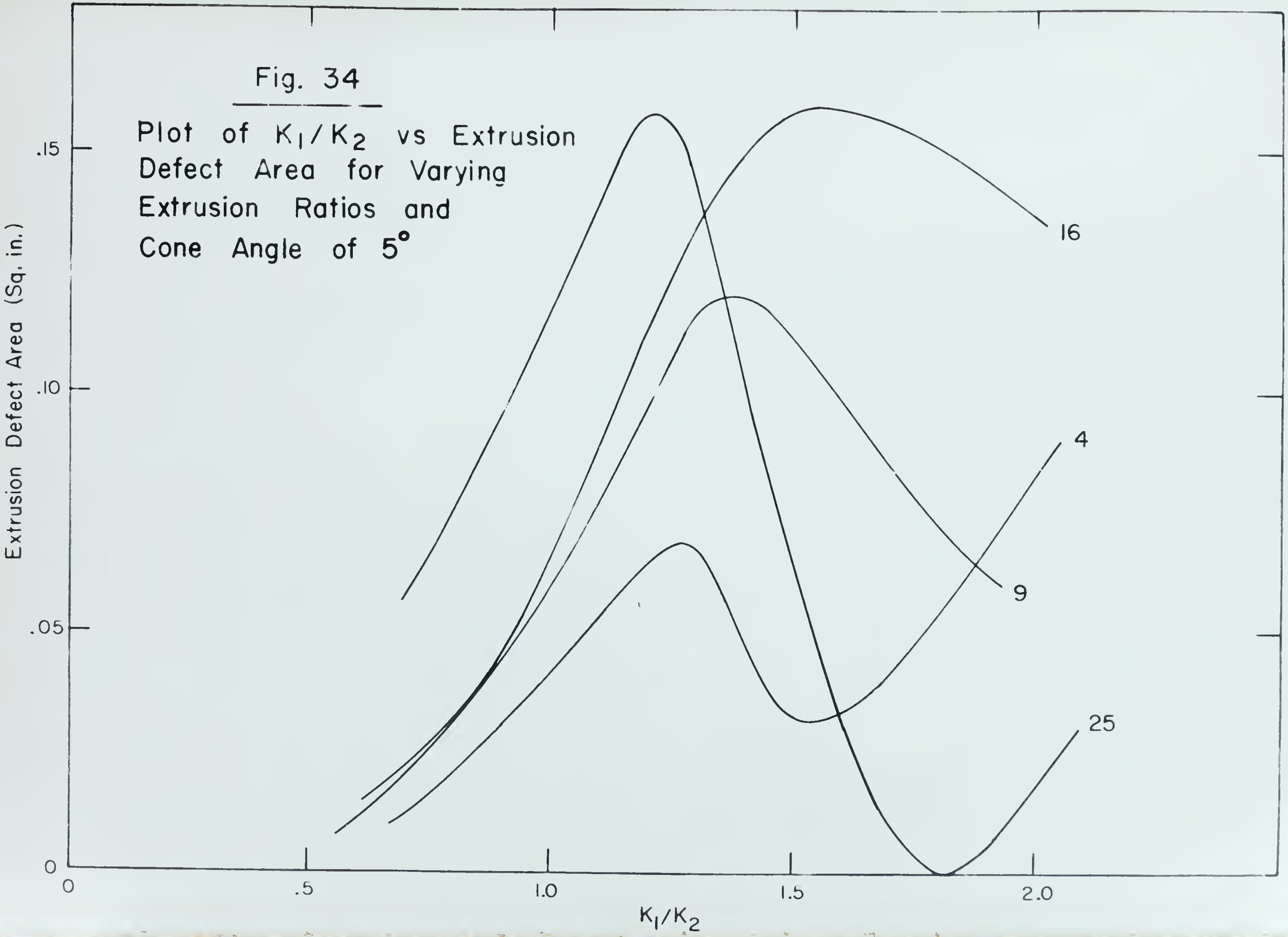

Fig. 34

Plot of $K_1/K_2$ vs Extrusion Defect Area for Varying Extrusion Ratios and Cone Angle of 5°

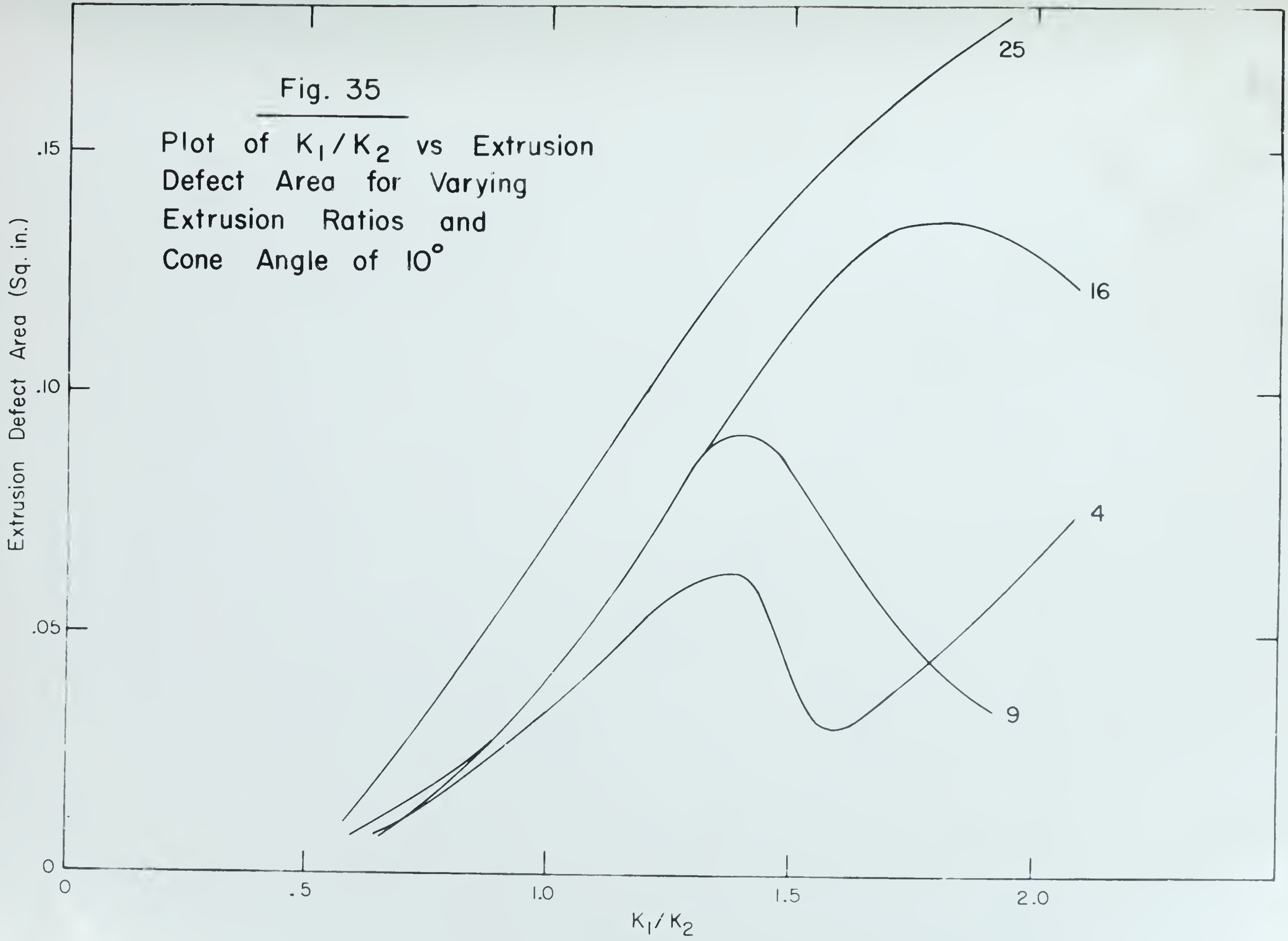

Fig. 35

Plot of $K_1/K_2$ vs Extrusion Defect Area for Varying Extrusion Ratios and Cone Angle of 10°

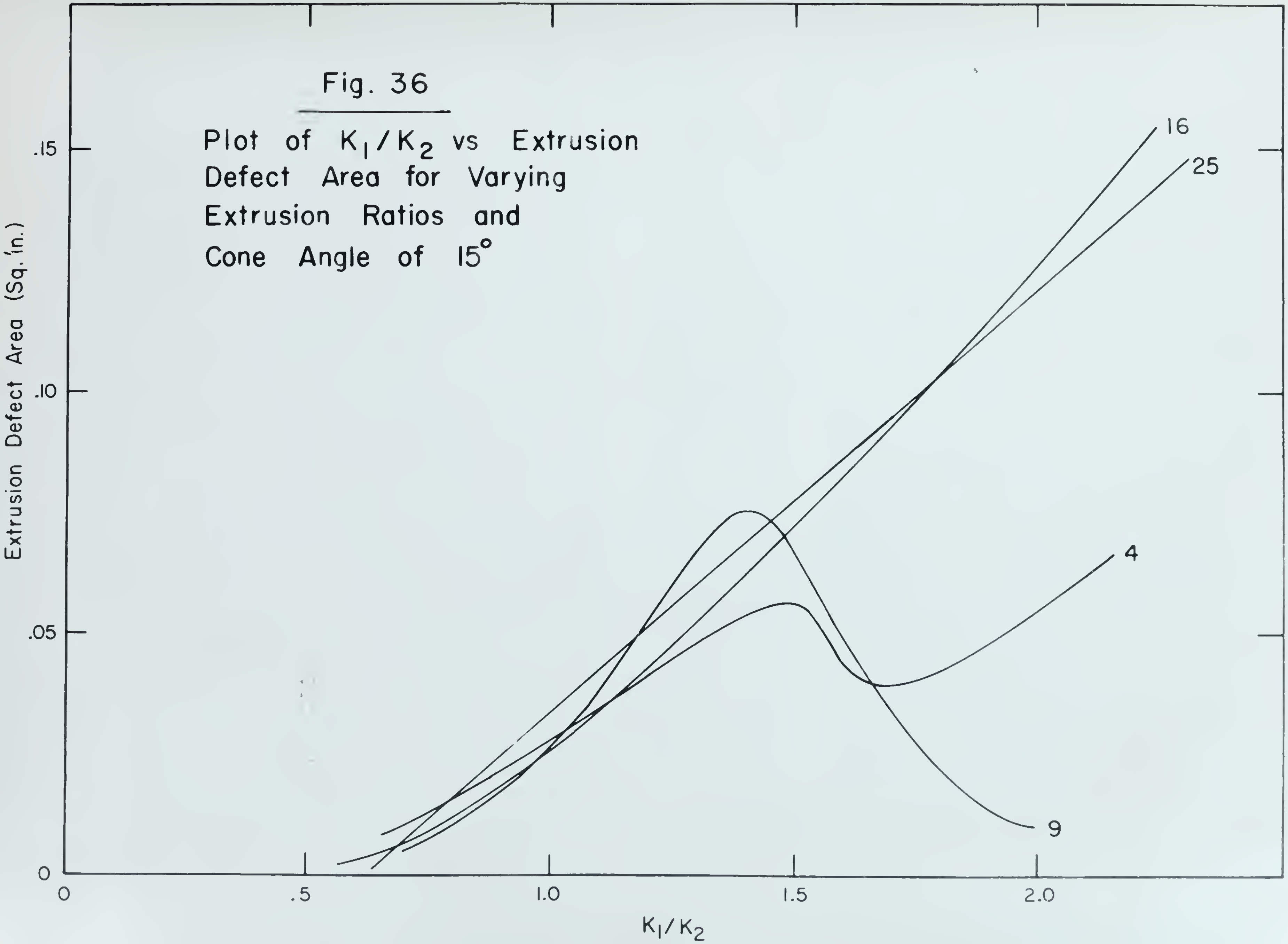

Fig. 36

Plot of $K_1/K_2$ vs Extrusion Defect Area for Varying Extrusion Ratios and Cone Angle of 15°

## C. Effect of Variation of Cone Angle

If attention is now directed to the variation of the defect area with cone angle it can be seen that no clear cut rule can be laid down. Generally, when the cone angle is increased from the flat interface ($0^{\circ}$ cone angle) the size of the defect decreases, but there are definite tendencies which show that for particular ratios of $K_1/K_2$ and extrusion ratios, increasing the cone angle actually increases the defect area. When the ratio of $K_1/K_2$ is around unity then the general rule holds. Beyond a value corresponding to the peaks, variation in cone angle is completely dependent upon the relative position of the maximum and minimum of the various S-curves.

In order to graphically illustrate the dependence of defect area on both $K_1/K_2$ and cone angle, Figures 37 - 40 have been plotted in a three-dimensional diagram showing the contours obtained for the various extrusion ratios.

In attempting to find some justification for the peak values of defect area as the $K_1/K_2$ ratio exceeds unity and then suddenly drops, it becomes paramount to again question the method by which the defect area was measured. This problem manifested itself from the beginning because no clear cut definition of the defect was available. In utilizing the area as finally selected, it was felt that this area was certainly as good as any other parameter which was available. It may be that the characteristic S-curve is a direct result of this selection and that no theoretical analysis can explain these curves. It is of interest to note that if the area acbf of Figure 15 is used as the defect area, the same type of curves are obtained. This fact, in some small way, substantiates the results found by using the parameter as chosen.

FIGURE 37.

THREE-DIMENSIONAL PLOT OF $K_1/K_2$ VS CONE ANGLE VS EXTRUSION DEFECT AREA

EXTRUSION RATIO = 4

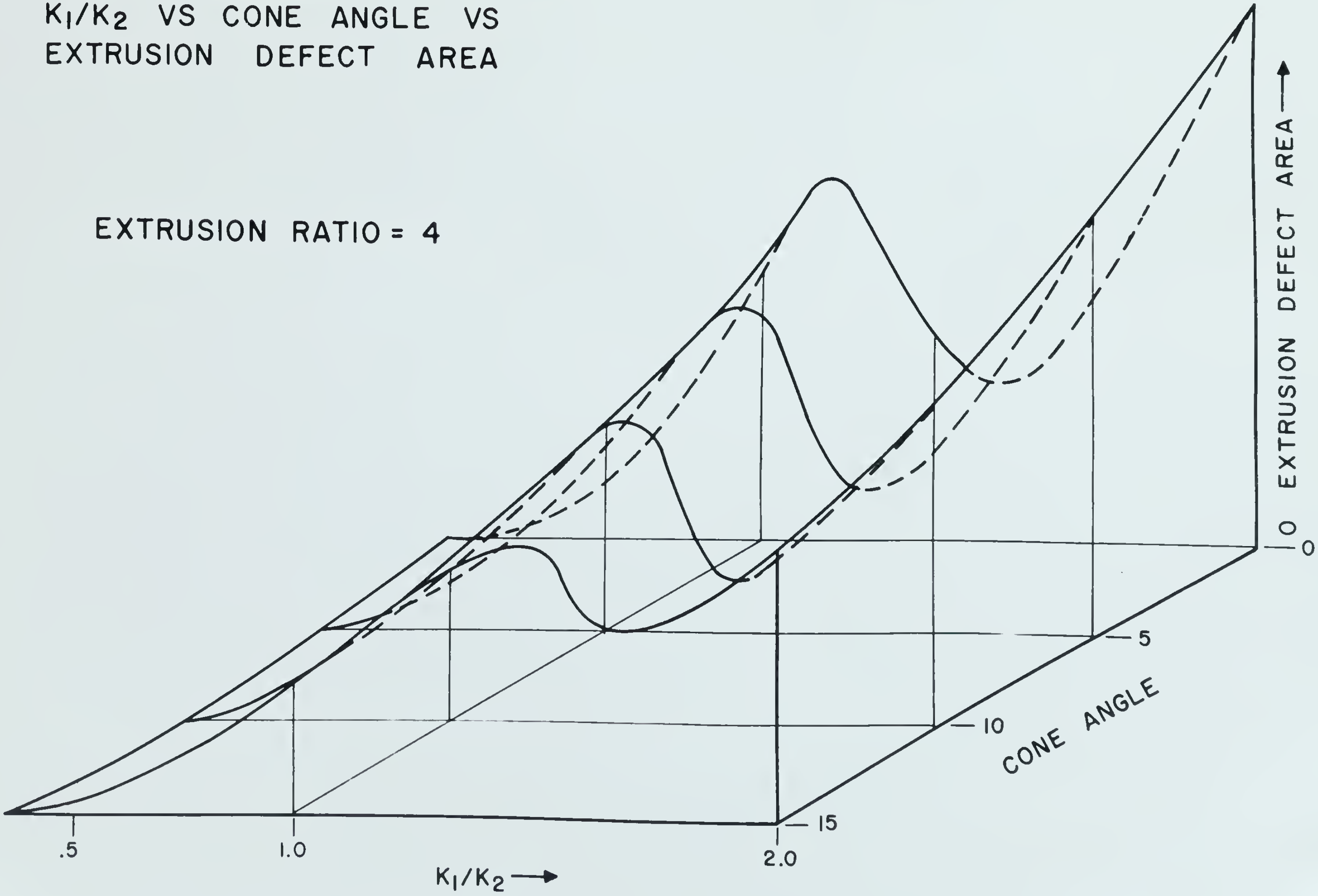

FIGURE 38.

THREE-DIMENSIONAL PLOT OF $K_1/K_2$ VS CONE ANGLE VS EXTRUSION DEFECT AREA

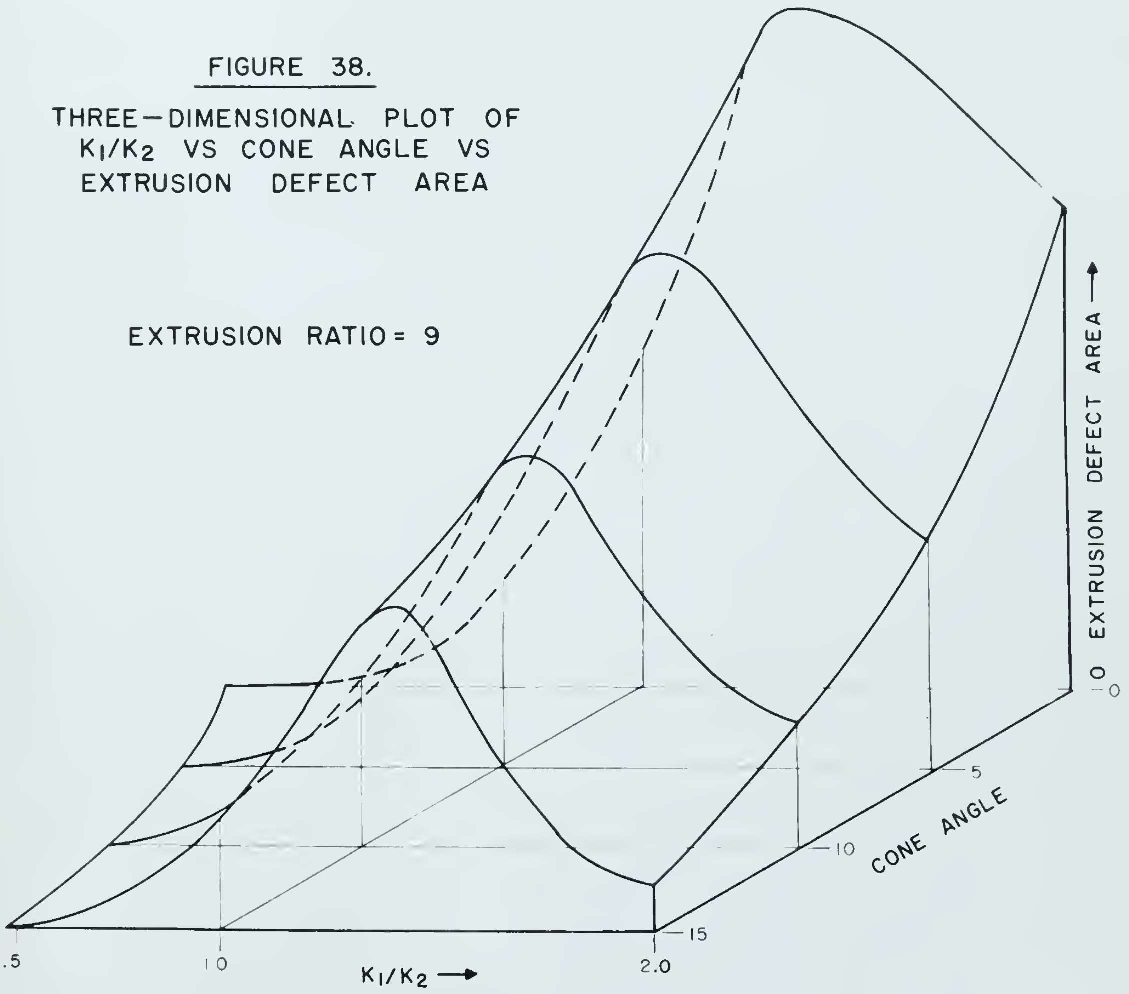

FIGURE 39.

THREE—DIMENSIONAL PLOT OF $K_1/K_2$ VS CONE ANGLE VS EXTRUSION DEFECT AREA

EXTRUSION RATIO = 16

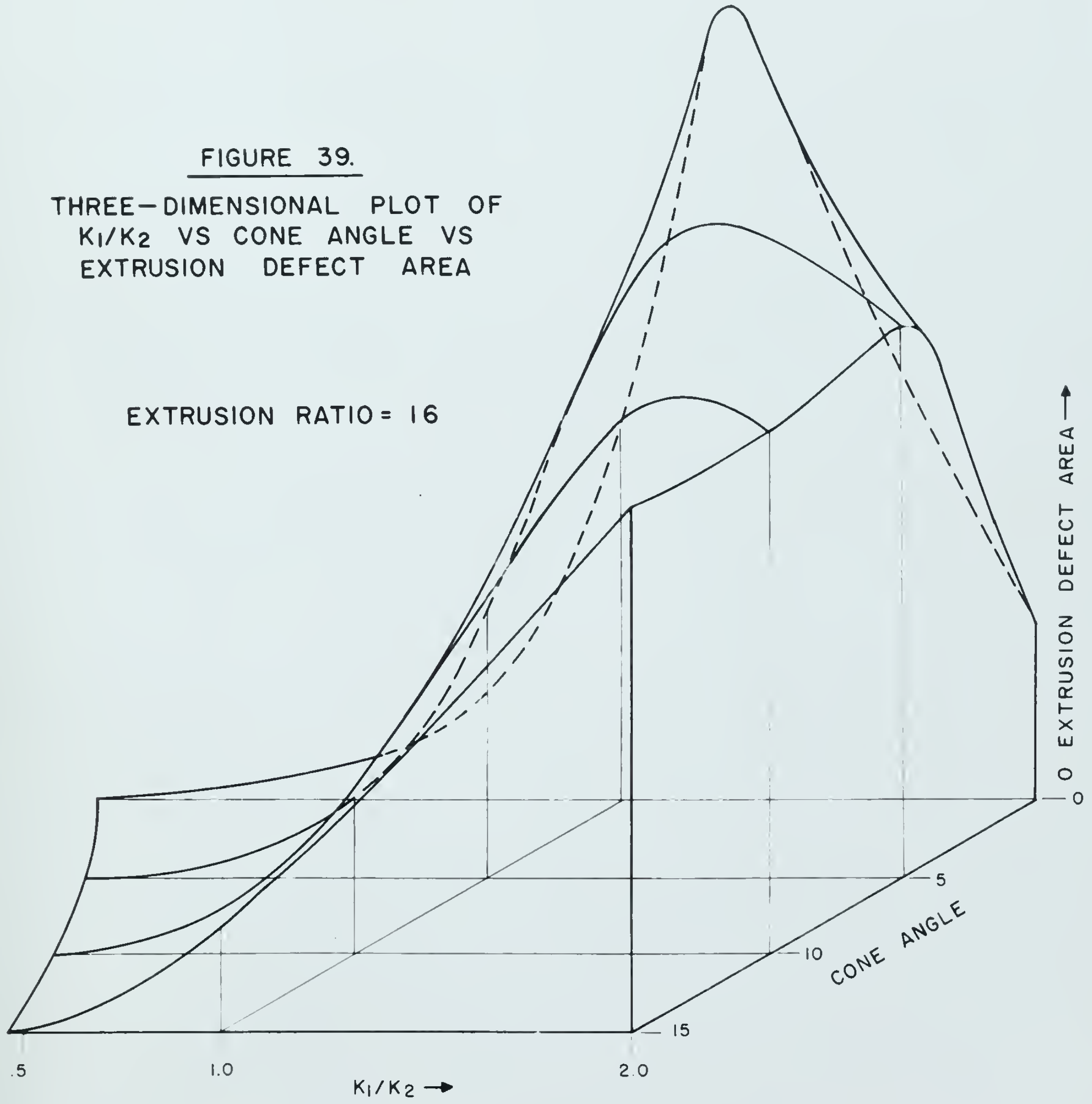

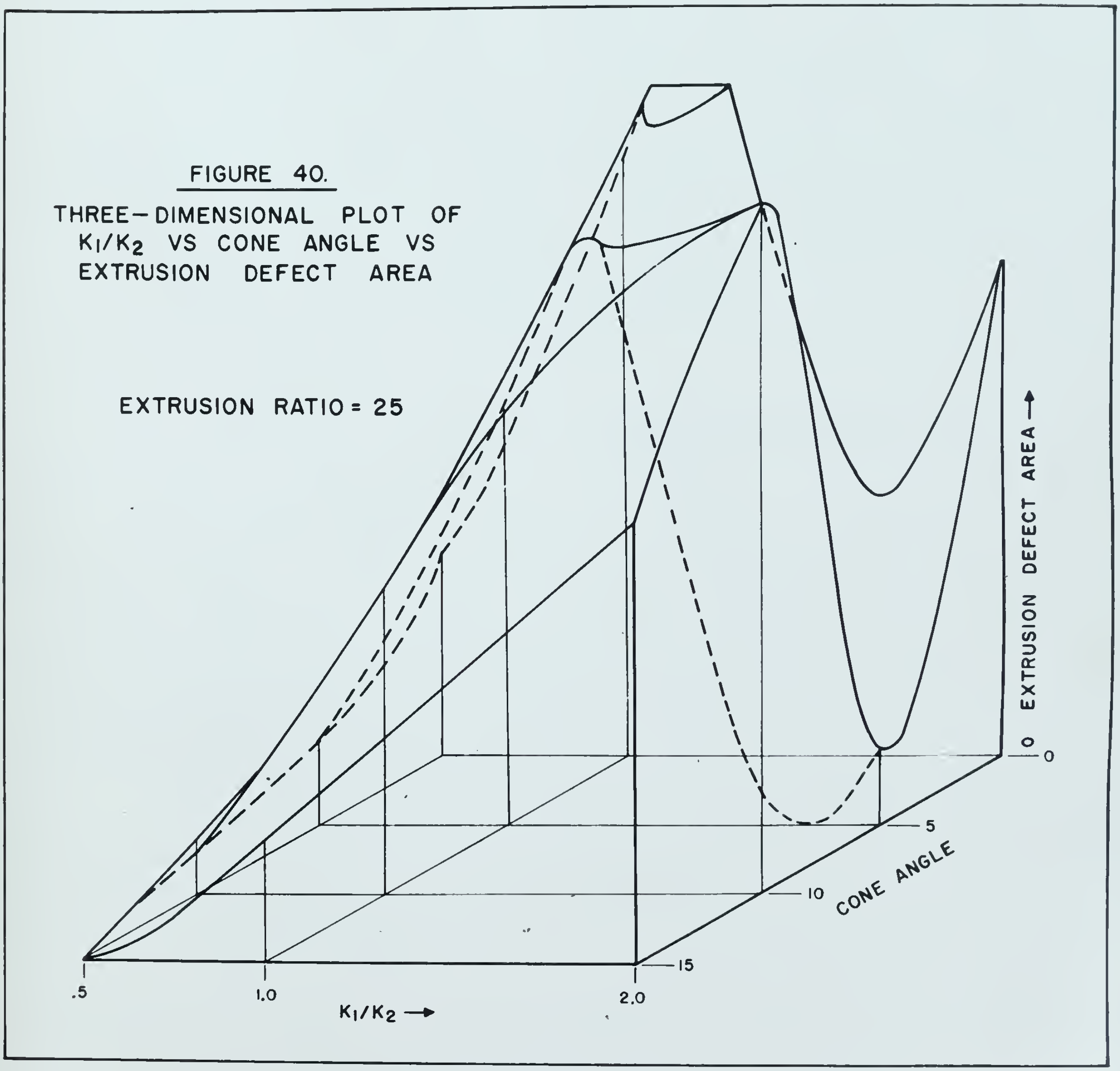

FIGURE 40.

THREE-DIMENSIONAL PLOT OF $K_1/K_2$ VS CONE ANGLE VS EXTRUSION DEFECT AREA

EXTRUSION RATIO = 25

## D. Formation of Voids

In 32 cases out of the 144 samples tested, voids were formed between the two metals after extrusion. Almost without fail the $K_1/K_2$ ratio was very low when the void formed. This is easily understood when it is realized that a hard metal is pushing the soft metal. As the interface passes through the die, the rear defect formed in the soft metal continues to increase by tailing back along the outer edge. The harder metal having a higher shear stress is incapable of keeping up with the faster moving soft metal in the center. As a result a void is formed.

Tabulated below is the result of void formation:

TABLE V

| TYPE* | NUMBER OF SAMPLES WHERE VOID FORMED |
|---|---|
| A (Low $K_1/K_2$) | 11 |
| B | 8 |
| C | 6 |
| D | 2 |
| E | 2 |
| F | 2 |
| G | 0 |
| H | 0 |
| I (High $K_1/K_2$) | 0 |

*See Table III

## VII. CONCLUSIONS

Before any conclusions can be reached it should be borne in mind that 144 test samples were investigated and that of these 144 samples no two were the same. Any analysis which might be based on the numerical data obtained from any one sample is very doubtful. Any curve drawn using as its basis the data from one sample is extremely doubtful. It is for this reason that great liberty was taken by the author in arriving at the curves. Many points fell entirely outside the range of reasonableness and were just discounted altogether. Thus, the conclusions that follow are based solely on the trends that this experimenter thought were evident. Another person, in viewing this data, might very well arrive at completely opposite views.

Based on the data found in this experiment and the interpretation placed thereon, certain conclusions can be reached.

A. To a certain degree, interfaces resulting from extruding two metals of differing stiffnesses can be predicted. If one knows $K_1/K_2$ and the extrusion ratio then it should be possible to select a preshaped cone angle which would result in the flattest interface obtainable under those circumstances. This interface will not necessarily be completely flat.

B. Extremely small defects result when $K_1/K_2$ is small, regardless of the extrusion ratio. However, the undesirable result of voids is prevalent at small $K_1/K_2$ ratios which means that little or no bonding would result at the interface. If bonding is important, then some means should be used to prevent extrusions at low $K_1/K_2$ ratios. This might be accomplished by the use of a buffer plate which has a stiffness

## VII. CONCLUSIONS

Before any conclusions can be reached it should be borne in mind that 144 test samples were investigated and that of these 144 samples no two were the same. Any analysis which might be based on the numerical data obtained from any one sample is very doubtful. Any curve drawn using as its basis the data from one sample is extremely doubtful. It is for this reason that great liberty was taken by the author in arriving at the curves. Many points fell entirely outside the range of reasonableness and were just discounted altogether. Thus, the conclusions that follow are based solely on the trends that this experimenter thought were evident. Another person, in viewing this data, might very well arrive at completely opposite views.

Based on the data found in this experiment and the interpretation placed thereon, certain conclusions can be reached.

A. To a certain degree, interfaces resulting from extruding two metals of differing stiffnesses can be predicted. If one knows $K_1/K_2$ and the extrusion ratio then it should be possible to select a preshaped cone angle which would result in the flattest interface obtainable under those circumstances. This interface will not necessarily be completely flat.

B. Extremely small defects result when $K_1/K_2$ is small, regardless of the extrusion ratio. However, the undesirable result of voids is prevalent at small $K_1/K_2$ ratios which means that little or no bonding would result at the interface. If bonding is important, then some means should be used to prevent extrusions at low $K_1/K_2$ ratios. This might be accomplished by the use of a buffer plate which has a stiffness intermediate between the two metals. Selection of this buffer material would have to be based on its nuclear as well as its mechanical properties.

C. Experimental determination of the S-curves would be very beneficial in determining the cone angle which should be used for obtaining flat interfaces.

# VIII. RECOMMENDATIONS

## A. Extension of Investigation

1. It is recommended that further study be made at cone angles in excess of the 15° tried in this report. Each particular group of experiments should be carried to the point where the defect area becomes negative, that is, completely reverses itself.

2. It is recommended that, if this experiment is continued, each particular test be run at least three times in order to minimize the probable error. One great problem in extrusions is the fact that it is not an exact science due to the pronounced effect each of the many variables can play on the final result and the inability to precisely control these variables. The only solution to a situation of this type is to repeat the particular test enough times so as to minimize the effect of the variables.

## B. Double Extrusion

It is recommended that the possibility of arriving at a flat interface by the use of double extrusion be investigated further, utilizing the apparatus for this experiment. The first extrusion should be done at extrusion ratios slightly over one and the second extrusion should be run at varying extrusion ratios in order to determine just what combination will result in a flat interface.

## C. Buffer Plates

It is recommended that the idea of using a metal of intermediate stiffness between two metals where $K_1/K_2$ is small be investigated in order to determine if formation of voids can be eliminated completely.

## APPENDIX A

1. Detailed Drawings of Apparatus

2. Photographs of Extruded Samples (Figures A-6 to A-21)

Each sheet of photographs contains those samples in which the extrusion ratio and cone angle remained fixed. Only the type of metal changed. See Table I for description of sample.

Arrow at top of sheet indicates direction of extrusion.

Note: Samples #55 and #144 were inadvertently placed in the opposite direction when photographed and consequently their direction of extrusion is opposite to that indicated.

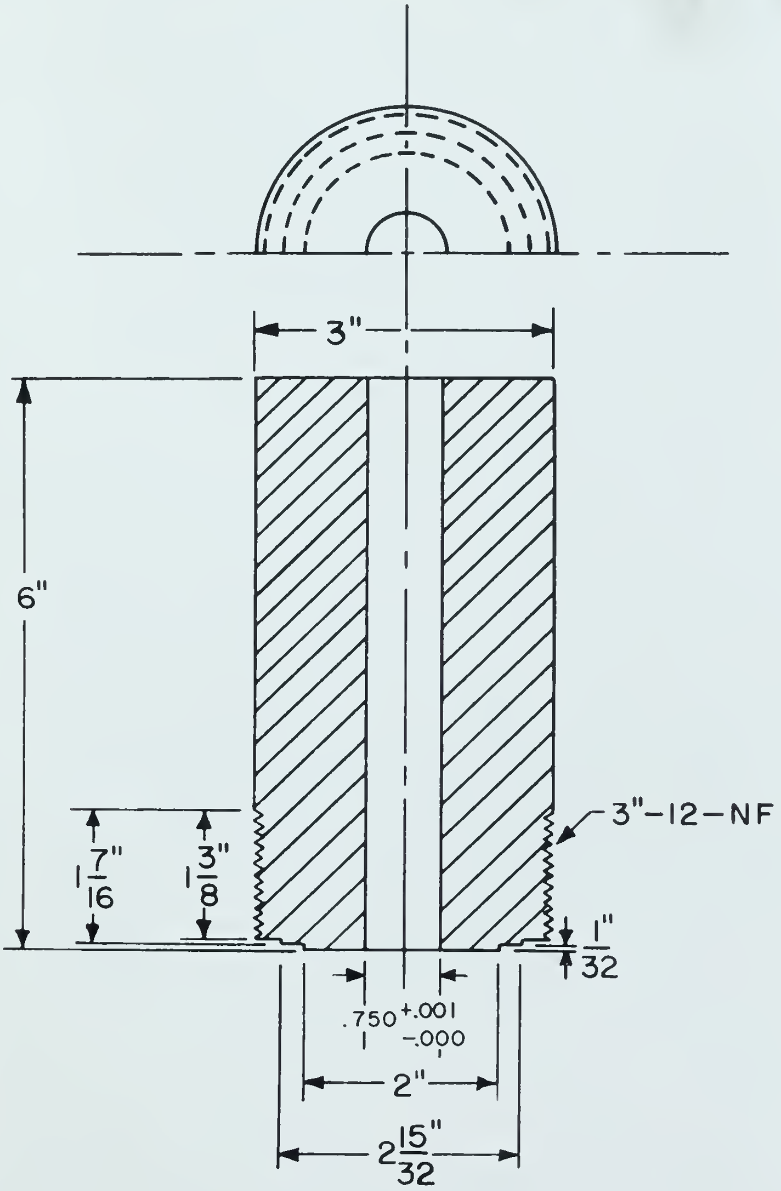

FIGURE A-1

Extrusion Cylinder

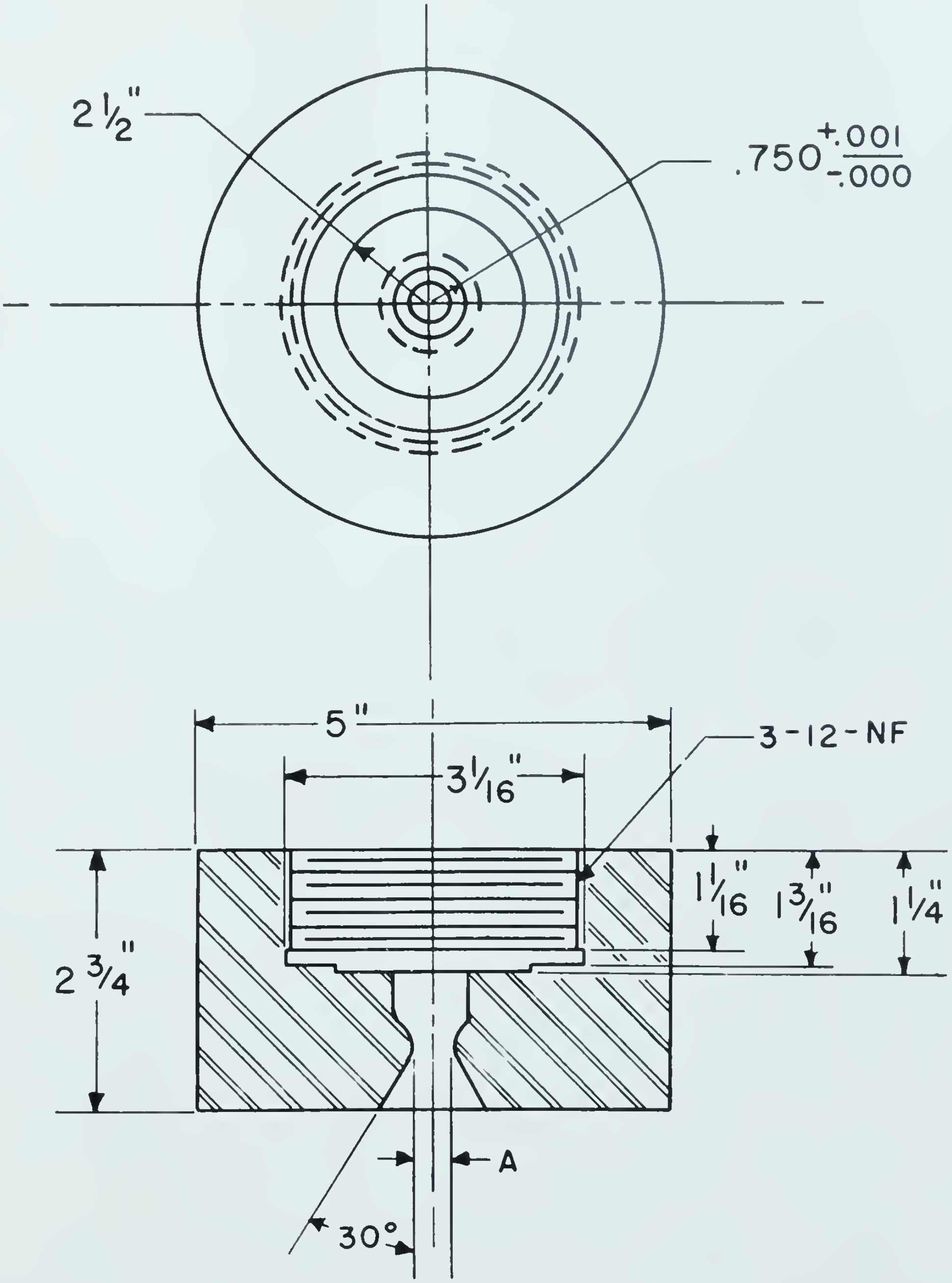

| | | | | |
|---|---|---|---|---|
| A | .375 | .250 | .1875 | .150 |

Fig. A-2. Extrusion Dies

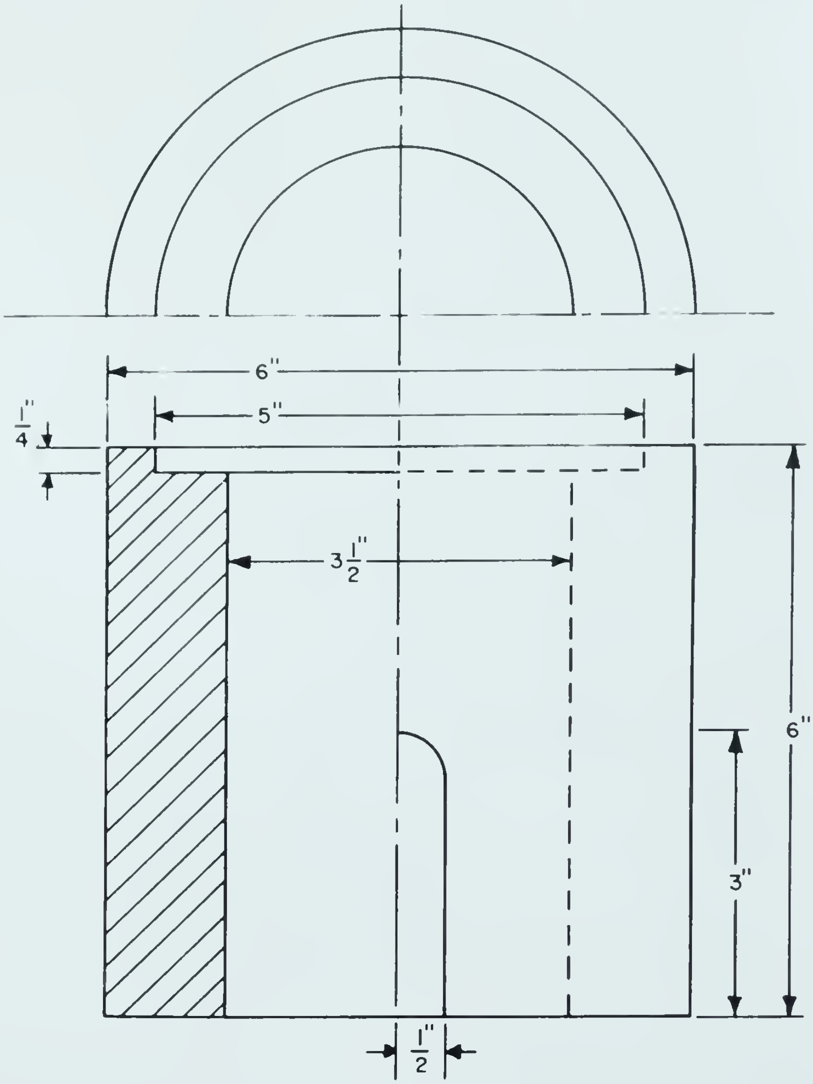

FIGURE A-3

Extrusion Stand

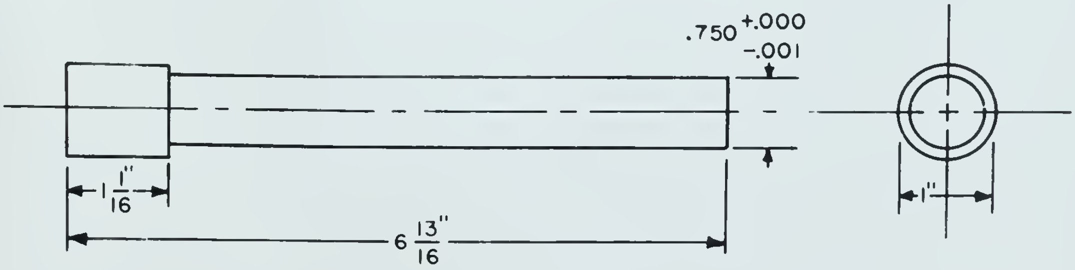

FIGURE A-4

Extrusion Ram

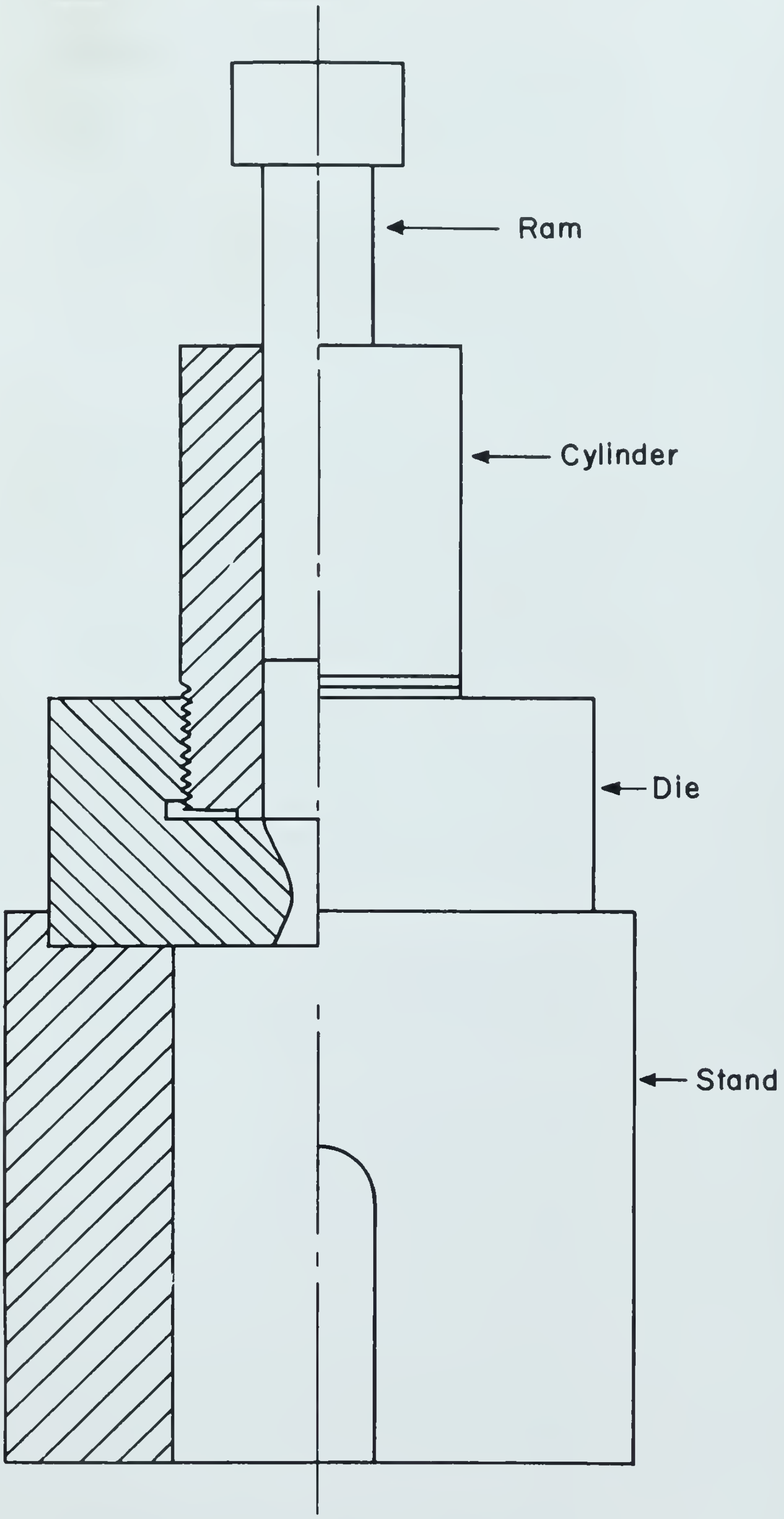

FIGURE A-5

Assembly of Extrusion Apparatus

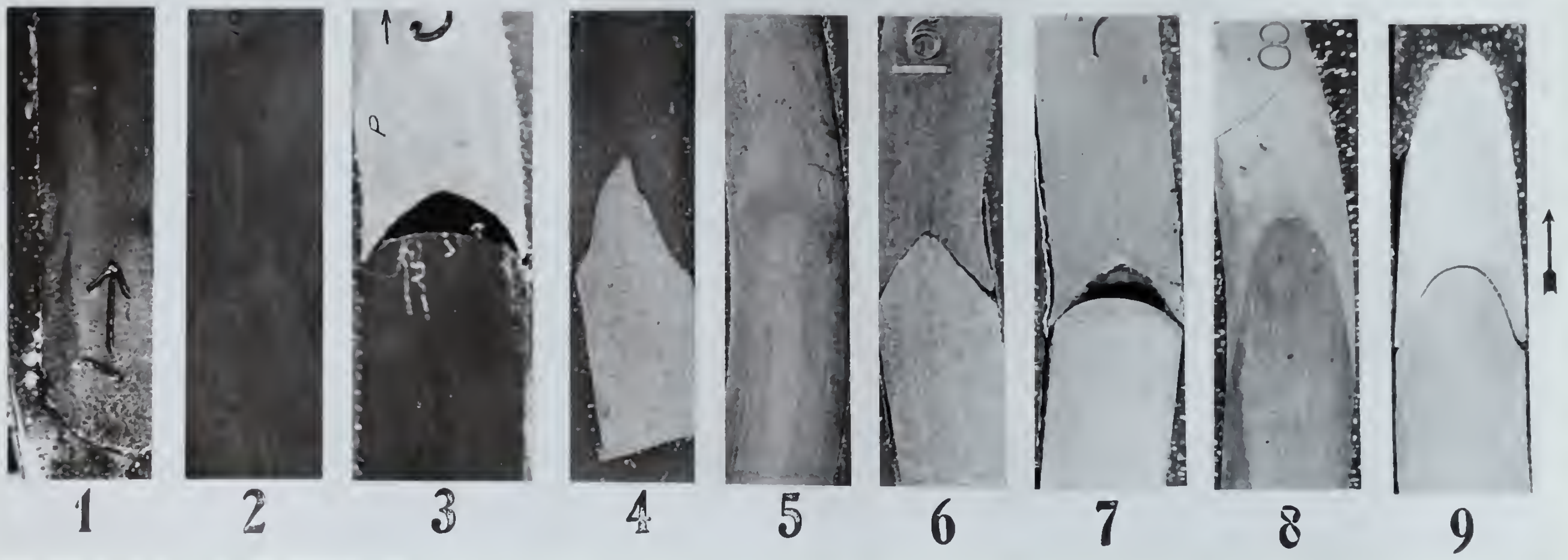

Figure A-6 - Photographs of Composite Lead Billets After Extrusion Showing Interface.
Extrusion Ratio = 4

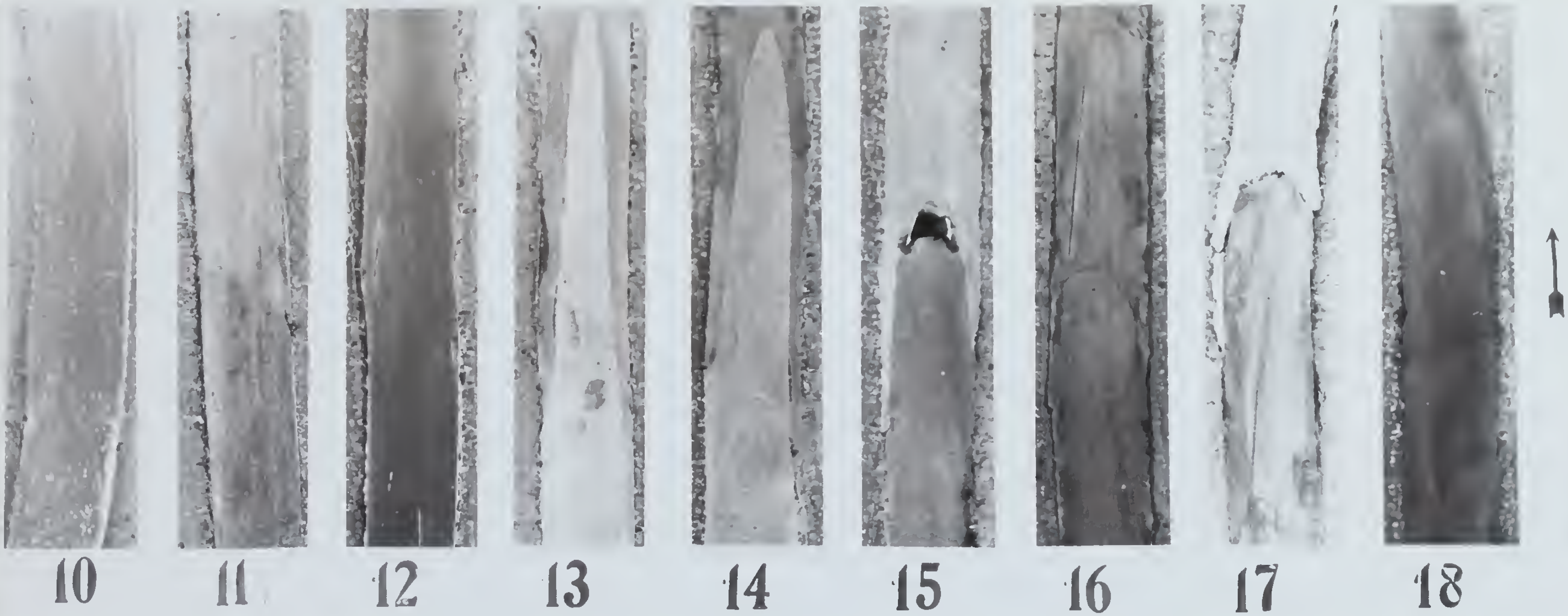

Figure A-7 - Photographs of Composite Lead Billets After Extrusion Showing Interface.
Extrusion Ratio = 9

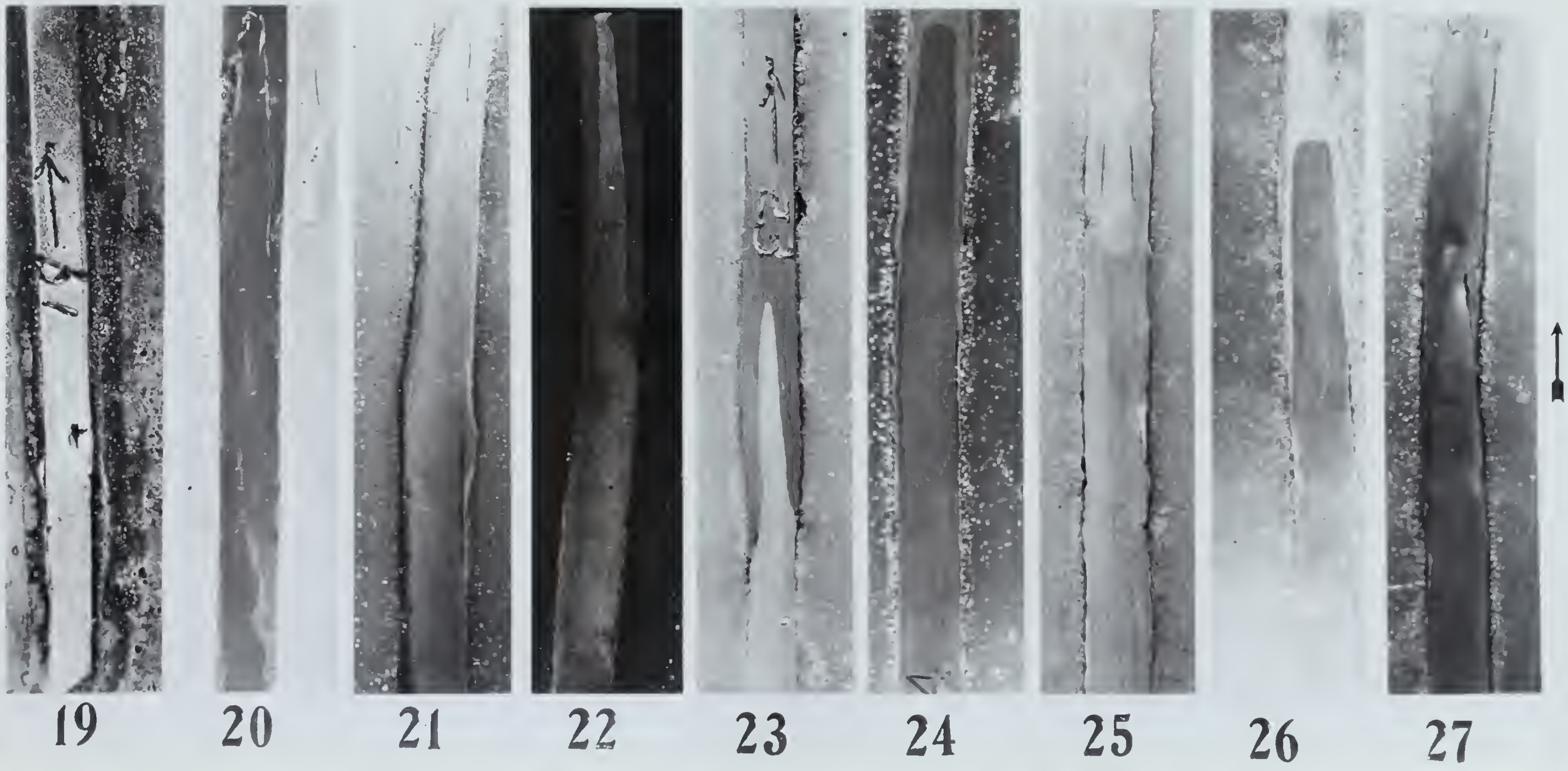

Figure A-8 - Photographs of Composite Lead Billets After Extrusion Showing Interface.
Extrusion Ratio = 16

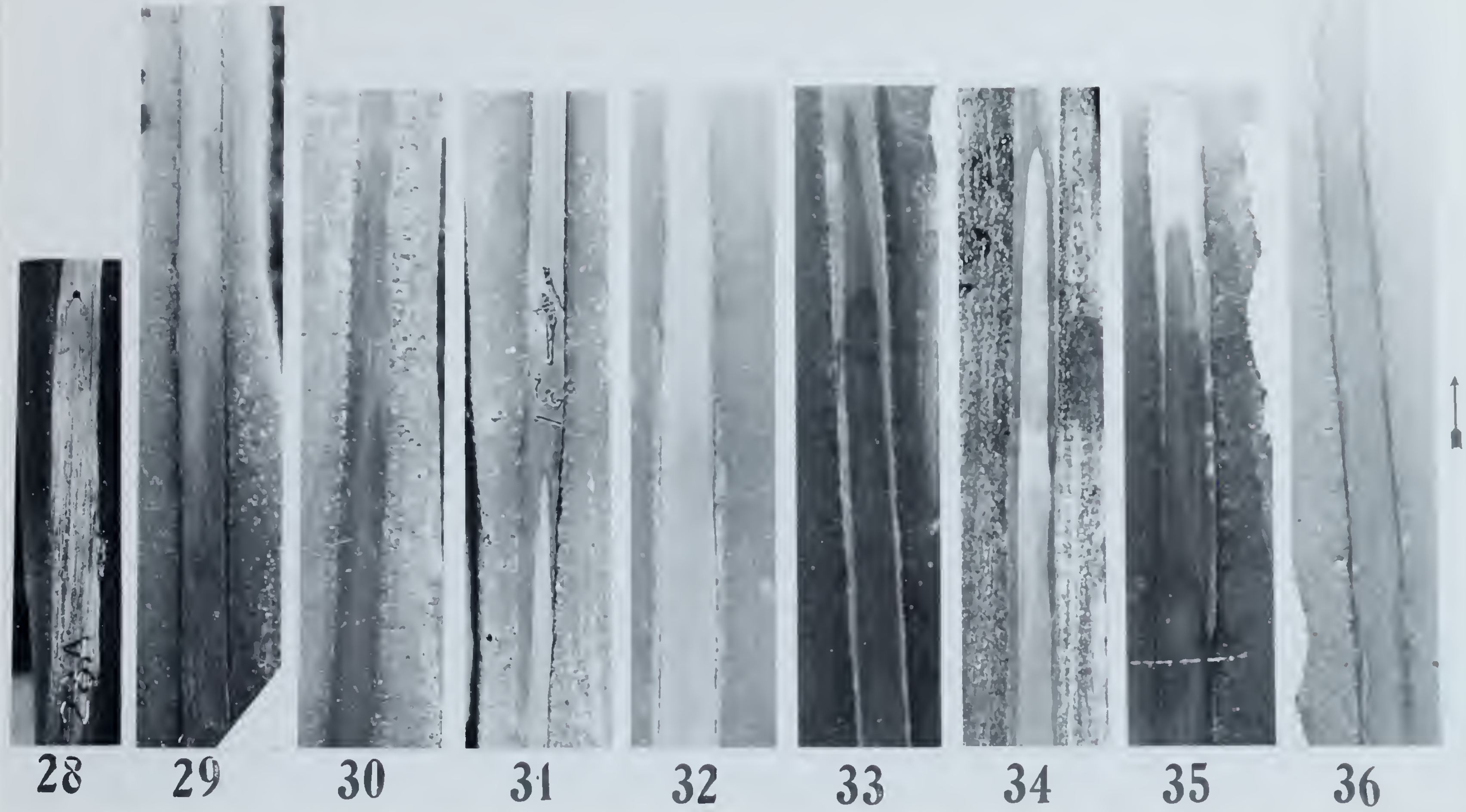

Figure A-9 - Photographs of Composite Lead Billets After Extrusion Showing Interface.
Extrusion Ratio = 25

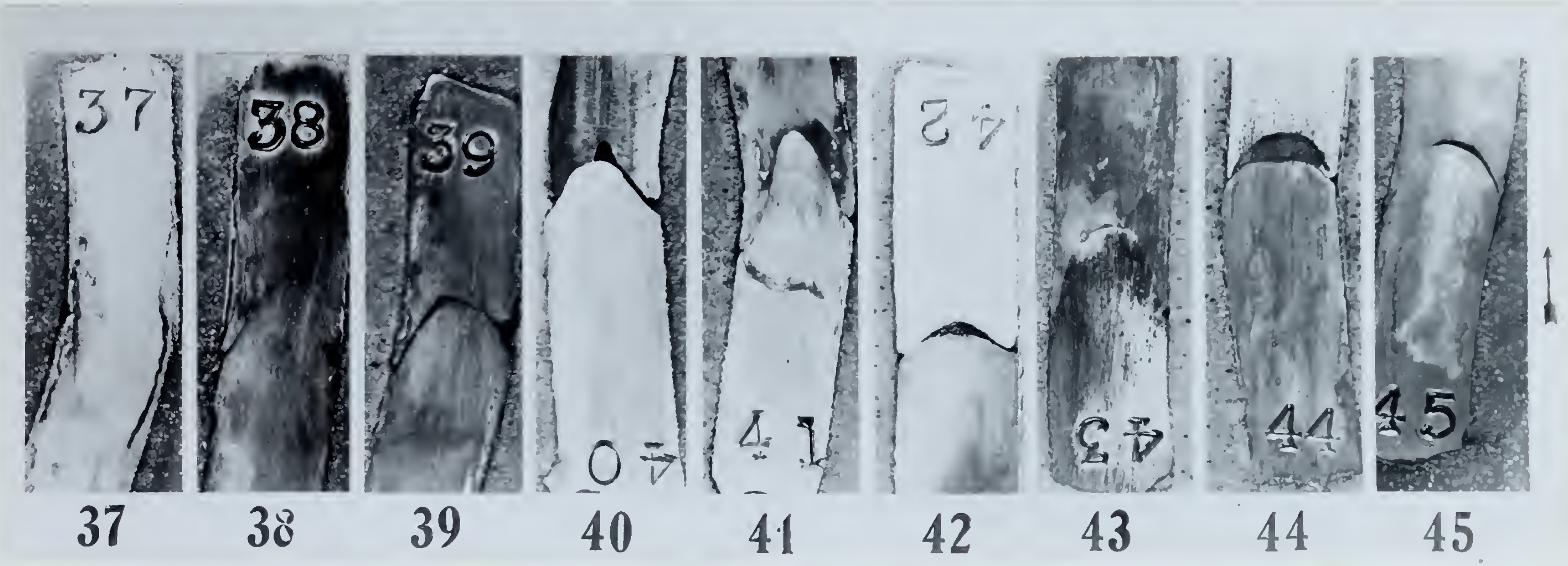

Figure A-10 - Photographs of Composite Lead Billets After Extrusion Showing Interface.
Extrusion Ratio = 4

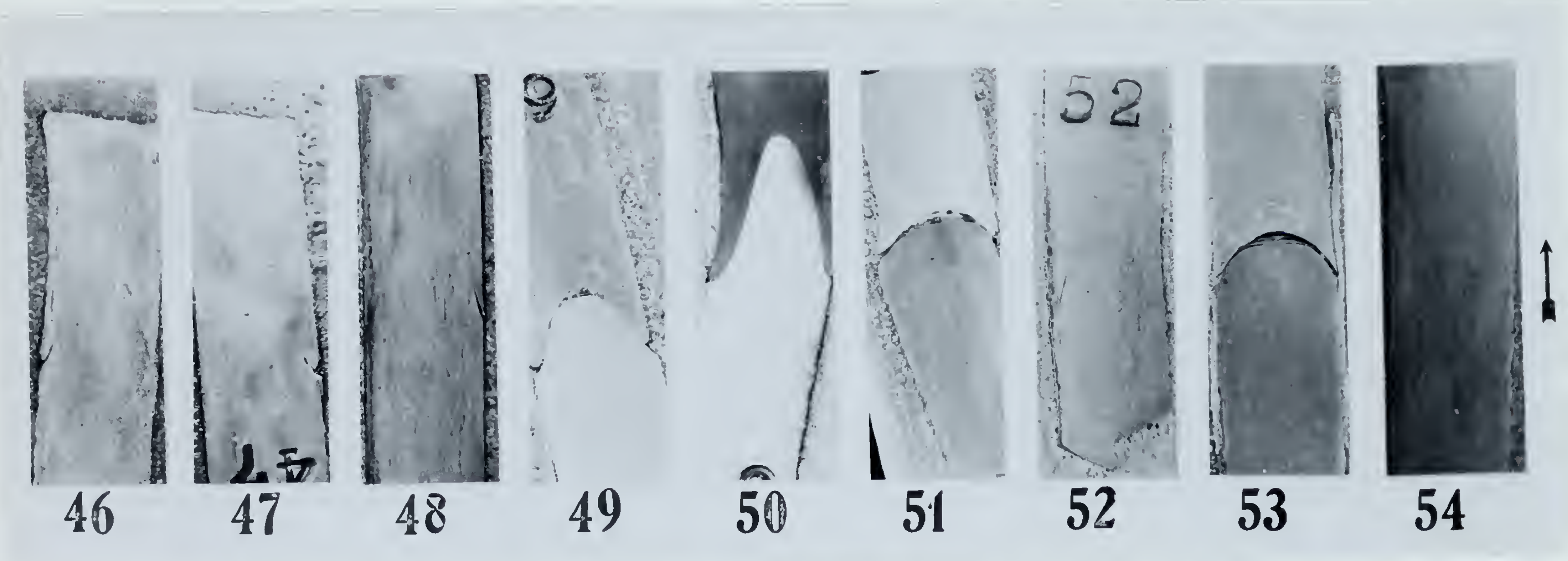

Figure A-11 - Photographs of Composite Lead Billets After Extrusion Showing Interface.
Extrusion Ratio = 4

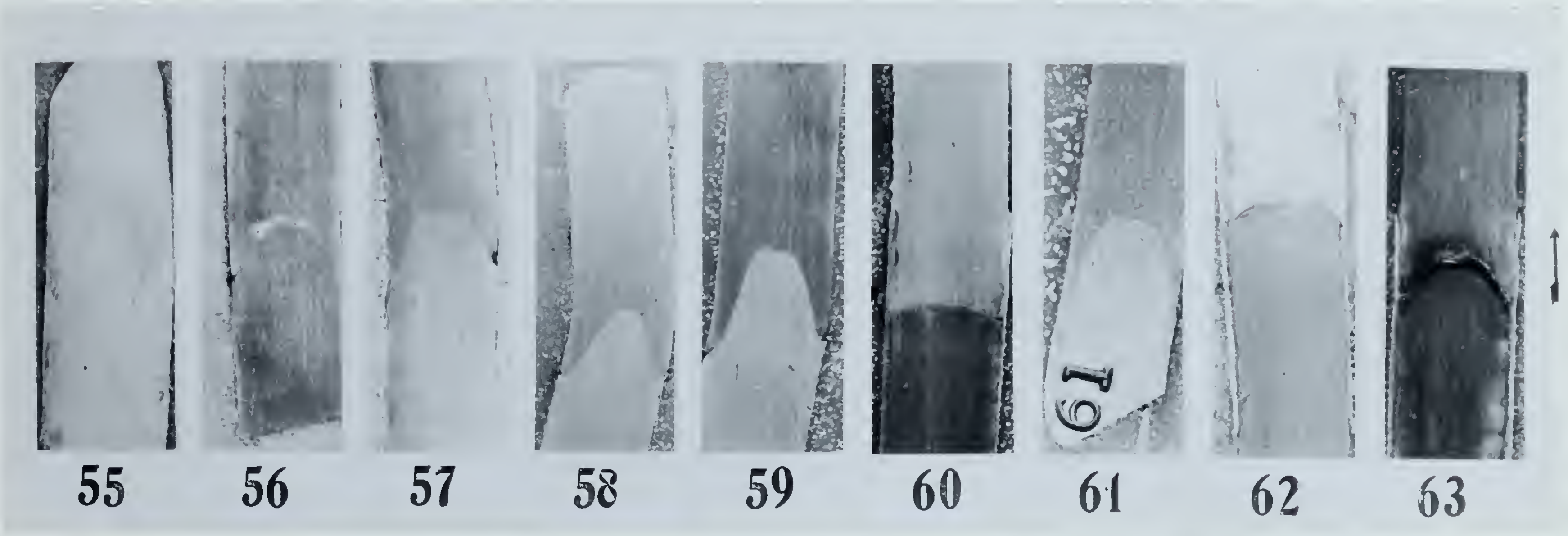

Figure A-12 - Photographs of Composite Lead Billets After Extrusion Showing Interface.
Extrusion Ratio = 4

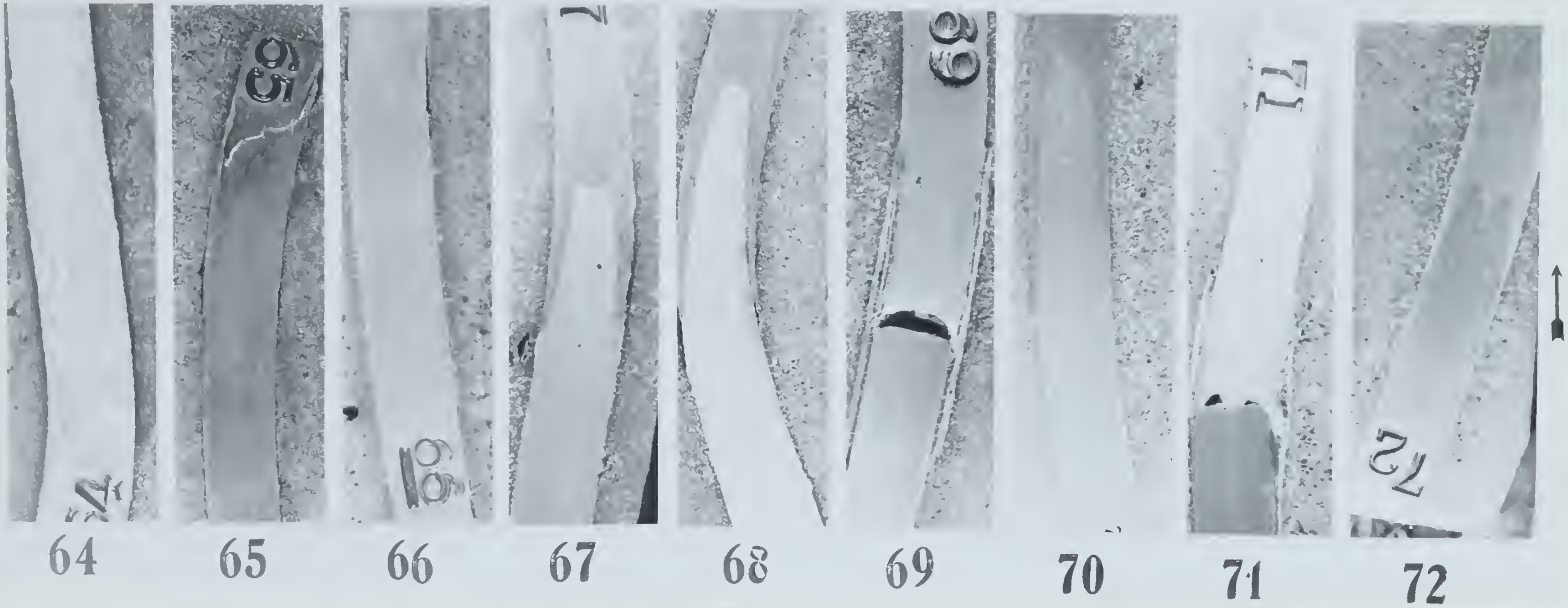

Figure A-13 - Photographs of Composite Lead Billets After Extrusion Showing Interface.
Extrusion Ratio = 9

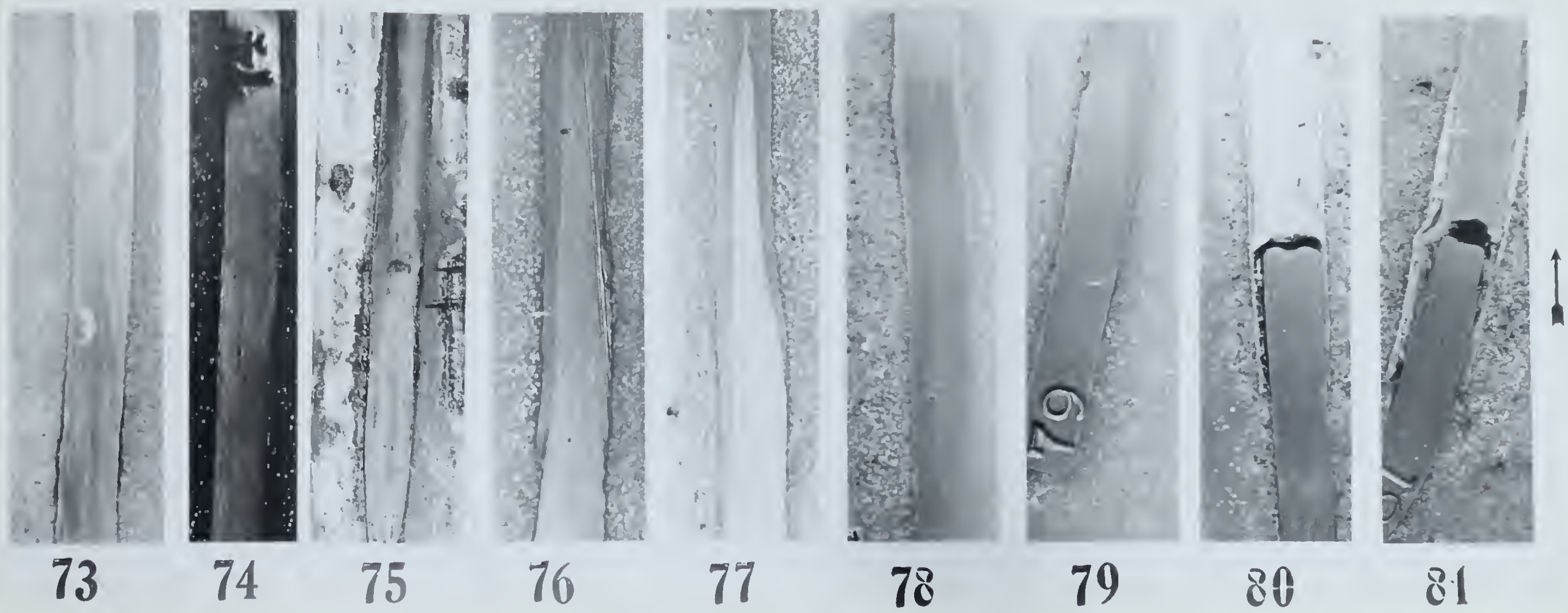

Figure A-14 - Photographs of Composite Lead Billets After Extrusion Showing Interface.
Extrusion Ratio = 16

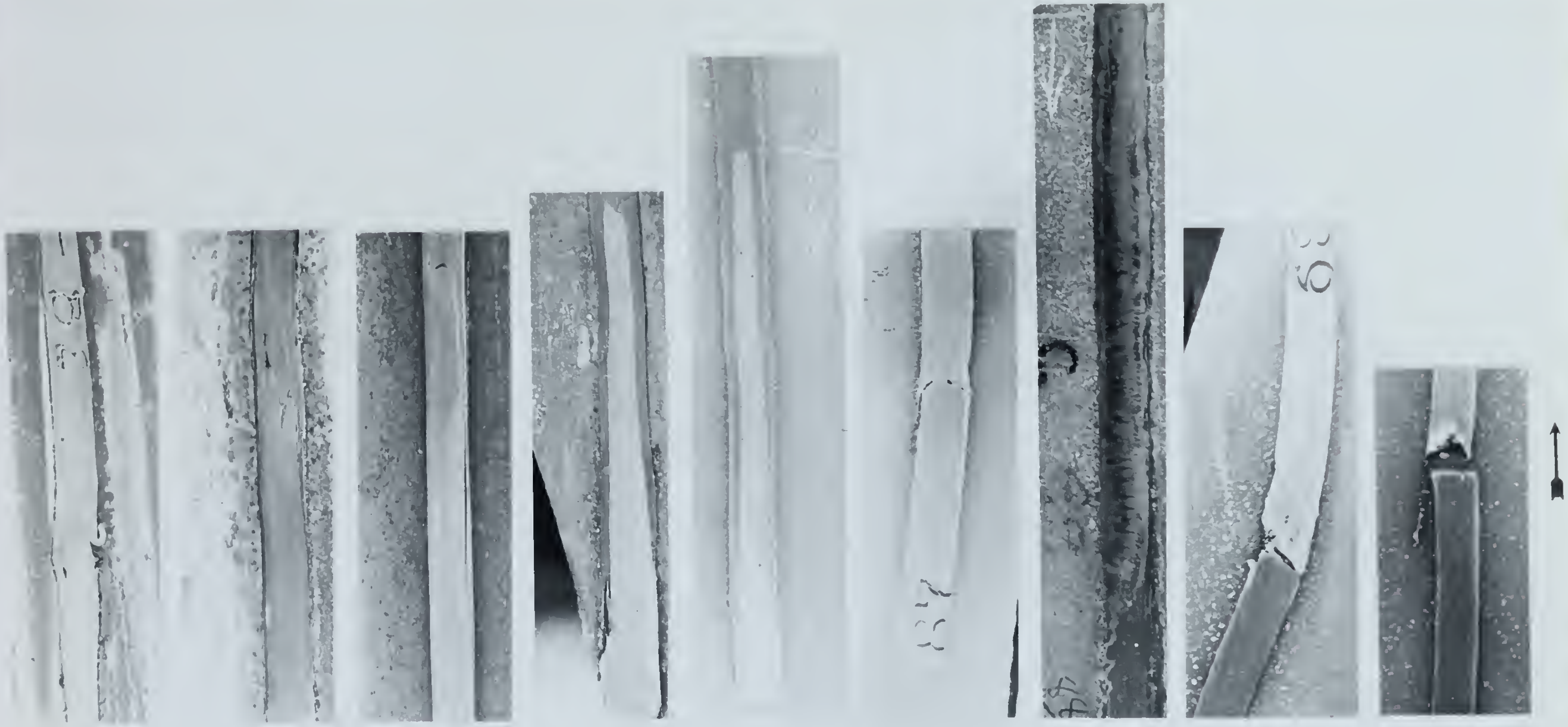

82 83 84 85 86 87 88 89 90

Figure A-15 - Photographs of Composite Lead Billets After Extrusion Showing Interface.
Extrusion Ratio = 25

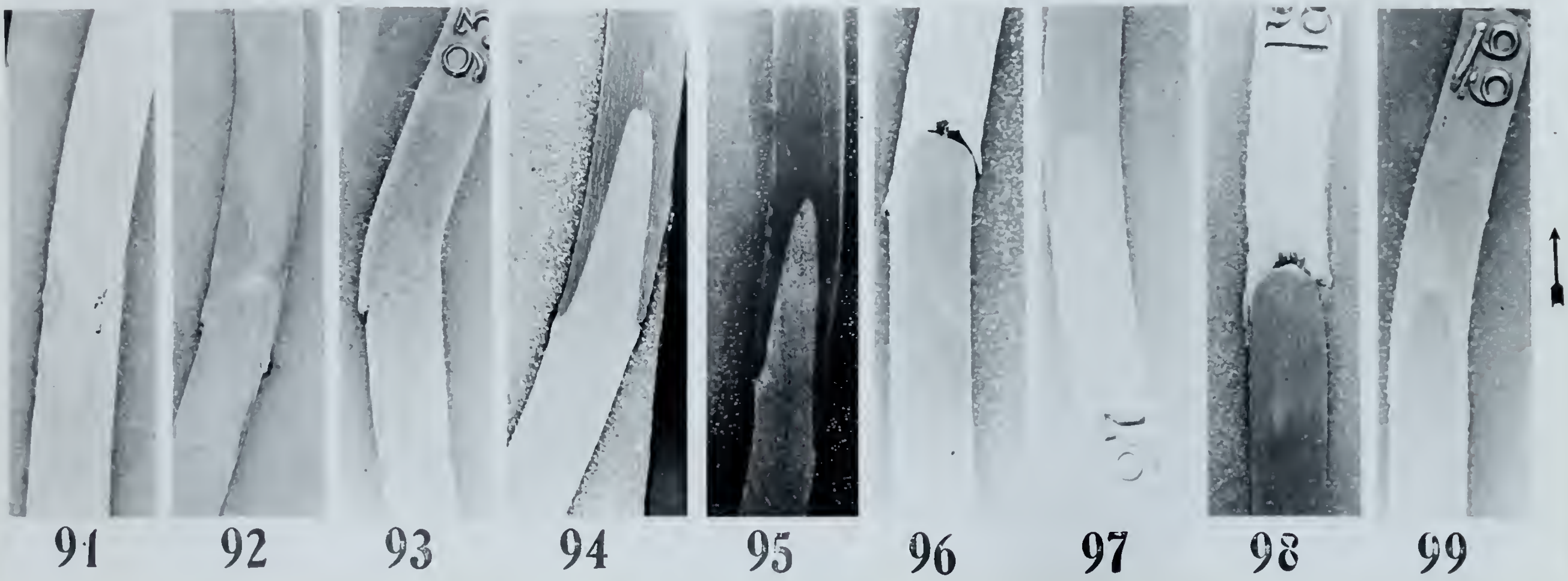

Figure A-16 - Photographs of Composite Lead Billets After Extrusion Showing Interface.
Extrusion Ratio = 9

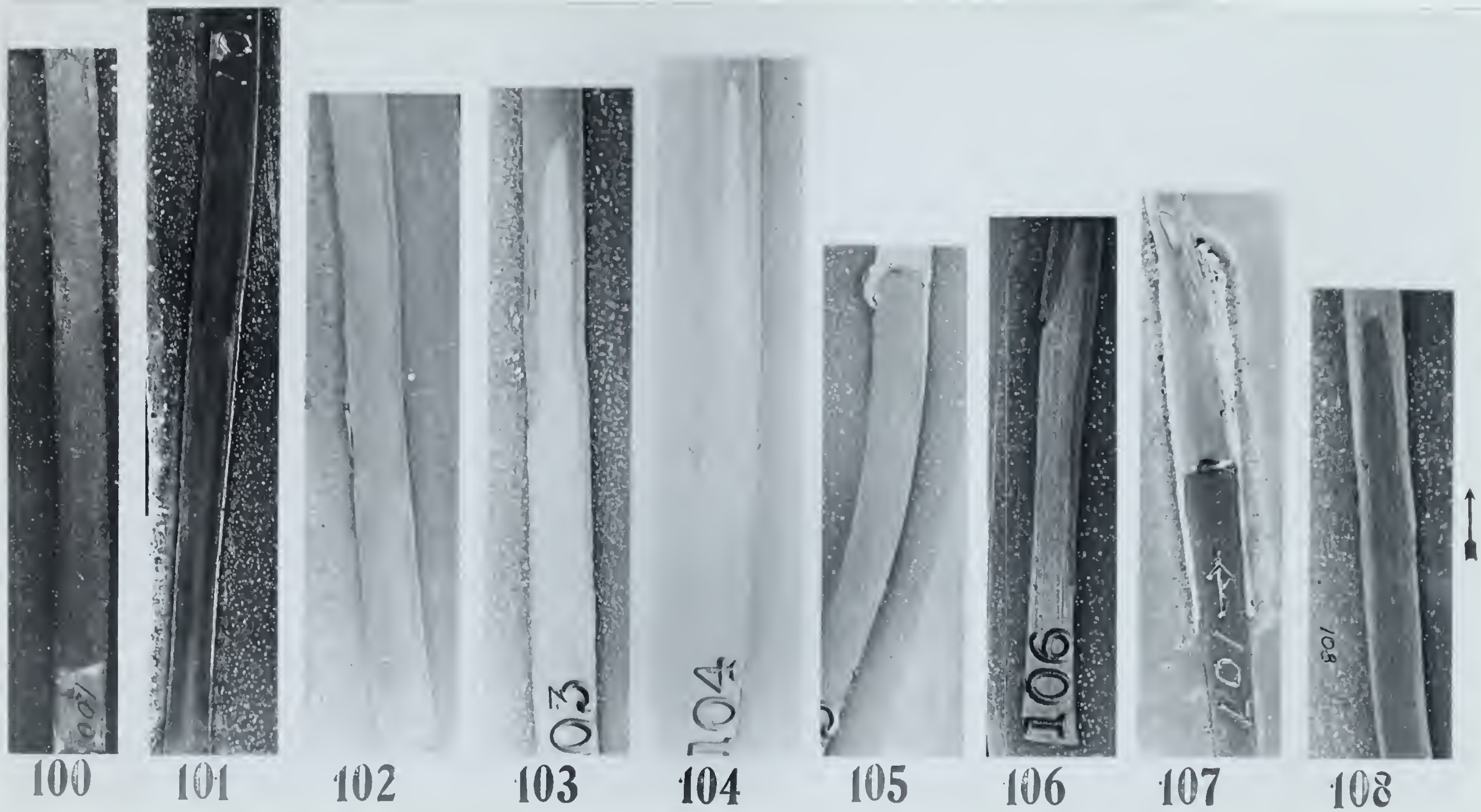

Figure A-17 - Photographs of Composite Lead Billets After Extrusion Showing Interface.
Extrusion Ratio = 16

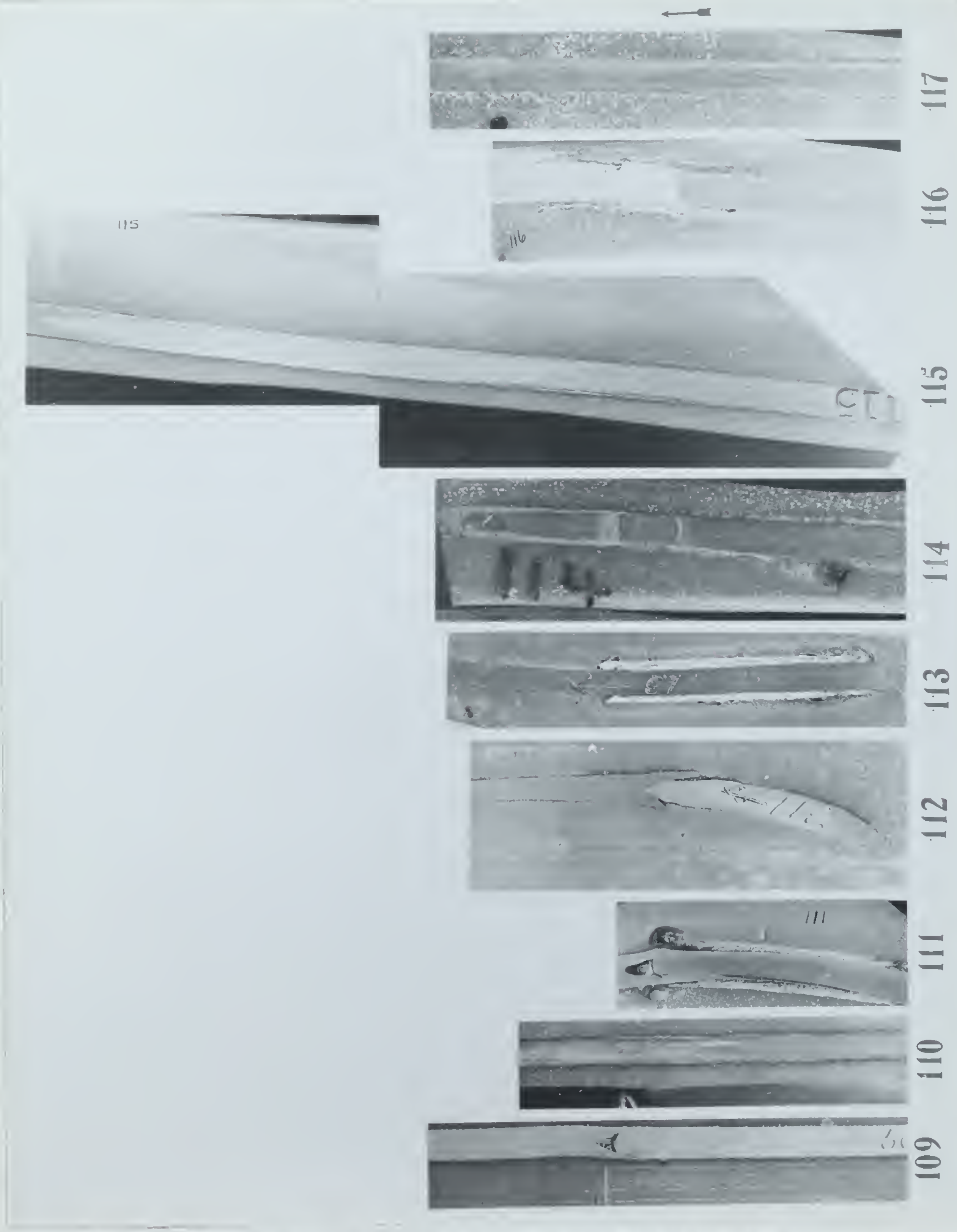

Figure A-18 - Photographs of Composite Lead Billets After Extrusion Showing Interface. Extrusion Ratio = 25

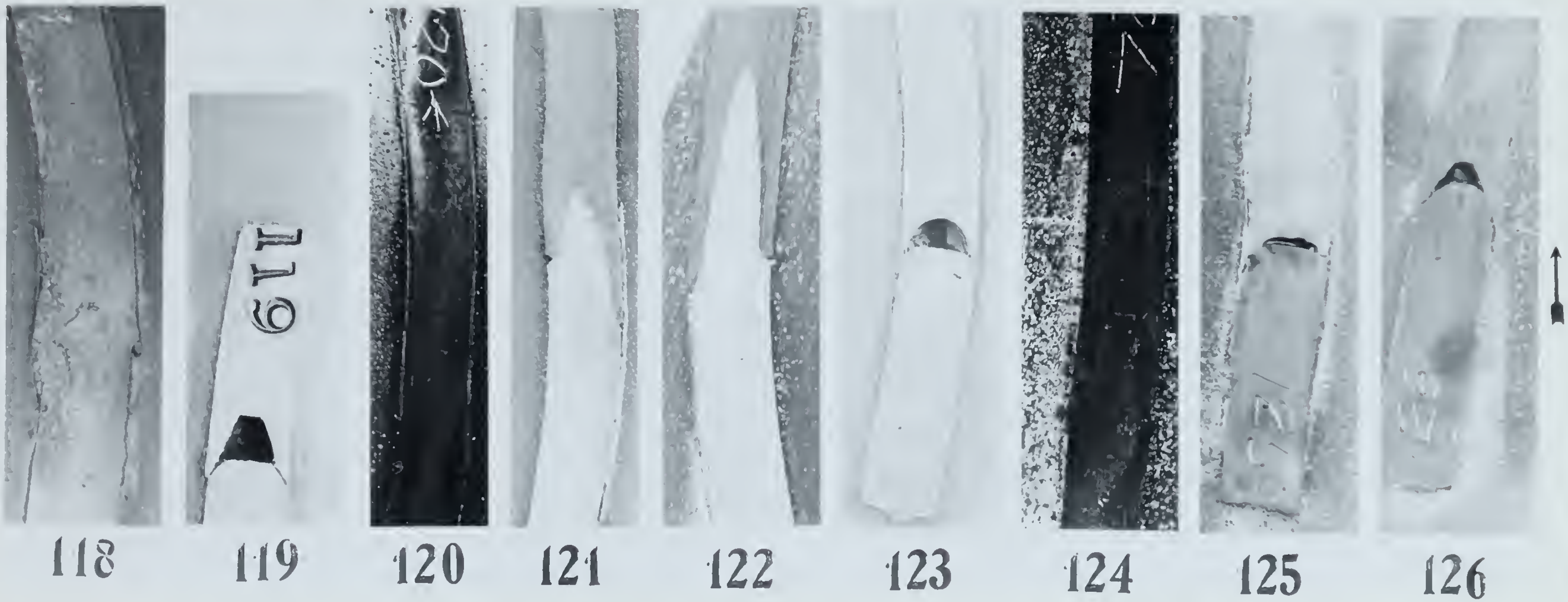

Figure A-19 - Photographs of Composite Lead Billets After Extrusion Showing Interface.
Extrusion Ratio = 9

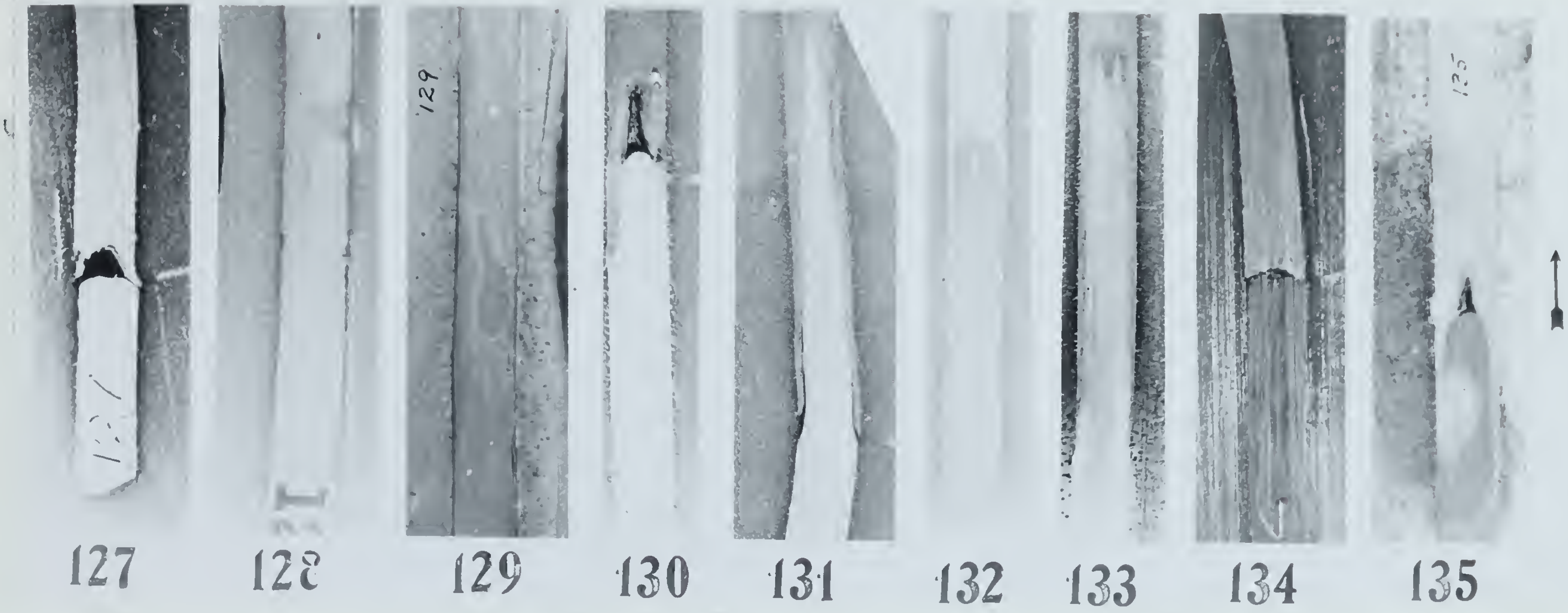

Figure A-20 - Photographs of Composite Lead Billets After Extrusion Showing Interface.
Extrusion Ratio = 16

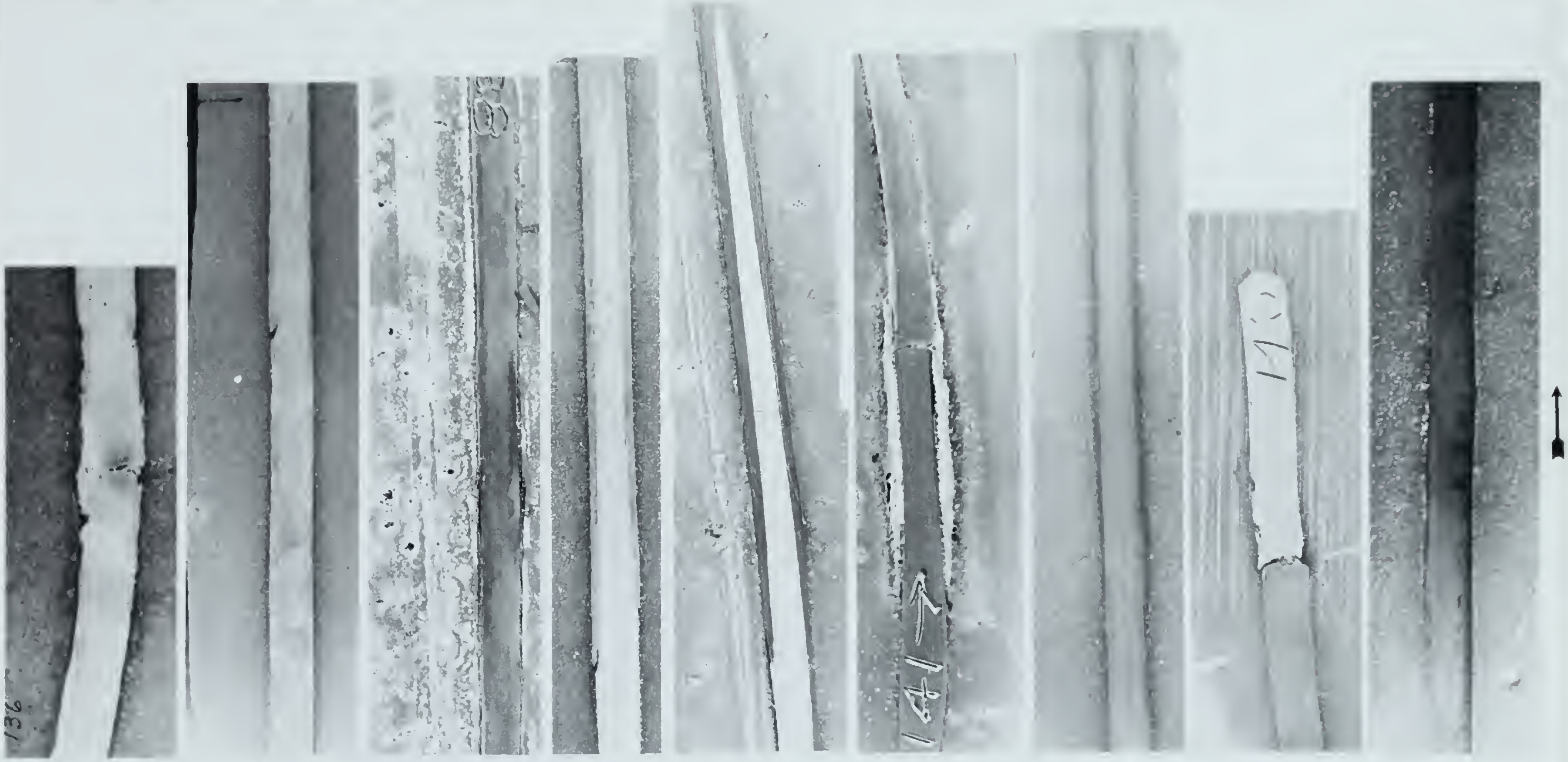

136 137 138 139 140 141 142 143 144

Figure A-21 - Photographs of Composite Lead Billets After Extrusion Showing Interface.
Extrusion Ratio = 25

# APPENDIX B

## PLASTICINE EXPERIMENTS

### 1. The Material Used

The Plasticine used was a plastic clay distributed under the trade name of "Plastalena", manufactured by the Stewart Clay Company of New York 13, New York. It was a non-hardening clay which came in a variety of colors and, much to the chagrin of the investigator, a variety of hardnesses. The color appeared to have a remarkable effect on the hardness, probably because in its manufacture, a batch consisted of one color. In conversation with the manufacturer, it was learned that precise methods were not used to any degree at all.

### 2. Lubrication

An attempt was made to determine the best lubricant for obtaining the least friction between the clay and a bright metal surface. The following substances were tried:

a. Talc

b. Dow Corning 703 Silicone Fluid

c. Dow Corning 9981 LT

d. Shell #140 Gear Box Oil

e. Teresso #65 Hydraulic Oil

f. Mineral Oil

g. Aquadag

h. Johnson #150 Wax Draw

i. Welsh Duo-seal Oil

j. Dumore Cool Bearing Oil

k. Lubriko Grease (Density M6)

l. Liquid Green Soap

m. Water

n. Ethyl Ricinoleate (Eastman Kodak)

o. Polyethylene Glycol "600"

The test consisted of extruding Plasticine through a circular die using an extrusion ratio of 4 and a billet diameter of .750-inch. The die, cylinder wall, ram, and billet were coated with the specified lubricant and the extrusion pressure was recorded. Without going into great details of the analysis, it was found that water was the best lubricant of all the materials tried. Most of the oils showed little if any variation. The Johnson Draw Wax closely approached the water value. In no cases was it possible to lubricate the throat of the die for more than a small portion of the extrusion, which indicated that the clay was soft enough to prevent the thin film lubricant from passing into the die. This was significant in that during the initial stage of extrusion the throat was lubricated; whereas, for most of the extrusion the throat had no lubricant whatsoever. This point should be remembered in analyzing the results of extrusion with very soft materials.

One point in favor of using plain water as a lubricant was that it was not a solvent for the binder in the clay.

### 3. Density Measurements

Some thought was given to kneading the clay in order to insure homogeneity. Invariably kneading resulted in lower extrusion pressures. Density measurements were made on different colors and with kneaded and unkneaded clay. As suspected, density varied with color but only from a batch-wise point of view. Significant, however, was the fact that the

unkneaded clay was always less dense, which can be attributed to the air bubbles existing in the clay prior to kneading. This variation amounted to about 1 percent.

### 4. Interface Study

A series of simple extrusions were conducted using two different colored Plasticines in order to study the formation of the interface which developed. No quantitative data was taken, since the object was to determine the feasibility of using the Plasticine as an extrusion medium. It was from these experiments that it was decided to use a metal such as lead. The main reason for its unacceptability was the lack of reproducibility and the difficulty experienced in obtaining accurate measurements.

# APPENDIX C

## DOUBLE EXTRUSION EXPERIMENT WITH ALUMINUM

In order to determine if the results obtained in the double extrusion experiment using Plasticine were applicable only to that material alone, the same basic experiment was carried out using aluminum.

A billet, shown in Figure C-1, was machined from 14S aluminum. A 1/8-inch hole was drilled as indicated and filled with powdered copper so that a radiograph could be taken in order to show the results of the extrusion on a transverse grid line. This billet was then heated to 400°C and extruded through a 1.054-inch die, giving an extrusion ratio of 4. Figure C-2 is the radiograph of the billet after the first extrusion. This billet was then re-extruded from the opposite direction, using a .55-inch die which gave an extrusion ratio again of 4. Figure C-3 is the radiograph of this final extrusion.

Note that the extrusion defect after the first extrusion is quite normal and is what one would expect; however in Figure C-3 the extrusion defect has not reversed itself anywhere along the line and has greatly increased in length. This inability of the defect to show even small signs of reversing itself indicates that this is an instance where the defect after the first extrusion was too great, and in fact, far exceeded the point at which it could be reversed.

It would be interesting to repeat this experiment and for the first extrusion use an extrusion ratio of around 1.5 and then re-extrude at about 10-16. In this way, the defect would be around the 15° cone angle range and could possibly result in a flat interface.

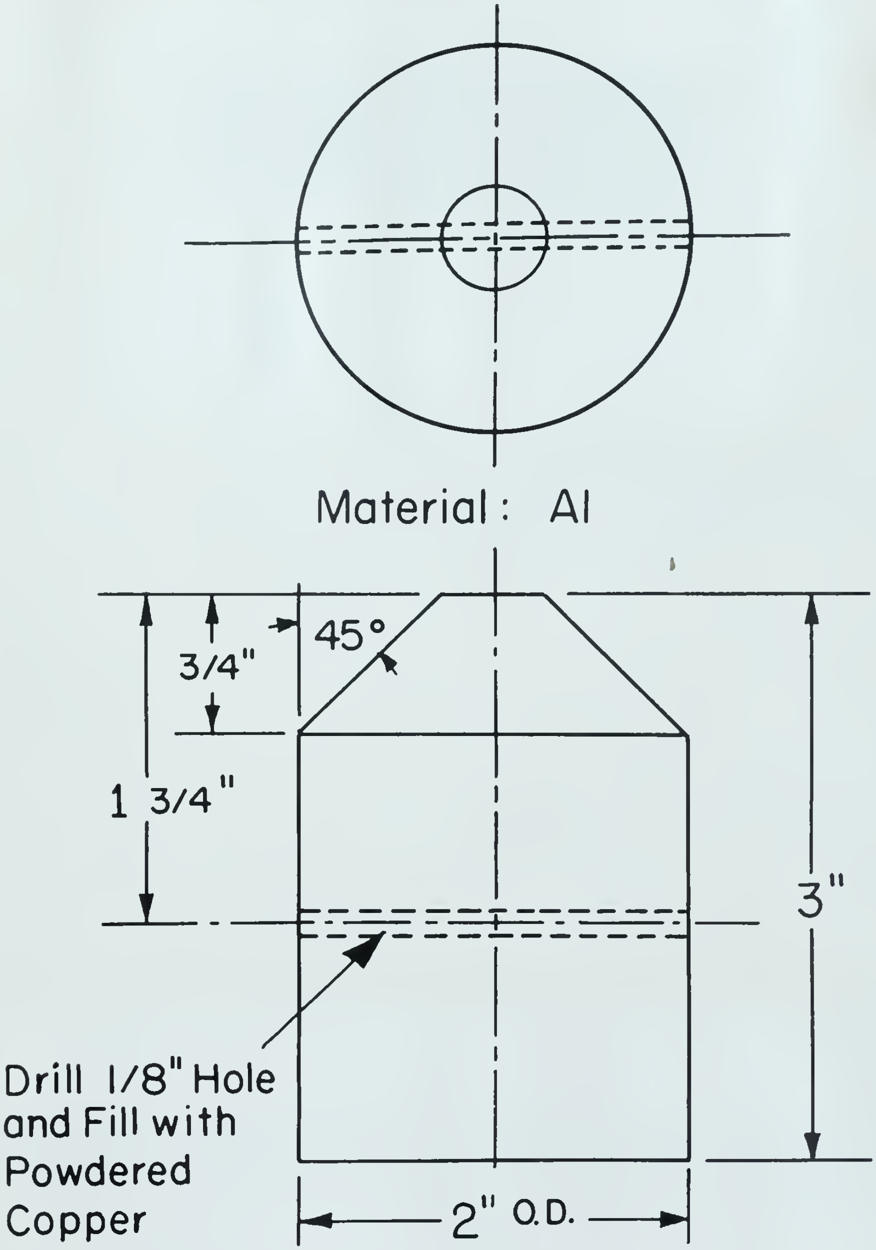

Figure C-1

Billet for Aluminum Double Extrusion

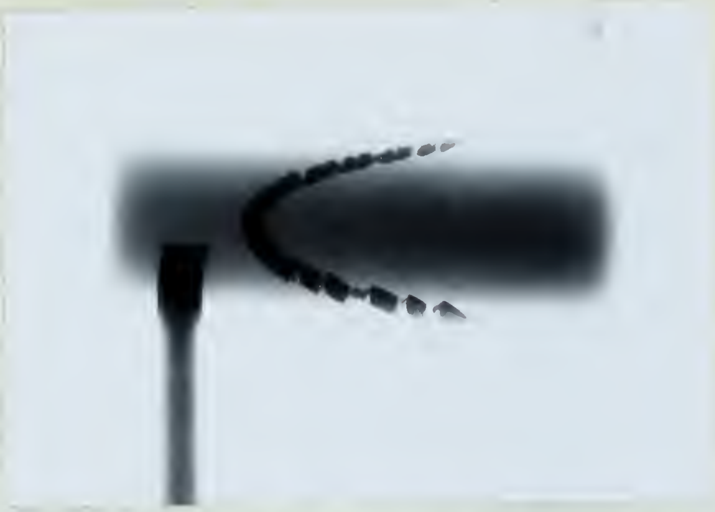

Figure C-2 - Radiograph of Aluminum Billet After First Extrusion Showing Distortion of Copper-Filled Hole. Direction of First Extrusion was from Right to Left.

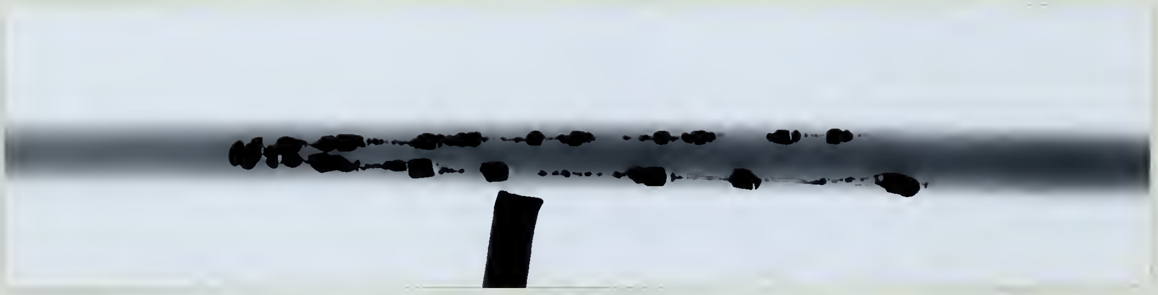

Figure C-3 - Radiograph of Aluminum Billet After Second Extrusion Showing Distortion of Copper-Filled Hole. Direction of Second Extrusion was from Left to Right.

23873

W335 Wegner

A study of metal flow during integral end closure extrusion cladding.

23873

W335 Wegner

A study of metal flow during integral end closure extrusion cladding.

thesW335
A study of the metal flow during integra
3 2768 001 95161 9
DUDLEY KNOX LIBRARY